Intercellular Signaling Activity Encoded by *hetN* in the Cyanobacterium *Anabaena* sp. strain PCC 7120

A DISSERTATION SUBMITTED TO THE GRADUATE DIVISION OF THE UNIVERSITY OF HAWAI'I AT MANOA IN PARTIAL FULFILMENT OF THE REQUIREMENTS FOR THE DEGREE OF

DOCTOR OF PHILOSOPHY
IN
MICROBIOLOGY

AUGUST 2017

By

Orion Silverstar Rivers

Dissertation Committee:

Sean Callahan, Chairperson
Dulal Borthakur
Sladjana Prisic
Steven Seifried
Floyd Reed

Keywords: *Anabaena*, intercellular signaling, HetN, cellular differentiation

ACHNOWLEDGEMENTS

I would like to express my sincerest thanks to Dr. Sean Callahan for his guidance and support throughout this process. I would also like to thank Dr. Patrick Videau for insightful discussions and technical assistance and Silvia Beurmann and Christina Runyon for intellectual support. I am also very grateful for the continued support of my family and friends.

ABSTRACT

Developmental regulators coordinate cellular differentiation in many organisms. Regulators can be small molecules or proteins. Developmental regulators called morphogens are produced in source cell(s) that determine the developmental fate of cells adjacent to the source in a concentration dependent manner. The filamentous cyanobacterium *Anabaena* sp. Strain PCC 7120 is a model organism used to study cellular differentiation. When *Anabaena* filaments are supplied a source of fixed nitrogen a single cell type, vegetative cells, comprise the filaments. However, removal of fixed nitrogen from the medium induces differentiation of one in every 10-15 cells into a heterocyst. Heterocysts are terminally differentiated cells that are the sites of atmospheric nitrogen fixation. Differentiation within *Anabaena* requires 24 hours and can be divided into four stages: induction, patterning, commitment, and morphogenesis. The periodic pattern of heterocyst is initially determined by the interplay of HetR, the primary activator of differentiation within *Anabaena*, and PatS, a diffusible inhibitor expressed during the patterning stage. The initial pattern of heterocysts in maintained during growth by a secondary inhibitor, HetN, which is expressed in mature heterocysts. The pentapeptide sequence RGSGR is conserved in the amino acid sequences of both inhibitors and has been shown to inhibit differentiation and induce HetR degradation when added to the medium, bind directly to HetR *in vitro*, and is required for the inhibitory function of PatS. In this work HetN was found to require the RGSGR sequence for inhibitory function and did not require predicted ketoacyl reductase activity. Full-length HetN was found to be confined to source cell(s) membranes, but a *hetN*-dependent inhibitory signal was shown to move away from source heterocysts in a manner similar to a paracrine-type intercellular signal. The *hetN*-dependent inhibitory signal was found not to require the intercellular channel forming protein SepJ. However, mutation of *sepJ* reduced

the signal range of the HetN-dependent inhibitory signal, suggesting its involvement in signal transport. Finally, evidence supporting the use of M119 of HetN as the developmentally regulated translational start site is presented. This work contributes to our knowledge of morphogen signals and supports the role of HetN as an inhibitory morphogen within *Anabaena*.

TABLE OF CONTENTS

List of Tables

List of Figures

Chapter 1. Introduction to *Anabaena* sp. Strain PCC 7120

Patterning of differentiation in many multicellular organisms is regulated by morphogens [44]. Morphogens are molecules that emanate from a source and determine the developmental fate of cells distant from the source based on the local concentration of the morphogen signal [42, 46]. In this dissertation, use is made of a model organism comprised of just two different cell types in an attempt to understand the action of a potential morphogen. The findings from this very simple organism will give insight into the complex interactions that are involved in the process of differentiation in more complex systems.

Cyanobacteria, as indicated by the fossil record, are as old as 3.5 billion years. Some cyanobacteria develop two distinct cell types in response to the availability of nitrogen within their environments. *Anabaena* sp. strain PCC 7120 (hereafter *Anabaena*), is one such cyanobacterium that develops two distinct cell types, vegetative cells for growth and heterocysts for fixation of atmospheric dinitrogen [16, 24, 54]. The generation of two distinct cell types elaborated by *Anabaena* in a periodic pattern has been used as a basic model system of cellular differentiation for over 50 years.

The *Anabaena* model system offers several advantages over eukaryotic systems for the study of cellular differentiation. Movement of developmental signals in *Anabaena* can be represented in one dimension as opposed to the 3-dimentional cellular arrangements of eukaryotic systems. *Anabaena* differentiates a single cell type, a heterocyst, within 24 hours of the removal of fixed nitrogen. *Anabaena* grows more rapidly than eukaryotes, doubling every 12 hours. Prokaryotic genomes, as found in *Anabaena*, are smaller than eukaryotic genomes and are haploid, which allows for easier genetic manipulation. The

availability of the complete *Anabaena* genome further aids in genetic manipulation within the system [21].

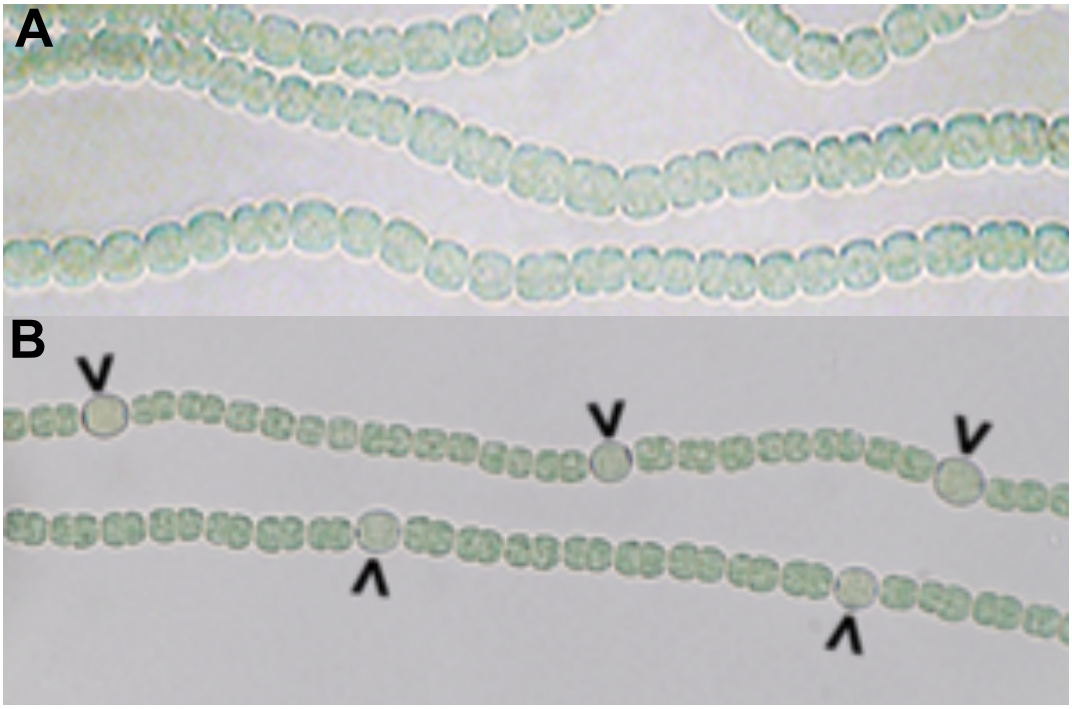

Figure 1. Bright-field micrographs of *Anabaena* sp. strain PCC 7120 grown with a source of nitrogen, N+ (A) and 24 hours after the removal of nitrogen from the medium, N- (B). Carets indicate heterocysts.

Anabaena is a filamentous cyanobacterium isolated from Lake Michigan during the 1950s. When the filaments are supplied a source of fixed nitrogen, such as nitrate or ammonium, a single cell type known as vegetative cells comprise the filaments (Fig. 1A). When fixed nitrogen is not available the filaments differentiate one in every 10-15 cells into a heterocyst (Fig. 1B) [16, 55, 59]. The heterocyst cells are arranged in a semi-regular periodic pattern along the filament. Heterocysts are terminally differentiated cells that are the sites of atmospheric nitrogen fixation, a process dependent on the enzyme nitrogenase [55]. Fixed nitrogen is supplied to the adjacent cells in the form of amino acids [32]. In exchange, vegetative cells supply heterocysts a source of carbon in the form

of sucrose (Fig. 2) [32, 52]. This interdependence of the two cell types makes *Anabaena* a good model organism for the study of patterned cellular differentiation.

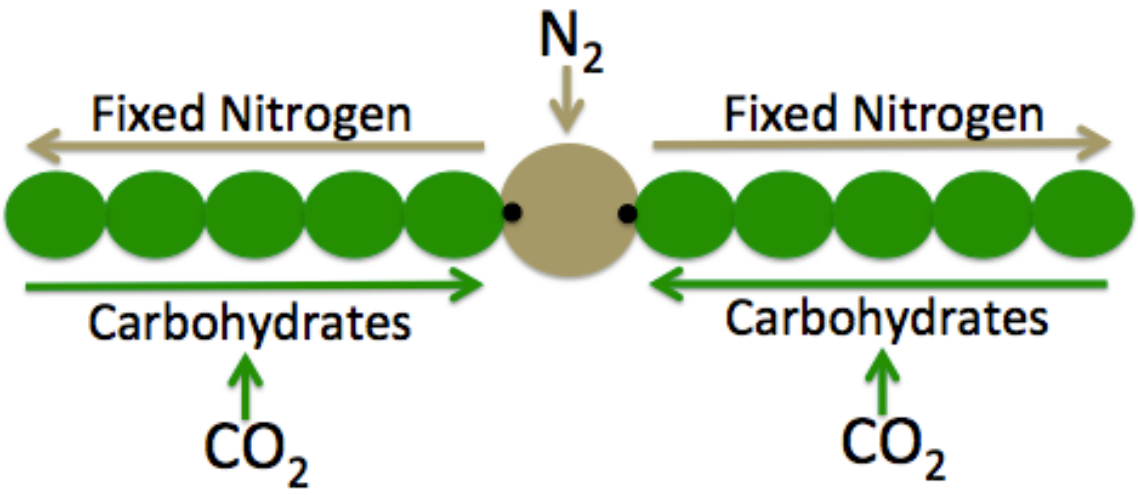

Figure 2. Diagram of the interdependence of heterocysts and vegetative cells. The brown heterocyst fixes atmospheric dinitrogen and exports the nitrogen, in the form of amino acids, to the adjacent vegetative cells. The green photosynthetic vegetative cells provide the heterocyst with carbohydrates, in the form of sucrose.

Overview of differentiation in *Anabaena*

Heterocyst differentiation in *Anabaena* proceeds through four developmental stages: induction, patterning, commitment, and morphogenesis. Induction begins when nitrogen starvation leads to the accumulation of 2-oxoglutarate, 2-OG [25, 28]. *Anabaena* lacks the tricarboxylic acid cycle-enzyme 2-oxoglutarate dehydrogenase. However, *Anabaena* contains a 2-oxoglutarate decarboxylase and succinic semialdehyde dehydrogenase, which together complement 2-oxoglutarate dehydrogenase function [62]. Regardless, when intracellular levels of carbon are abundant and fixed nitrogen is scarce 2-oxoglutarate accumulates [28]. 2-OG then binds to NtcA, a CRP/CAP-like transcriptional regulator of nitrogen metabolism [17, 48]. The NtcA/2-OG complex up

regulates the transcription of *nrrA*, leading to the transcription of *hetR* (Fig. 3) [9, 10]. HetR is the primary activator of differentiation and its expression initiates the beginning of the patterning stage.

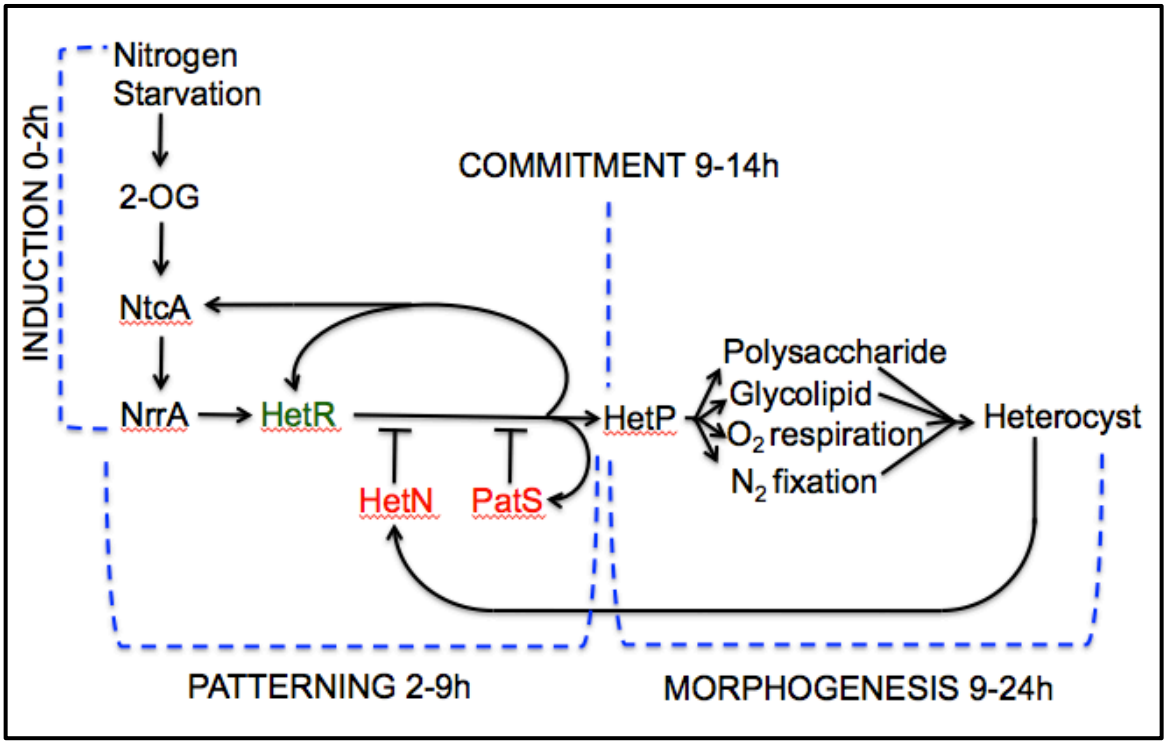

Figure 3. Model of key genetic interactions involved in the differentiation of heterocysts in *Anabaena* sp. strain PCC 7120. The approximate timing for each stage: initiation, patterning, commitment, and morphogenesis are indicated in hours. Arrows represent positive interactions and bars negative interactions.

Patterning begins with the production of the transcriptional regulator HetR (Fig 3). Deletion of *hetR* results in a lack of differentiation, even in nitrogen-depleted environments [4]. Overexpression of *hetR* results in the formation of heterocysts regardless of nitrogen availability [5]. HetR is a transcriptional regulator that binds directly to DNA and controls a regulon, many genes of which are involved in differentiation [49]. HetR up-regulates its own transcription as well as that of *patS*, an

inhibitor of differentiation (Fig. 3) [5]. The interplay of the activator HetR and the inhibitor PatS determine the initial pattern of heterocysts that will form in a population of vegetative cells.

Once the initial pattern has been established, filaments enter the commitment stage. This represents a point at which the developmental fate of the cells has been determined and differentiation will occur, despite the nitrogen status of the environment [58]. The timing of commitment appears to be dependent on four proteins similar to HetP, a protein of unknown function [18, 51]. Once a cell has committed to differentiation a number of morphological changes occur. Together these changes comprise the morphogenesis stage.

During morphogenesis exterior laminated glycolipid and exopolysaccharide layers are added to the developing heterocyst [43, 53]. The glycolipid layer serves as a barrier to entry of molecular oxygen to achieve a microoxic environment that is required for the function of the nitrogenase complex [53, 55]. The deposition of these layers is accompanied by the degradation of photosystem II, a complex that evolves molecular oxygen, and the Calvin cycle. As a result, heterocysts are dependent on vegetative cells for carbon and vegetative cells are dependent on heterocysts for fixed nitrogen [55]. During morphogenesis a secondary inhibitor of differentiation, HetN, is produced (Fig. 3) [45].

HetR, PatS, and HetN in heterocyst patterning

Mathematical models have been developed to study the molecular interactions that produce biological patterns. The activator-inhibitor model, a reaction-diffusion type model, is one [15, 33, 47]. In order to apply the activator-inhibitor model to *Anabaena*

the system must fulfill four criteria; the activator must be auto-catalytic, production of the inhibitor must be dependent on the activator, the inhibitor must inhibit the auto-catalysis of the activator or promote activator decay, and the inhibitor must move over a greater distance than the activator (Fig. 4) [15].

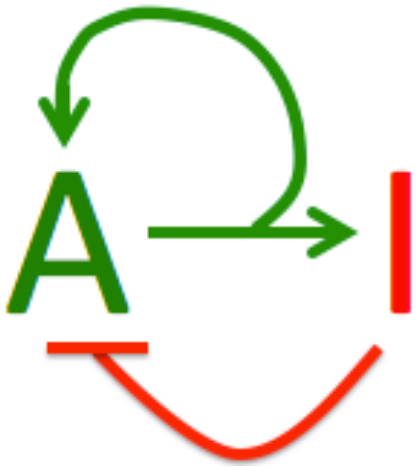

Figure 4. Diagram of the interactions described by the activator-inhibitor model of biological pattern formation. The activator (green A) catalyzes the production of the inhibitor (red I) as well as itself. The inhibitor then blocks activator function. Green arrows represent positive interactions. Red bars represent negative interactions.

In the case of *Anabaena*, HetR can be defined as the activator and PatS and HetN can be defined as inhibitors (Fig. 4). The production of HetR, PatS, and HetN are dependent on HetR [38], whose function as an activator is abrogated by PatS and HetN [20]. Finally, although HetR is likely confined to source cells, PatS has been shown to move several cell diameters away from its source [7] and a portion of HetN or something dependent on HetN has been shown to move several cell diameters from the source of production [7, 41]. The combination of these findings allows for the activator-inhibitor

model to be applied to the *Anabaena* model system to predict further molecular interactions leading to differentiation [33].

HetR is the primary activator of differentiation [2]. A *hetR* deletion strain is unable to differentiate heterocysts, and a strain overexpressing *hetR* forms an excess number of heterocysts in medium containing a source of nitrogen (N+) and in medium lacking a source of nitrogen (N-) [4, 5]. The crystal structure of HetR reveals four domains: two flap domains involved in non-specific binding of DNA, a hood domain thought to be the site were the inhibitory peptides interact with HetR, and a helix-turn-helix motif involved in binding to specific DNA sequences [22]. HetR has been shown to be a transcriptional regulator that binds directly to DNA [18, 23] and regulates the transcription of a regulon of genes, many of which are involved in the differentiation process [44, 49, 50]. Both the inhibitors of differentiation, PatS and HetN, contain the sequence RGSGR as part of the protein. This penta-peptide binds directly to HetR at amino acids 250-256, and this binding has been shown to abrogate the DNA-binding ability of HetR *in vitro* and cause degradation of HetR *in vivo* [11, 12, 40]. Mutation of amino acids 250-256 in HetR creates a protein that can act as a transcriptional regulator that is insensitive to inhibition and promotes the formation of heterocysts in the presence of excess inhibitor derived from *hetN* or *patS* [39]. HetR was further shown to bind with 30 times more affinity to the hexa-peptide ERGSGR, the wild-type amino acid sequence found in both PatS and HetN [11, 40].

PatS and HetN are inhibitors directly and indirectly up regulated by HetR, respectively. Removal of *patS* or *hetN* results in a mutant phenotype where multiple contiguous heterocysts (Mch) are present within the filaments, whereas the wild-type

differentiates primarily individual heterocysts [3]. Overexpression of *patS* or *hetN* results in an inability to form heterocysts in N- conditions [3, 6]. PatS, a 17aa peptide, and HetN, a 287aa protein, both contain the penta-peptide sequence RGSGR. Exogenous addition of the penta-peptide RGSGR to the growth medium results in the suppression of heterocyst formation [56, 57]. Any mutation in the RGSGR sequence of PatS results in a mutant Mch phenotype [8]. PatS is expressed in the patterning phase and is thought to be involved in pattern formation [57].

HetN can be divided into four domains based on the hydrophobicity of the linear peptide sequence. An N-terminal hydrophobic domain at amino acids 1-46; an N-terminal hydrophilic domain containing the RGSGR and catalytic triad motifs at amino acids 47-176; a second hydrophobic domain consistent with a membrane spanning domain at amino acids 177-196; and a C-terminal hydrophilic domain at amino acids 197-287 (Fig. 3A) [19]. The presence of an internal hydrophobic region within HetN suggests that the protein localizes to a membrane. There are two likely membrane types that HetN could be localizing to, the plasma membrane or the thylakoid membranes. HetN also contains both the RGSGR sequence at residues 132-136, and ketoacyl reductase activity, which would depend on residues 142, 155, and 159 [1]. These latter residues are conserved in ketoacyl reductases and represent the catalytic site. HetN is produced in mature heterocysts and is thought to be responsible for pattern maintenance as cells within the filament grow and divide [6].

Previous work has addressed the importance of the catalytic triad residues to the inhibitory function of HetN with mixed results. It was reported that mutation of one of the residues in the catalytic triad prevented the allele from inhibiting differentiation when

overexpressed, while mutation of the other two had no effect [29]. The results are inconsistent with those that you would expect when mutating residues in the catalytic site of an enzyme, where all mutations of catalytic residues usually produce a similar phenotype.

A second study found that when each of the three alleles of *hetN*; S142A, Y155F, and K159R, where overexpressed in wild-type, the strains failed to differentiate heterocysts after 24 hours growth in N- conditions [19]. The result indicated that a functional inhibitor is being produced in the absence of ketoacyl reductase activity. These semi-conflicting studies suggest that more work is required to determine the developmental importance of the ketoacyl reductase activity of HetN.

Work on the importance of the RGSGR sequence to the inhibitory function of HetN has also yielded mixed results. It has been reported that mutation of residues within the RGSGR sequence had no effect on the inhibitory function of HetN [26, 27]. A second study reported the ability of HetN to induce post-translational decay of HetR was abrogated when the allele *hetN*(RGDAR) was used in place of native *hetN*, indicating that the RGSGR sequence is important for the inhibitory function of HetN [40]. A third study found that when each of the five alleles encoding the substitutions R132K, G133A, S134A, G135A, and R136K in HetN separately were overexpressed in wild-type the strains where able to differentiate heterocysts after 24 hours of growth in N- conditions [19]. Notably, the R132K and R136K alleles showed no inhibitory activity and allowed differentiation comparable to that of the wild-type containing an empty vector [19]. The result indicated that little to no functional inhibitor is being produced in the absence of individual residues within the RGSGR sequence of HetN. The conflicting results suggest

that more work is required to determine the developmental importance of the RGSGR sequence in HetN.

For PatS or HetN to be classified as morphogens, the proteins must first be shown to fulfill the requirements of a morphogen. Importantly, the inhibitory protein that moves from cell to cell must be identified, and that protein's control over the developmental fate of the surrounding cells must be defined. Signals, such as morphogens and hormones, have been classified based on the distance travelled away from the source. Examples are juxtacrine signals, which act on cells immediately adjacent to source cells, paracrine signals, which act over several cell lengths, and endocrine signals, which act throughout the entire organism [35].

How the PatS and HetN-dependent inhibitory signals move from cell to cell is unknown but is likely achieved through one, or a combination, of three possible routes of protein transfer between cells in *Anabaena* filaments. First, the periplasm of cells in filaments is contiguous, and there is evidence both for and against the diffusion of proteins between cells via the periplasmic space [30, 37, 60, 61]. The second potential route of transfer is direct exchange between the membranes of adjacent cells. Although the cytoplasmic membranes at cell septa are not shared by adjacent cells and so are not continuous between cells, they are in close proximity [13], and could be bridged by an, as yet, uncharacterized inter-membrane transport system. The third potential route of transfer is via inter-cytoplasmic exchange mediated by channel forming proteins, which allow for direct exchange between the cytoplasms of adjacent cells in a filament. Intercellular channel-forming proteins, such as SepJ, FraC, or FraD, have been shown to

localize to cell junctions and facilitate the movement of molecules between cells [14, 31, 34, 36, 41].

Work described in the following chapters expands the current knowledge surrounding the developmental inhibitors present within the *Anabaena* model system, with a focus on the inhibitor HetN. In chapter 2 the developmentally important regions within the HetN protein are identified. Specifically, the contribution to development of the predicted domains of HetN based on hydrophobicity, the amino acid sequence ERGSGR, and the predicted ketoacyl reductase function of HetN. Chapter 3 explores the subcellular localization of HetN, the ability of HetN to be transported from cell to cell as a full-length protein, and the spatial range of the HetN-dependent inhibitory signal within *Anabaena*. Chapter 4 investigates the ability of HetN or PatS to be transported from cell to cell via protein channels connecting the cytoplasm of adjacent cells to one another. In Chapter 5 a HetN-dependent inhibitory signal is shown to influence differentiation at a distance in a paracrine type manner. Finally, chapter 6 supports the translation of HetN from a start site different from the annotated translational start site.

Implications for Current Work

Cellular differentiation within multi-cellular organisms has allowed for the specialization of different cell types for specific functions during the evolutionary contest of survival. Differentiation has been found to be controlled by morphogens, diffusible small molecules or proteins produced in source cell(s), which determine the developmental fate of adjacent cells in a concentration-dependent manner. Mathematical models have been developed to study the molecular interactions that produce biological

patterns. The activator-inhibitor model, a reaction-diffusion type model, is one model that appears to be applicable to differentiation in *Anabaena* [15, 47].

Rigorous demonstration of paracrine signaling is complicated by the need to conclusively show that the effect of a given molecule cannot be explained by cell autonomous activity. Since its discovery in 1998, PatS has been regarded as an intercellular signaling molecule that regulates the patterning of heterocyst differentiation [57] and has been described as a morphogen within the *Anabaena* model system [7] despite a lack of identification of the exact inhibitory peptide. The secondary inhibitor HetN, which is predicted to have ketoacyl reductase activity, is less well defined.

The identification of developmental regulators in less complex model organisms is an important step in the understanding of more complex developmental systems. The work presented here defines the domains required for HetN-dependent inhibitory activity, investigates the route of transfer of inhibitory signals within Anabaena, and describes the role of internal methionine residues to the translation of HetN. The results support the presence of a HetN-dependent paracrine type inhibitory morphogen within the *Anabaena* developmental system. Defining the mode of action of developmental regulators like HetN is important for both the understanding of multicellular organisms and contributes to our potential to control cellular differentiation for medical purposes in future generations.

References

1. Black, T., A. and C.P. Wolk, *Analysis of a Het⁻ mutation in Anabaena sp. strain PCC 7120 implicates a secondary metabolite in the regulation of heterocyst spacing.* J. Bacteriol., 1994. **176**: p. 2282-2292.
2. Black, T.A., Y. Cai, and C.P. Wolk, *Spatial expression and autoregulation of hetR, a gene involved in the control of heterocyst development in Anabaena.* Mol. Microbiol., 1993. **9**: p. 77-84.
3. Borthakur, P.B., et al., *Inactivation of patS and hetN causes lethal levels of heterocyst differentiation in the filamentous cyanobacterium Anabaena sp. PCC 7120.* Mol. Microbiol., 2005. **57**: p. 111-123.
4. Buikema, W.J. and R. Haselkorn, *Characterization of a gene controlling heterocyst development in the cyanobacterium Anabaena 7120.* Genes Dev., 1991. **5**: p. 321-330.
5. Buikema, W.J. and R. Haselkorn, *Expression of the Anabaena hetR gene from a copper-regulated promoter leads to heterocyst differentiation under repressing conditions.* Proc. Natl. Acad. Sci., U.S.A., 2001. **98**: p. 2729-2734.
6. Callahan, S.M. and W.J. Buikema, *The role of HetN in maintenance of the heterocyst pattern in Anabaena sp. PCC 7120.* Mol. Microbiol., 2001. **40**: p. 941-950.
7. Corrales-Guerrero, L., et al., *Functional dissection and evidence for intercellular transfer of the heterocyst-differentiation PatS morphogen.* Mol. Microbiol., 2013. **88**(6): p. 1093-1105.
8. Corrales-Guerrero, L., et al., *Functional dissection and evidence for intercellular transfer of the heterocyst-differentiation PatS morphogen.* Molecular microbiology, 2013. **88**(6): p. 1093-1105.
9. Ehira, S. and M. Ohmori, *NrrA directly regulates expression of hetR during heterocyst differentiation in the cyanobacterium Anabaena sp. strain PCC 7120.* J. Bacteriol., 2006. **188**: p. 8520-8525.
10. Ehira, S. and M. Ohmori, *NrrA, a nitrogen-responsive response regulator facilitates heterocyst development in the cyanobacterium Anabaena sp. strain PCC 7120.* Mol. Microbiol., 2006. **59**: p. 1692-1703.
11. Feldman, E.A., et al., *Differential binding between PatS C-terminal peptide fragments and HetR from Anabaena sp. PCC 7120.* Biochemistry, 2012. **51**: p. 2436-2442.
12. Feldman, E.A., et al., *Evidence for direct binding between HetR from Anabaena sp. PCC 7120 and PatS-5.* Biochmistry, 2011. **50**: p. 9212-9224.
13. Flores, E., et al., *Is the periplasm continuous in filamentous multicellular cyanobacteria?* Trends Microbiol., 2006. **14**: p. 439-443.
14. Flores, E., et al., *Septum-localized protein required for filament integrity and diazotrophy in the heterocyst-forming cyanobacterium Anabaena sp. strain PCC 7120.* J. Bacteriol., 2007. **189**(10): p. 3884-3890.
15. Gierer, A. and H. Meinhardt, *A theory of biological pattern formation.* Kybernetik, 1972. **12**: p. 30-39.
16. Golden, J.W. and H.-S. Yoon, *Heterocyst development in Anabaena.* Curr. Opin. Microbiol., 2003. **6**: p. 557-563.

17. Herrero, A., A.M. Muro-Pastor, and E. Flores, *Nitrogen control in cyanobacteria.* J. Bacteriol., 2001. **183**: p. 411-425.
18. Higa, K.C. and S.M. Callahan, *Ectopic expression of hetP can partially bypass the need for hetR in heterocyst differentiation by Anabaena sp strain PCC 7120.* Mol. Microbiol., 2010. **77**: p. 562-574.
19. Higa, K.C., et al., *The RGSGR amino acid motif of the intercellular signaling protein, HetN, is required for patterning of heterocysts in Anabaena sp. strain PCC 7120.* Mol. Microbiol., 2012. **83**: p. 682-693.
20. Huang, X., Y. Dong, and J. Zhao, *HetR homodimer is a DNA-binding protein required for heterocyst differentiation, and the DNA-binding activity is inhibited by PatS.* Proc. Natl. Acad. Sci. U.S.A., 2004. **101**(14): p. 4848-4853.
21. Kaneko, T., et al., *Complete genome sequence of the filamentous nitrogen-fixing cyanobacterium Anabaena sp. strain PCC 7120.* DNA Res., 2001. **8**: p. 205-213; 227-253.
22. Kim, Y., et al., *Structure of the transcription factor HetR required for heterocyst differentiation in cyanobacteria.* Proc. Natl. Acad. Sci., 2011. **108**: p. 10109-10114.
23. Kim, Y., et al., *Structures of complexes comprised of Fischerella transcription factor HetR with Anabaena DNA targets.* Proc. Natl. Acad. Sci. USA, 2013. **110**(19): p. E1716-1723.
24. Kumar, K., R.A. Mella-Herrera, and J.W. Golden, *Cyanobacterial Heterocysts.* Cold Spring Harbor Perspectives in Biology, 2010. **2**(4): p. a000315.
25. Laurent, S., et al., *Nonmetabolizable analogue of 2-oxoglutarate elicits heterocyst differentiation under repressive conditions in Anabaena sp. PCC 7120.* Proc. Natl. Acad. Sci. U.S.A., 2005. **102**: p. 9907-9912.
26. Li, B., X. Huang, and J. Zhao, *Expression of hetN during heterocyst differentiation and its inhibition of hetR up-regulation in the cyanobacterium Anabaena sp. PCC 7120.* FEBS letters, 2002. **517**(1): p. 87-91.
27. Li, B., X. Huang, and J. Zhao, *Expression of hetN during heterocyst differentiation and its inhibition of hetR up-regulation in the cyanobacterium Anabaena sp. PCC 7120.* FEBS Lett., 2002. **517**: p. 87-91.
28. Li, J.-H., et al., *An increase in the level of 2-oxoglutarate promotes heterocyst development in the cyanobacterium Anabaena sp. strain PCC 7120.* Microbiology, 2003. **149**: p. 3257-3263.
29. Liu, J. and W.-L. Chen, *Characterization of HetN, a protein involved in heterocyst differentiation in the cyanobacterium Anabaena sp. strain PCC 7120.* FEMS microbiology letters, 2009. **297**(1): p. 17-23.
30. Mariscal, V., A. Herrero, and E. Flores, *Continuous periplasm in a filamentous, heterocyst-forming cyanobacterium.* Mol. Microbiol., 2007. **65**: p. 1139-1145.
31. Mariscal, V., et al., *Functional dissection of the three-domain SepJ protein joining the cells in cyanobacterial trichomes.* Mol Microbiol, 2011. **79**(4): p. 1077-88.
32. Meeks, J.C., et al., *Pathways of assimilation of $[^{13}N]N_2$ and $^{13}NH_4^+$ by cyanobacteria with and without heterocysts.* J. Bacteriol., 1978. **134**(1): p. 125-130.

33. Meinhardt, H., *Models of biological pattern formation: from elementary steps to the organization of embryonic axes.* Curr. Top. Dev. Biol., 2008. **81**: p. 1-63.
34. Merino-Puerto, V., et al., *FraC/FraD-dependent intercellular molecular exchange in the filaments of a heterocyst-forming cyanobacterium, Anabaena sp.* Mol. Microbiol., 2011. **82**: p. 87-98.
35. Müller, P. and A.F. Schier, *Extracellular movement of signaling molecules.* Developmental cell, 2011. **21**(1): p. 145-158.
36. Mullineaux, C.W., et al., *Mechanism of intercellular molecular exchange in heterocyst-forming cyanobacteria.* EMBO J, 2008. **27**: p. 1299-1308.
37. Nicolaisen, K., et al., *The outer membrane of a heterocyst-forming cyanobacterium is a permeability barrier for uptake of metabolites that are exchanged between cells.* Mol Microbiol, 2009. **74**(1): p. 58-70.
38. Rajagopalan, R. and S.M. Callahan, *Temporal and Spatial Regulation of the Four Transcription Start Sites of hetR from Anabaena sp. Strain PCC 7120.* J. Bacteriol., 2010. **192**(4): p. 1088-1096.
39. Risser, D.D. and S.M. Callahan, *Mutagenesis of hetR reveals amino acids necessary for HetR function in the heterocystous cyanobacterium Anabaena sp. strain PCC 7120.* J. Bacteriol., 2007. **189**: p. 2460-2467.
40. Risser, D.D. and S.M. Callahan, *Genetic and cytological evidence that heterocyst patterning is regulated by inhibitor gradients that promote activator decay.* Proceedings of the National Academy of Sciences, 2009. **106**(47): p. 19884-19888.
41. Rivers, O.S., P. Videau, and S.M. Callahan, *Mutation of sepJ reduces the intercellular signal range of a hetN-dependent paracrine signal, but not of a patS-dependent signal, in the filamentous cyanobacterium Anabaena sp. strain PCC 7120.* Mol. Microbiol., 2014. **94**(6): p. 1260-1271.
42. Rogers, K.W. and A.F. Schier, *Morphogen gradients: from generation to interpretation.* Annu Rev Cell Dev Biol, 2011. **27**: p. 377-407.
43. Stanier, R.Y. and G. Cohen-Bazire, *Phototrophic prokaryotes: the cyanobacteria.* Ann. Rev. Microbiol., 1977. **31**: p. 225-74.
44. Tabata, T. and Y. Takei, *Morphogens, their identification and regulation.* Development, 2004. **131**: p. 703-712.
45. Tandeau de Marsac, N. and G. Cohen-Bazire, *Moleclular composition of cyanobacterial phycobilisomes.* Proc. Natl. Acad. Sci. USA, 1977. **74**: p. 1635-1639.
46. Teleman, A.A., M. Strigini, and S.M. Cohen, *Shaping morphogen gradients.* Cell, 2001. **105**(5): p. 559-562.
47. Turing, A., *The chemical basis of morphogenesis.* Phil. Trans. R. Soc. Ser. B, 1952. **237**: p. 37-72.
48. Vega-Palas, M.A., E. Flores, and A. Herrero, *NtcA, a global nitrogen regulator from the cyanobacterium Synechococcus that belongs to the Crp family of bacterial regulators.* Mol. Microbiol., 1992. **6**(13): p. 1853-1859.
49. Videau, P., et al., *Expanding the direct HetR regulon in Anabaena sp. strain PCC 7120.* J. Bacteriol., 2014. **196**(5): p. 1113-1121.
50. Videau, P., et al., *Expanding the direct HetR regulon in Anabaena sp. strain PCC 7120.* Journal of bacteriology, 2014. **196**(5): p. 1113-1121.

51. Videau, P., et al., *The heterocyst regulatory protein HetP and its homologs modulate heterocyst commitment in Anabaena sp. strain PCC 7120.* Proceedings of the National Academy of Sciences, 2016. **113**(45): p. E6984-E6992.
52. Wolk, C.P., *Movement of carbon from vegetative cells to heterocysts in Anabaena cylindrica.* J. Bacteriol., 1968. **96**: p. 2138-2143.
53. Wolk, C.P., *Heterocyst formation.* Annu. Rev. Genet., 1996. **30**: p. 59-78.
54. Wolk, C.P., *Heterocyst formation in Anabaena*, in *Prokaryotic Development*, Y.V. Brun and L.J. Shimkets, Editors. 2000, American Society for Microbiology Press: Washington, DC. p. 83-104.
55. Wolk, C.P., A. Ernst, and J. Elhai, *Heterocyst metabolism and development*, in *The Molecular Biology of Cyanobacteria*, D.A. Bryant, Editor. 1994, Kluwer Academic Publishers: Dordrecht, The Netherlands. p. 769-823.
56. Wu, X., et al., *patS minigenes inhibit heterocyst development of Anabaena sp. strain PCC 7120.* J. Bacteriol., 2004. **186**: p. 6422-6429.
57. Yoon, H.-S. and J.W. Golden, *Heterocyst pattern formation controlled by a diffusible peptide.* Science, 1998. **282**: p. 935-938.
58. Yoon, H.-S. and J.W. Golden, *PatS and products of nitrogen fixation control heterocyst pattern.* J. Bacteriol., 2001. **183**: p. 2605-2613.
59. Zhang, C.-C., et al., *Heterocyst differentiation and pattern formation in cyanobacteria: a chorus of signals.* Mol. Microbiol., 2006. **59**(2): p. 367-375.
60. Zhang, L.-C., et al., *Existence of periplasmic barriers preventing green fluorescent protein diffusion from cell to cell in the cyanobacterium Anabaena sp. strain PCC 7120.* Mol. Microbiol., 2008. **70**: p. 814-823.
61. Zhang, L.C., et al., *Exploring the size limit of protein diffusion through the periplasm in cyanobacterium Anabaena sp. PCC 7120 using the 13 kDa iLOV fluorescent protein.* Res Microbiol, 2013. **164**(7): p. 710-7.
62. Zhang, S. and D.A. Bryant, *The tricarboxylic acid cycle in cyanobacteria.* Science, 2011. **334**(6062): p. 1551-3.

Chapter 2. Regions of HetN That Contribute to Inhibitory Function

Introduction

To better understand if HetN is acting as a morphogen, the active regions or residues of the protein should be defined. Previous studies have identified areas of interest that warrant more rigorous scrutiny. Specific areas of study in this work were the domains of the protein defined by hydrophobicity, predicted residues involved in ketoacyl reductase function, an RGSGR motif similar to that found in PatS, and residue 131, which occurs immediately upstream of the RGSGR motif.

HetN can be divided into four domains based on hydrophobicity. An N-terminal hydrophobic domain with the properties of a signal sequence occurs at amino acids 1-46; an N-terminal hydrophilic domain containing the RGSGR and catalytic triad motifs occurs at amino acids 47-176; a second hydrophobic domain consistent with a membrane spanning domain occurs at amino acids 177-196; and a C-terminal hydrophilic domain occurs at amino acids 197-287 (Fig. 5A) [14]. To determine which domain(s) are required, five alleles of HetN were created. Each of the four domains described above was individually deleted, and a fifth allele lacking residues 47-128 was also created. This latter allele encoded a protein that lacks most of the internal hydrophilic domain but has both the RGSGR and ketoacyl reductase residues. The five alleles were overexpressed in the wild-type to determine if inhibitory protein is being produced. The alleles were also used to replace the native copy of *hetN* in the chromosome to determine the domain(s) required for patterning.

To determine if the five mutant alleles of *hetN* are capable of producing an inhibitory protein they were individually expressed from a copper inducible promoter, P_{petE}, on a multi-copy replicative plasmid in the wild-type [5, 6]. After 24 hours of growth in N- medium the filaments were viewed under a light microscope and the presence and abundance of heterocysts was determined.

As a positive control, full-length *hetN* was placed on the same vector to ensure that functional inhibitor is being produced as evidenced by suppression of heterocysts in N- conditions. As a negative control, the parent vector was introduced into the wild-type and its impact on heterocyst differentiation in N- conditions was determined. The negative control should result in the formation of a wild-type number of heterocysts. The comparisons between the controls and the mutant alleles determined if inhibitory protein was being produced.

To determine which domain(s) of *hetN* are required to produce the characteristic periodic pattern of heterocysts elaborated by the wild-type, the above five alleles were used to individually replace native *hetN* in the chromosome. The alleles were introduced into strain UHM150 (Δ*hetN*) at the native locus [14]. The resulting strains avoided any complications with plasmid copy number or transcriptional activation because the alleles were present at a native copy number, under the control of the native promoter, at the native locus. To ensure the introduction approach is a viable method native *hetN* was also introduced to UHM150. This strain displayed a wild-type phenotype in N- conditions. The phenotypes produced by the five mutants were compared to wild-type, UHM150, and the native *hetN* introduction strain to determine the domain(s) required for pattering.

In addition to the multi-residue domains of HetN, specific residues of HetN located within the catalytic triad of ketoacyl reductase function or the RGSGR motif were altered to assess their potential function in inhibition or patterning of heterocysts. Based on the amino acid sequence of HetN, the protein is predicted to have ketoacyl reductase function. These enzymes are known to catalyze fatty acid biosynthesis and are involved with production of the cell wall, in addition to other cellular functions. Ketoacyl reductases have conserved amino acids at their catalytic sites. The conserved catalytic residues in HetN are S142, Y155, and K159. HetN is produced in mature heterocysts and could be involved in maintaining a microoxic environment required for nitrogen fixation.

To determine if the predicted ketoacyl reductase activity of HetN is important for inhibitory function, three mutant alleles, each encoding one of the conservative substitutions S142A, Y155F, and K159R, were created. As for the domain-deletion alleles, these substitution alleles were introduced, via double-homologous recombination of a suicide vector, into UHM150 (Δ*hetN*). The resulting strains had their phenotypes determined after 48 hours of growth in N- conditions. The phenotypes were compared to those of the wild-type, UHM150, and a positive control strain in which native *hetN* was re-introduced to its native locus. The comparative phenotypes were used to determine if the ketoacyl reductase activity of HetN is important for inhibitory and/or patterning function.

PatS has been defined as a morphogen, and the RGSGR sequence within the protein has been identified as the source of its inhibitory function. HetN is one of four proteins within the *Anabaena* genome that contains an RGSGR sequence [23]. However when all3299 and orf77 were deleted from the genome differentiation was not affected

[23] unlike the Mch phenotype produced by a *hetN* or *patS* mutant [2]. The implied function of HetN as an inhibitor and the conflicting results found in previous studies suggest that more work is required to determine the developmental importance of the RGSGR sequence in HetN.

To determine if the RGSGR sequence of HetN is important for inhibitory function, five mutant alleles, each encoding one of the conserved substitutions R132K, G133A, S134A, G135A, and R136K were created. The alleles were introduced, via double-homologous recombination of a suicide vector, into UHM150 (Δ*hetN)*. The resulting strains were observed after 48 hours of growth in N- conditions. The phenotypes were compared to the wild-type, UHM150, and a positive control strain where native *hetN* was re-introduced into UHM150. The comparative phenotypes were used to determine the importance of the RGSGR sequence to the inhibitory function of HetN.

The similarity in amino acid sequence between PatS and HetN is not limited to the RGSGR sequence. The shared amino acid sequence of both proteins extends one residue more to ERGSGR. The position of the sequence within each protein is very different, being found at positions 12-17 of the 17aa PatS protein and positions 131-136 of the 287aa HetN protein. Previous work has shown that mutation of E12 of PatS to alanine produced a mutant with an increased number of heterocyst doublets, suggesting a potential role in PatS-dependent inhibition [9]. It has further been shown that the peptide ERGSGR (PatS-6) binds thirty times stronger to HetR than the peptide RGSGR (PatS-5) *in vitro* [11, 12]. Substitution of the glutamine residue with an aspartate, lysine, or glycine did not alter binding affinity, while HetR bound to residues consistent with PatS-7 (DERGSGR) and PatS-8 (CDERGSGR) 1200 times less than PatS-6 and at

undetectable levels, respectively [11]. The previous findings suggest that more work is required to determine the developmental importance of the glutamate at position 131 of HetN.

To determine if the glutamate at position 131 of HetN contributes to the HetN-dependent inhibitory function the residue was individually mutated to alanine, leucine, or glutamine. The alleles were introduced into strain UHM150 (Δ*hetN)* at the native *hetN* locus. The phenotypes produced by the three strains were compared to those of the wild-type and UHM150 to determine the involvement of E131 in the inhibitory function of HetN.

Materials and Methods

Culture conditions. *Anabaena* sp. PCC 7120 and its derivatives were grown in BG-11 medium as previously described [4]. Media were supplemented with neomycin at 45 μg ml^{-1} or spectinomycin and streptomycin at 2.5 μg ml^{-1} each as appropriate. *Escherichia coli* strains were grown in Luria-Bertani (LB) broth for liquid cultures and LB solidified with 15% agar for plate cultures. For selective growth, media were supplemented with 100 μg ml^{-1} spectinomycin, 50 μg ml^{-1} kanamycin, 100 μg ml^{-1} ampicillin or 10 μg ml^{-1} chloramphenicol.

To induce heterocyst formation, early exponential phase cultures grown in BG-11 were washed three times with BG-11 medium without combined nitrogen (BG-11_0), re-suspended in BG-11_0 without antibiotics, and incubated under growth conditions. To induce the copper inducible *petE* promoter, media were supplemented with 2 μM $CuSO_4$. Heterocyst percentages were determined by counting 300 cells or more and scoring

heterocysts as previously described [25]. These counts were done on three separate cultures, and the percentages reported are an average of the three counts.

Plasmid construction. Tables 1 and 2 list the plasmids and oligonucleotide primers, respectively, used in this study. Plasmid pDR382 is a suicide used to reintroduce the wild-type *hetN* to a *hetN*-deletion strain, recreating wild-type *Anabaena*. A 2129-bp fragment starting 747 bp upstream and ending 518 bp downstream of the *hetN*-coding region was amplified via PCR using wild-type *Anabaena* chromosomal DNA as template with the primers HetMF-BamHI and hetIR-SacI. The resulting fragment was cloned into the *Eco*RV site of pBluescript SK+ (Stratagene) as a blunt end fragment, and subsequently moved as a *Bam*HI-*Sac*I fragment using restriction sites introduced on primers into pRL277 [7] cut with *Bgl*II and *Sac*I to create pDR382.

Plasmids pCO100, pCO102, pCO103, pCO104, and pCO111 were used to create strains with an allele of *hetN* encoding proteins lacking a range of amino acids: Δ2-46, Δ47-176, Δ177-195, Δ196-287, and Δ47-128 respectively. The fragments used to create the domain deletions were amplified via overlap extension PCR using pDR382 as template. The outer primers used to create the constructs were PhetN-BamHI-F and pRL-SacI. The following were the internal primers used: hetN-(Δ2-46)-F and hetN-(Δ2-46)-R for pCO100; hetN-(Δ47-176)-F and hetN-(Δ47-176)-R for pCO102; hetN-(Δ177-195)-F and hetN-(Δ177-195)-R for pCO103; hetN-(Δ196-287)-F and hetN-(Δ196-287)-R for pCO104; and hetN-(Δ47-128)-F and hetN-(Δ47-128)-R for pCO111. The overlap extension PCR products were cloned as *Spe*I-*Sac*I fragments into pDR382, replacing the wild-type allele of *hetN*.

Plasmid pSMC187 is a mobilizable shuttle vector based on pAM505 [22], in which the *Eco*RI site was removed by restriction digest with *Eco*RI and blunt-ending with T4 polymerase followed by ligation. Plasmid pKH256 is a mobilizable shuttle vector based on pam505 containing the *petE* promoter and used to make transcriptional fusions to the promoter. A fragment containing P_{petE} was amplified via PCR using the primers PpetE-SacI-F and PpetE-EcoRI-BamHI-R and cloned into pSMC187 as a *Bam*HI-*Sac*I fragment to create pKH256.

Plasmid pCO110 is a shuttle vector based on pAM505 carrying the wild-type allele of *hetN* transcriptionally fused to the *petE* promoter. Wild-type *hetN* was amplified by PCR using *Anabaena* chromosomal DNA as template and the primers hetN-EcoR1 and hetN-BamH1-R. The PCR product was cloned as an *Eco*RI-*Bam*HI fragment into pKH256.

The plasmids pCO105, pCO107, pCO108, pCO109, and pCO113 are shuttle vectors based on pAM505 carrying *hetN* encoding the deletions Δ2-46, Δ47-176, Δ177-195, Δ196-287, and Δ47-128, respectively, transcriptionally fused to the *petE* promoter. The fragments used to make the *hetN* variants were amplified via overlap extension PCR. The outer primers used were hetN-EcoRI and hetN-BamHI-R. The following are the internal primers used: hetN-(Δ2-46)-F and hetN-(Δ2-46)-R for pCO105; hetN-(Δ47-176)-F and hetN-(Δ47-176)-R for pCO107; hetN-(Δ177-195)-F and hetN-(Δ177-195)-R for pCO108; hetN-(Δ196-287)-F and hetN-(Δ196-287)-R for pCO109; hetN-(Δ47-128)-F and hetN-(Δ47-128)-R for pCO113. The overlap extension products were cloned as *Eco*RI-*Bam*HI fragments into pKH256.

Plasmids pDR387, pDR388, pDR389, pDR390, pDR391, pDR392, pDR393, and pDR394 were used to reintroduce *hetN* alleles encoding R132K, G133A, S134A, G135A, R136K, S142A, Y155F, and K159R substitutions, respectively, to strain UHM150 (Δ*hetN*), replacing the wild-type *hetN* locus of *Anabaena*. The fragments used to make base substitutions were amplified via overlap extension PCR using pDR382 as a template [15]. The outer primers used to create the constructs were PhetN-BamHI-F and pRL-SacI. The following internal primers were used to make specific *hetN* alleles: R132K Fwd and R132K Rev for pDR387; G133A Fwd and G133A Rev for pDR388; S134A Fwd and S134A Rev for pDR389; G135A Fwd and G135A Rev for pDR390; R136K Fwd and R136K Rev for pDR391; S142A Fwd and S132A Rev for pDR392; Y155F Fwd and Y155F Rev for pDR393; and K159R Fwd and K159R Rev for pDR394. The overlap extension PCR products were cloned as *spe*I-*Sac*I fragments into pDR382, replacing the wild-type allele of *hetN*. The *spe*I site is naturally occurring in the upstream region of *hetN* amplified by PhetN-BamHI-F.

Plasmids pOR115 and pOR116 are suicide vectors based on pRL277 to introduce *hetN*(*E131A*) and *hetN*(E131L), respectively, at the native locus. The fragments used to make base substitutions were amplified via overlap extension PCR using pDR382 as a template. The outer primers used to create the constructs were PhetN-Bam-F and hetN-SacI-R. The internal primers used to make specific *hetN* alleles were HetN E->A Fwd and HetN E->A Rev for pOR115 and HetN E->L Fwd and HetN E->L Rev for pOR116. The overlap extension PCR products were cloned as a *Spe*I-*Sac*I fragments into pDR382, replacing the wild-type allele of *hetN*.

Plasmid pPJAV369 is a suicide vector based on pRL277 to introduce *hetN*(*E131Q*) at the native locus. The fragment used to make the base substitution was amplified via overlap extension PCR using pDR382 as a template. The outer primers used to create the construct were PhetN-Bam-F and hetN SacI-R. The internal primers used to make the specific *hetN* allele were HetN E->Q Fwd and HetN E->Q Rev. The overlap extension PCR product was cloned as a *Spe*I-*Sac*I fragment into pDR382, replacing the wild-type allele of *hetN*.

Strain construction. Table 1 lists the strains used in this study. The *hetN* gene was cleanly deleted from the chromosome of *Anabaena* using allelic replacement as previously described [8] using plasmid pCCO103 to create strain UHM150. Allelic replacement was used with the following plasmids and strain UHM150 to create the following strains with altered alleles of *hetN* at the original *hetN* locus: pCO100 for UHM192; pCO102 for UHM209; pCO103 for UHM210; pCO104 for UHM211; pCO111 for UHM212; pDR387 for UHM202; pDR388 for UHM200; pDR389 for UHM203; pDR390 for UHM201; pDR391 for UHM204; pDR392 for UHM205; pDR393 for UHM206; pDR394 for UHM207; pOR115 for UHM352; pOR116 for UHM353; and pPJAV369 for UHM354. As a control to recreate wild-type *Anabaena*, pDR382 was introduced into UHM150 (Δ*hetN)* using the same technique to create strain UHM208. Strains were confirmed as double recombinants using the primers up-hetN-F and down-hetN-R.

Microscopy. Cells were routinely viewed and imaged as previously described [3]. All images were processed in Adobe Photoshop CS2.

Table 1. Strains and Plasmids used in Chapter 2

Strain or Plasmid	Relevant Characteristic(s)*	Source or Reference
***Anabaena* sp. strains**		
PCC 7120	Wild-type	Pasteur Culture Collection
UHM150	Δ*hetN*	[14]
UHM192	*hetN*(Δ2-46)	This study
UHM200	*hetN*(G133A)	This study
UHM201	*hetN*(G135A)	This study
UHM202	*hetN*(R132K)	This study
UHM203	*hetN*(S134A)	This study
UHM204	*hetN*(R136K)	This study
UHM205	*hetN*(S142A)	This study
UHM206	*hetN*(Y155F)	This study
UHM207	*hetN*(K159R)	This study
UHM208	UHM150 with *hetN* reintroduced	This study
UHM209	*hetN*(Δ47-176)	This study
UHM210	*hetN*(Δ177-195)	This study
UHM211	*hetN*(Δ196-287)	This study
UHM212	*hetN*(Δ47-128)	This study
UHM352	*hetN*(*E131A*)	This study
UHM353	*hetN*(*E131L*)	This study
UHM354	*hetN*(*E131Q*)	This study
Plasmids		
pAM505	Shuttle vector for replication in *E. coli* and *Anabaena*; Km^r Nm^r	[22]
pRL277	Suicide vector; Sm^r Sp^r	[7]
pDR382	pRL277 used to make UHM208	This study
pDR387	pRL277 used to make UHM202	This study
pDR388	pRL277 used to make UHM200	This study
pDR389	pRL277 used to make UHM203	This study
pDR390	pRL277 used to make UHM201	This study
pDR391	pRL277 used to make UHM204	This study
pDR392	pRL277 used to make UHM205	This study
pDR393	pRL277 used to make UHM206	This study
pDR394	pRL277 used to make UHM207	This study
pKH256	pAM505 with P_{petE}	This study
pCO100	pRL277 used to make UHM192	This study
pCO102	pRL277 used to make UHM209	This study
pCO103	pRL277 used to make UHM210	This study
pCO104	pRL277 used to make UHM211	This study
pCO105	pAM505 with P_{petE}-*hetN*(Δ2-46)	This study
pCO107	pAM505 with P_{petE}-*hetN*(Δ47-176)	This study

Table 1 continued.

pCO108	pAM505 with P_{petE}-*hetN*(Δ177-195)	This study
pCO109	pAM505 with P_{petE}-*hetN*(Δ196-287)	This study
pCO110	pAM505 with P_{petE}-*hetN*	This study
pCO111	pRL277 used to make UHM212	This study
pCO113	pAM505 with P_{petE}-*hetN*(Δ47-128)	This study
pSMC187	pAM505 with the *Eco*RI site removed	This study
pOR115	pRL277 to make UHM352	This study
pOR116	pRL277 to make UHM353	This study
pPJAV369	pRL277 to make UHM354	This study

*Km, kanamycin; Nm, neomycin; Sm, streptomycin; Sp, spectinomycin

Table 2. Oligonucleotide primers used in Chapter 2

Oligonucleotide*	Sequence
HetMF-BamHI	GGATCCTAGAACGCTGGTCTGATGAACAA
hetIR-SacI	GAGCTCTGGAACCAGGGCAAGTTAAATTT
PhetN-BamHI-F	ATATAGGATCCAGGAGAAGACGCGATGAATC
pRL-SacI	TGTAGATAACTACGATACGG
hetN-(Δ2-46)-F	GGTTACAATGTGTAATGCGGTTAAGGCTGC
hetN-(Δ2-46)-R	CCGCATTACACATTGTAACCTGCTAGTCTC
hetN-(Δ47-176)-F	AGCCCAAACGGGTGTCAACATTTCGGTGGTTTG
hetN-(Δ47-176)-R	TGTTGACAGCCGTTTGGGCTAATCCTGATTG
hetN-(Δ177-195)-F	AGTTGGTACTGATACTCGTGTCTCTGCGCC
hetN-(Δ177-195)-R	CACGAGTATCAGTACCAACTAATTCCTGAC
hetN-(Δ196-287)-F	GATGACTGTTTGACTCCGCAGTTGCTTAGGGAATG
hetN-(Δ196-287)-R	AACTGCGGAGTCAAACAGTCATCCCAGTTTG
hetN-(Δ47-128)-F	AGCCCAAACGATGATGGAACGCGGTAGTG
hetN-(Δ47-128)-R	GTTCCATCATCGTTTGGGCTAATCCTGATTG
PpetE-SacI-F	ATATAGAGCTCGCTGAGGTACTGAGTACACAGC
PpetE-EcoRI-BamHI-R	ATAGGATCCGAATTCTCCTAACCTGTAG
hetN-EcoRI	ATATAGAATTCTATGACAACTCTTACAGGTAAG
hetN-BamHI-R	ATATAGGATCCTCATGAGCGATGAGACTCAAC
R132K Fwd	AGCATGATGGAAAAGGGTAGTGGTCGGATTGTCAAT
R132K Rev	CCGACCACTACCCTTTTCCATCATGCTGGGTAGTAAC
G133A Fwd	ATGATGGAACGCGCTAGTGGTCGGATTGTCAATATTG
G133A Rev	AATCCGACCACTAGCGCGTTCCATCATGCTGGGTAG
S134A Fwd	GTCAATATTGCTGCTTTAGCTGGTAAAAAGGGCG
S134A Rev	GACAATCCGACCAGCACCGCGTTCCATCATGCTGG
G135A Fwd	GAACGCGGTAGTGCTCGGATTGTCAATATTGCTTC
G135A Rev	ATTGACAATCCGAGCACTACCGCGTTCCATCATGC
R136K Fwd	GCGGTAGTGGTAAGATTGTCAATATTGCTTCTTTAG
R136K Rev	AATATTGACAATCTTACCACTACCGCGTTCCATC
S142A Fwd	GTCAATATTGCTGCTTTAGCTGGTAAAAAGGGCG
S142A Rev	TTTACCAGCTAAAGCAGCAATATTGACAATCCGACC
Y155F Fwd	TTCAACAGCGTTTTCTCAGCTAGCAAGGCAGGTTTG
Y155F Rev	CTTGCTAGCTGAGAAAACGCTGTTGAAAGCAACGC
K159R Fwd	TACTCAGCTAGCAGAGCAGGTTTGATTATGTGGAC
K159R Rev	AATCAAACCTGCTCTGCTAGCTGAGTAAACGCTG
hetN-SacI-R	ATATAGAGCTCTCATGAGCGATGAGACTCAAC
HetN E->A Fwd	GCATGATGGCACGCGGTAGTGGTCGGATTG
HetN E->A Rev	CAATCCGACCACTACCGCGTGCCATCATGC
HetN E->L Fwd	GCATGATGCTACGCGGTAGTGGTCGGATTG
HetN E->L Rev	CAATCCGACCACTACCGCGTAGCATCATGC
HetN E->Q Fwd	GCATGATGCAACGCGGTAGTGGTCGGATTG
HetN E->Q Rev	CAATCCGACCACTACCGCGTTGCATCATGC
Up-hetN-F	GAGCTCGGCAAGCAGAGTTAATC
Down-hetN-R	GGATCCGCCCATTAATATAAGTCTC

Table 2 continued.

HetN E->Q Fwd	GCATGATGCAACGCGGTAGTGGTCGGATTG
HetN E->Q Rev	CAATCCGACCACTACCGCGTTGCATCATGC
PhetN-Bam-F	ATATAGGATCCAGGAGAAGACGCGATGAATC
hetN SacI-R	CGCCGAGCTCGCTGCTATTAACCTTGCAAAGTTC

*Oligonucleotides are shown in the 5' to 3' direction

Results

Domain(s) required for HetN-dependent inhibitory function. To identify the domains of HetN that are necessary for its suppression of heterocyst differentiation, alleles of *hetN* coding for protein that lacks one of the four domains were overexpressed from the copper inducible *petE* promoter on a replicating plasmid introduced to wild-type *Anabaena*. Strains containing alleles encoding deletions of the N-terminal hydrophobic domain (Δ2-46), central hydrophobic domain (Δ177-195), and C-terminal hydrophilic domain (Δ197-287) behaved the same way as those containing the wild-type allele and did not produce heterocysts (Fig. 5B). Conversely, *Anabaena* containing an allele of *hetN* encoding a deletion of the N-terminal hydrophilic domain (Δ47-176) formed a number and pattern of heterocysts similar to the negative control, the same strain containing the empty shuttle vector pAM505 (Fig. 5B). A fifth allele of *hetN* encoding protein with a partial deletion of the N-terminal hydrophilic domain was also constructed and tested for its ability to suppress differentiation. An allele encoding protein with deletion of residues 47-128, three amino acids before the RGSGR motif, fully suppressed differentiation of heterocysts (Fig. 5B)[14]. The results indicate that the inhibitory function of HetN is present in the N-terminal hydrophilic domain between residues 129-176.

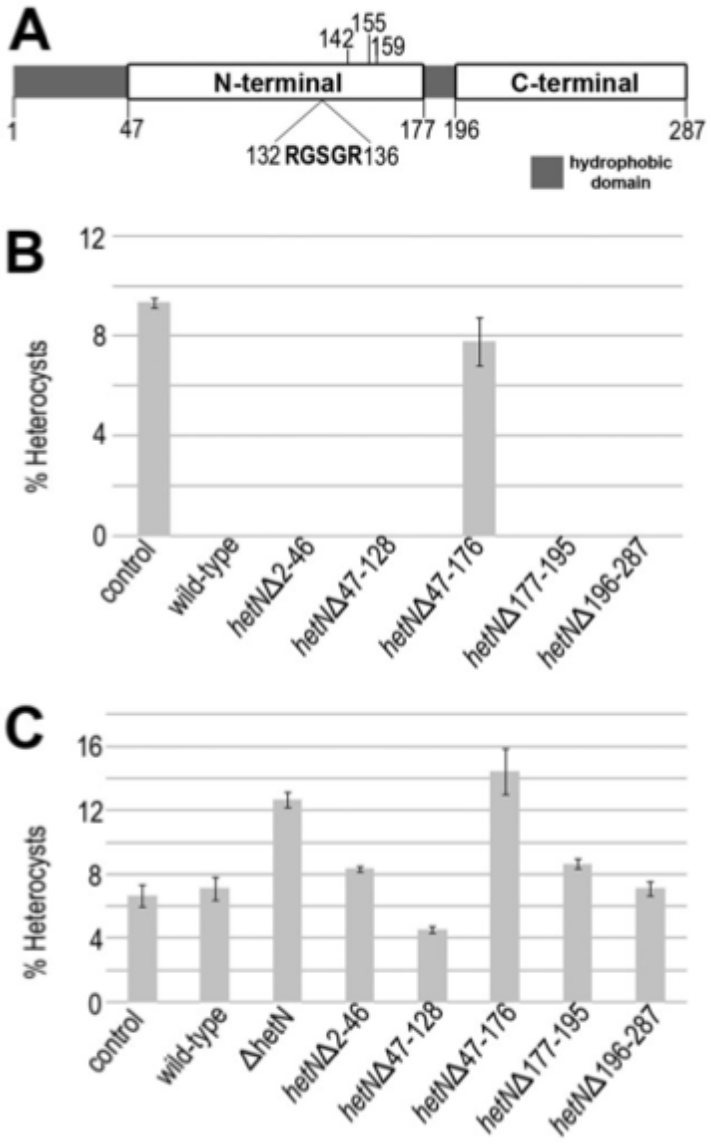

Figure 5: Domain(s) responsible for HetN's inhibitory function. Schematic depicting the domains based on hydrophobicity, RGSGR sequence, and putative ketoacyl reductase catalytic residues of HetN (A). Heterocyst percentages for *Anabaena* carrying the control plasmid pKH256, pKH256 with wild-type *hetN* and pKH256 carrying the indicated alleles of *hetN* (B). Heterocyst percentages for strains wild-type *Anabaena*; strain UHM208, which has wild-type *hetN* reintroduced into the native locus of the Δ*hetN* strain UHM150; strain UHM150; and strains with the indicated *hetN* alleles (C). Percent heterocysts where determined after 24 h (B) and 48 h (C) of growth in N- conditions. Error bars represent standard error of the mean.

To identify regions of HetN that are necessary for heterocyst patterning, strains with one of the alleles of *hetN* tested above in place of the wild-type chromosomal *hetN* gene were created and heterocyst patterning was examined. Strains containing alleles encoding deletions of the N-terminal hydrophobic domain (Δ2-46), central hydrophilic domain (Δ177-195), and C-terminal hydrophilic domain formed a pattern of heterocysts similar to that of the wild-type (Fig 5C) [14]. The strain containing the allele encoding the deletion of the N-terminal hydrophilic domain (Δ47-176), which includes the RGSGR motif and the catalytic site for ketoacyl reductase function, differentiated a pattern and number of heterocysts similar to the *hetN*-deletion strain UHM150. The fifth allele of *hetN* encoding protein with a partial deletion of the N-terminal hydrophilic domain (Δ47-128) differentiated 4.6% individual heterocysts separated by regions of vegetative cells (Fig. 5C). This strain formed fewer heterocysts than the wild-type, indicating that this allele has an increased ability to suppress differentiation.

Contribution of the RGSGR motif and ketoacyl reductase function to HetN-dependent inhibitory function. Previous studies on suppression of heterocyst differentiation with mutant alleles of *hetN* suggest that the RGSGR motif and not the putative catalytic site of HetN is involved in the regulation of heterocyst differentiation [14]. However, expression of *hetN* from the *petE* promoter on a multicopy plasmid likely results in much higher expression of *hetN* than in normally found in the wild-type, potentially compensating for reduced activity of some of the substituted proteins. In addition, the patterned expression of *hetN* from its native promoter is lost with the *petE* promoter. To examine heterocyst patterning and number in strains with the mutant alleles of *hetN*, strains were created that had a wild-type genotype except for a change in the

chromosome of one or two nucleotides that corresponded to one of the amino acid substitutions: R132K, G133A, S134A, G135A, R136K, S142A, Y155R, and K159R. Strains were created by re-introduction of the mutant alleles of *hetN* to the *hetN*-deletion strain, UHM150. In wild-type and the strain with the wild-type allele of *hetN* reintroduced to UHM150, 7.1% and 6.9% of cells were heterocysts, respectively, 48 h after the removal of combined nitrogen (Fig. 6A and B). These heterocysts occurred as single heterocysts flanked on each side by groups of vegetative cells (Fig. 6B). In the *hetN*-deletion strain, UHM150, 12.2% of the cells were heterocysts, and heterocysts were often found in groups of 2, 3, or more contiguous heterocysts, indicative of the Mch phenotype (Fig. 6A and C). In strains with alleles of *hetN* encoding one of the S142A, Y155F, and K159R conservative substitutions in the putative catalytic site, 7.1%, 7.3% and 6.3% of the cells were heterocysts, respectively, arranged in a pattern similar to that of the wild-type (Fig 6A and D). Conversely, strains with alleles of *hetN* encoding R132K, G133A, S134A, G135A, and R136K conservative substitutions formed an average of 12.9%, 9.7%, 10.1%, 9.7%, and 11.9% heterocysts respectively (Fig 6A, E and F). For each of these strains, heterocysts were often found in groups of 2, 3, or more, indicative of the Mch phenotype and similar to UHM150 (Fig. 6). These results indicate that each of the amino acids of the RGSGR motif and not those of the putative catalytic site of HetN is necessary for differentiation of the number and pattern of heterocysts found in the wild-type organism.

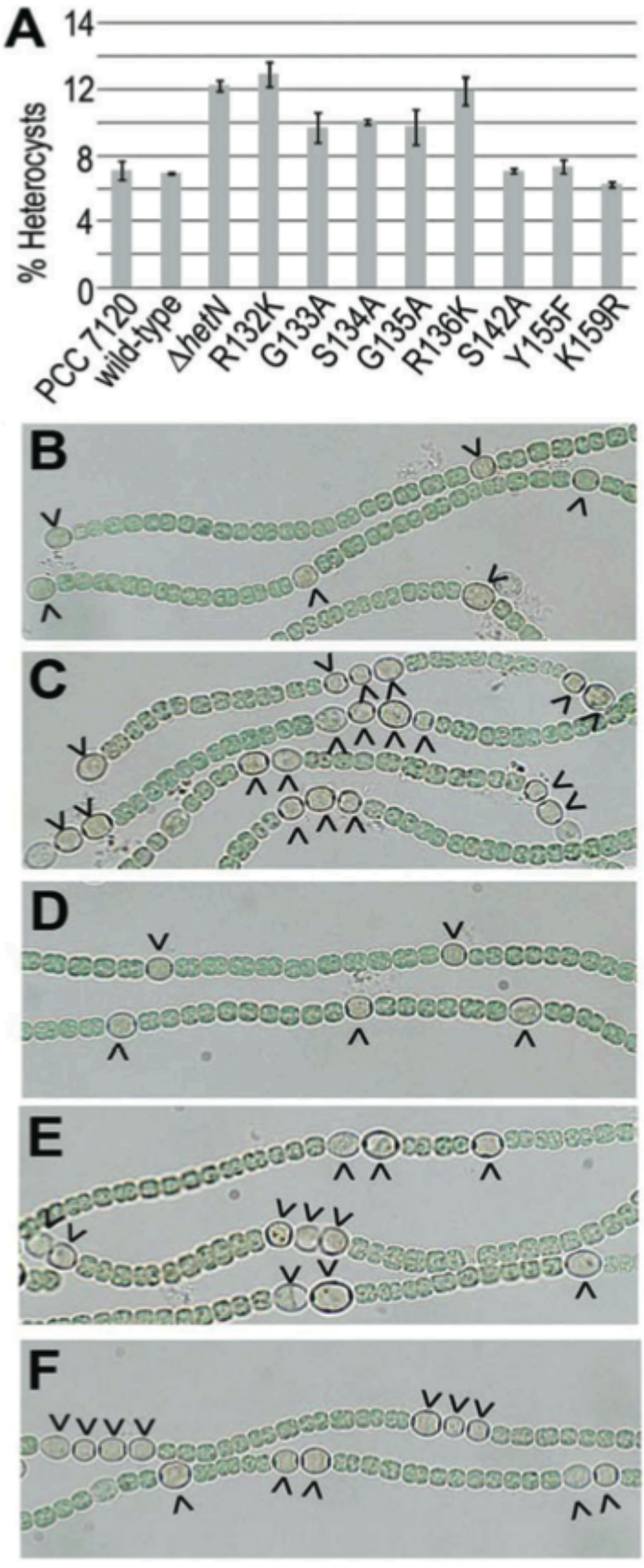
A
14
12
8
4
0
% Heterocysts
PCC 7120 wild-type
ΔhetN
R132K
G133A
S134A
G135A
R136K
S142A
Y155F
K159R
B
C
D
E
F

Figure 6: Determine the importance of ketoacyl reductase activity and the RSGSR sequence to the inhibitory function of HetN. Heterocyst percentages for strains wild type *Anabaena*, wild type *hetN* reintroduced to a Δ*hetN* strain, a Δ*hetN* strain UHM150, and strains with the indicated chromosomal alleles (A). brightfield images of wild type *Anabaena* (B); UHM150 which is Δ*hetN* (C);UHM207, which is *hetN*(K159R) (D); UHM203, which is *hetN*(S134A) (E); and UHM201, which is *hetN*(G135A) (F). Micrographs were taken 48 h after the removal of combined nitrogen. Carets indicate heterocysts.

Contribution of the HetN(E131) residue to HetN-dependent inhibitory function. The glutamate at position 12 in PatS is also present in HetN at position 131 conserving a hexapeptide sequence, ERGSGR, in both proteins. To assess the contribution of glutamate 131 in HetN the residue was individually mutated to an alanine, leucine, or glutamine.

When glutamate 131 in HetN was mutated to an alanine, E131A, or leucine, E131L, the resulting strains produced 13.6 ± 0.6 and 15 ± 0.6 percent heterocysts after 48 h of growth on N- medium, respectively (Figure 7, Table 3). A one-way ANOVA followed by a post-hoc Tukey HDS test indicated that both phenotypes are significantly different from the wild-type and the *hetN* mutant, UHM150, which differentiated 9.47 ± 0.31 and 16.2 ± 0.2 percent heterocysts after 48H of growth in N-, respectively (Fig. 7, Table 3, Table 4). Both E131A and E131L displayed Mch phenotypes similar to UHM150, while the wild-type did not (Table 3). The increased percentage of heterocysts and the presence of an Mch phenotype in both E131A and E131L suggest that glutamate 131 is important for HetN-dependent inhibitory function.

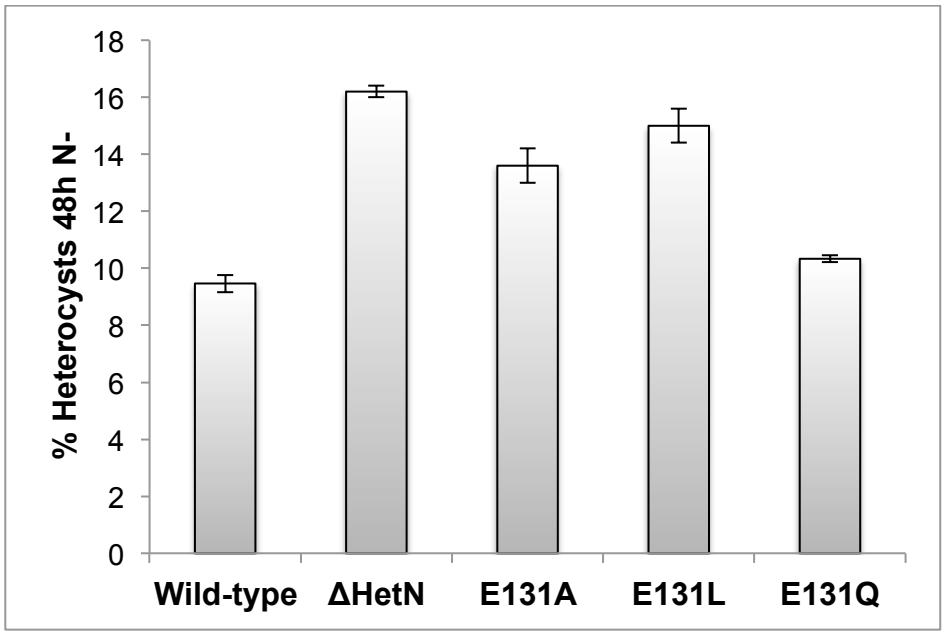

Figure 7: Determine the role of the E131 residue to the inhibitory function of HetN. Phenotypes were determined 48 h after the removal of combined nitrogen. The phenotype for each strain was determined in triplicate; error bars represent one standard deviation.

When glutamate 131 in HetN was mutated to glutamine, E131Q, the resulting strain produced 10.33 ± 0.12 percent heterocysts after 48H of growth on N- (Fig. 7, Table 3). A one-way ANOVA followed by a post-hoc Tukey HDS test indicated that the percentage of hertrocysts differentiated by E131Q is not significantly different from the wild-type (Table 4). However, the phenotype of E131Q is significantly different from UHM150 (Table 4). E131Q did not produce an Mch phenotype at any time. The percentage and arrangement of heterocysts differentiated by E131Q suggests that glutamate 131 of HetN may not contribute to HetN-dependent inhibitory function.

Table 3. Patterns of heterocysts produced by strains of *Anabaena*.

Strain (Genotype)	Hours N-	Heterocyst Percentage	Mean Vegetative Cell Interval	Heterocyst Occurrence
Wild-type	24	9.07 ± 0.31	10.3 ± 0.46	96 ± 1.73; 4 ± 1.73
	48	9.47 ± 0.31	11.5 ± 0.31	96.67 ± 1.53; 3.33 ± 1.53
	72	8.93 ± 0.23	12.7 ± 0.38	95.33 ± 0.58; 6.67 ± 0.58
UHM150 (Δ*hetN*)	24	9.47 ± 0.5	10.4 ± 0.32	88.33 ± 3.79; 10.67 ± 2.08 1 ± 1.73
	48	16.2 ± 0.2	5.9 ± 0.17	41.67 ± 2.08; 33.33 ± 4.04; 25 ± 4.36
	72	16.07 ± 0.12	6.1 ± 0.45	29 ± 1; 29.11 ± 2.08; 42 ± 2.52
UHM352 (Δ*hetN*(*E131A*))	24	9.33 ± 0.58	10.8 ± 0.48	96.33 ± 0.58; 3.67 ± 0.58
	48	13.6 ± 0.6	7 ± 0.52	63.33 ± 9.29; 25 ± 7.94; 11.67 ± 1.53
	72	15.53 ± 1.15	6.6 ± 0.33	47.67 ± 1.15; 32 ± 3.61; 20.33 ± 4.51
UHM353 (Δ*hetN*(*E131L*))	24	10.67 ± 1.01	8.5 ± 0.76	91.67 ± 4.62; 7.67 ± 4.16; 0.67 ± 1.15
	48	15 ± 0.6	6.5 ± 0.47	65.67 ± 4.62; 24.67 ± 7.57; 9.66 ± 3.06
	72	15.87 ± 0.76	5.8 ± 0.28	55.33 ± 2.52; 32 ± 1; 12.67 ± 2.08
UHM354 (Δ*hetN*(*E131Q*))	24	8.73 ± 0.7	11.8 ± 0.35	98 ± 1; 2 ± 1
	48	10.33 ± 0.12	9.1 ± 0.26	97.67 ± 1.53; 2.33 ± 1.53
	72	10.73 ± 0.31	8.3 ± 0.17	93.67 ± 1.53; 6.33 ± 1.53

At the indicated times following nitrogen stepdown, 500 cells were counted in triplicate and total heterocysts are presented as the mean ± the standard deviation. The presence of single (top line), double (second line), or multiple contiguous heterocysts (third line) was

determined for 300 heterocyst occurrences in triplicate and are presented as the average percent ± the standard deviation. The number of vegetative cell between heterocysts was counted for 300 intervals and is presented as the mean ± the standard deviation of the mean.

Table 4. Statistical analysis of UHM352, UHM353, and UHM354.

	wild-type	UHM150
ANOVA p-value	$1.09 * 10^{-6}$	$1.12 * 10^{-6}$
Strain:	post-hoc Tukey HSD p-value	post-hoc Tukey HSD p-value
UHM352 (*hetN*(E131A))	0.001	0.001
UHM353 (*hetN*(E131L))	0.001	0.041
UHM354 (*hetN*(E131Q))	0.168	0.001

One-way ANOVA with post-hoc Tukey HDS test comparing UHM352, UHM353, and UHM354 to the wild-type and UHM150 (Δ*hetN*). All phenotypes being compared were observed 48h after the removal of combined nitrogen (Table 3). Values written in green indicate a significant difference in the comparison being tested. Values written in red indicate no significant difference in the comparison being tested.

Discussion

HetN and PatS are required for different stages of heterocyst patterning. PatS is necessary for formation of the initial pattern of cells in a filament composed exclusively of vegetative cells that will differentiate after a transition to conditions that require diazotrophy for growth. A *hetN* mutant strain is capable of forming this *de novo* pattern whereas a *patS* mutant is not [8, 24]. HetN is necessary for stabilization of this initial pattern. The wild-type pattern of heterocysts initially formed in a *hetN* mutant becomes Mch after 48 hours [8]. Genetic and mathematical modeling evidence relating to placement of additional heterocysts between existing ones as vegetative cells divide to maintain the pattern and ratio of heterocysts to vegetative cells suggests that a HetN-dependent signal produced in mature heterocysts is responsible for specification of a region of cells at the midpoint between two heterocysts, and that PatS resolves this region to a single cell that will differentiate [13, 24, 26]. Despite the different roles of PatS and

HetN in patterning, the RGSGR motif is likely essential to the function of both. To take the analysis of HetN further, a single nucleotide or two corresponding to a codon in the RGSGR motif was changed in the chromosome of the wild-type. Each of the strains with an allele of *hetN* encoding a conservative substitution in one of the amino acids of the RGSGR motif resembled the *hetN*-deletion strain more than the wild-type and instead of a periodic pattern of single heterocysts, the Mch phenotype was observed. These results are comparable with those found with substitutions in PatS. In this case, a genetic selection identified four of the five amino acids of the RGSGR motif as necessary for suppression of differentiation [24]. A further study confirmed that all five amino acids in the RGSGR motif as well as E12 of PatS are required for proper differentiation and patterning [9]. In contrast, conservative substitutions in the putative ketoacyl reductase catalytic site had no effect on the function of HetN. The RGSGR motif of HetN and not the ketoacyl reductase activity is necessary for patterning of heterocysts.

Three previous studies have addressed the quality of HetN necessary for its ability to suppress heterocyst differentiation, with varied results. In the first, mutation of residues in the RGSGR sequence of HetN was reported to have no effect on the ability of HetN to suppress differentiation when the corresponding alleles of *hetN* were overexpressed [17]. In addition to R132K and R136L substitutions, the report states that G134S and S135D substitutions were made and had no effect. However, this is confusing because the HetN sequence is S134 and G135, not G134 and S135 as indicated, so what substitutions were actually made is unclear. In the second study, substitutions of one of the three amino acids in the predicted catalytic site for ketoacyl reductase activity in HetN prevented suppression of heterocyst differentiation by overexpression of the

corresponding mutant allele [19]. However, substitution of the other two had no effect. In the third study, overexpression of *hetN* was shown to cause post-translational decay of HetR, which presumably contributes to suppression of heterocyst formation. When the RGSGR motif was replaced by RGDAR, overexpression of the corresponding allele of *hetN* did not lower levels of HetR in filaments nor did it suppress differentiation, suggesting that the RGSGR motif is necessary for suppression [21]. The present study is the most comprehensive with respect to the regions of HetN that are necessary for inhibition and patterning. It clearly shows that the RGSGR motif of HetN and not the ketoacyl reductase activity is necessary for patterning of heteocysts within *Anabaena*.

The RGSGR motif as the primary functional group of HetN and PatS in patterning is consistent with known activities of HetN and PatS. In electrophoretic mobility shift assays the synthetic RGSGR peptide prevents the binding of HetR to a region of *hetR* promoter DNA that includes the auto-regulated transcriptional start point at position -271, and overexpression of *hetN* or *patS* prevents transcription from this start site [16, 20]. Isothermal titration calourimetry has shown synthetic RGSGR binds directly to HetR, while ERGSGR binds with 30 times greater affinity than RGSGR [11, 12]. Addition of RGSGR peptide to medium causes post-translational decay of HetR protein in whole filaments, as does overexpression of *hetN* or *PatS* in all cells of filaments [21]. Overexpression of *hetN* or *patS* in individual cells of filaments also causes decay of HetR in adjacent groups of cells, suggesting that the HetN- and PatS-dependent signal that moves from cell to cell contains the RGSGR sequence.

Individual deletions of the predicted signal sequence, internal hydrophobic domain, and the C-terminal hydrophilic domain had no effect on suppression of

differentiation or patterning. However, two pieces of evidence suggest that it is not solely the RGSGR motif of HetN that is necessary for normal suppression and patterning of heterocysts. First, it has been reported that a K159E substitution prevents the ability of HetN to suppress differentiation when overexpressed [18]. This non-conservative substitution of a positively charged amino acid with a negatively charged one, unlike the conservative K159R substitution used in the work presented here, apparently alters HetN sufficiently to prevent it from suppressing heterocyst formation. The second piece of evidence is the formation of fewer heterocysts by a strain with the wild-type *hetN* replaced with an allele encoding a deletion of amino acids 47-128, deleting a portion of the N-terminal hydrophilic domain up to three amino acids before the RGSGR sequence. The resulting protein appears to lead to the suppression of differentiation in a larger region of a filament than wild-type HetN. Possible explanations of this enhanced range of lateral inhibition include a more active form of the protein, a longer half-life, an increased rate of diffusion or increased production of the mature form of HetN that presumably is transferred between cells.

Despite sharing a functional protein motif, the forms of HetN and PatS that diffuse from cell to cell and interact with HetR may be different and remain unknown. Increased expression of *hetN* in cells that will become heterocysts around the time of commitment to differentiation is very different from that of *patS*, which occurs in groups of cells soon after induction of filaments to differentiate [1, 25]. The difference in expression patterns reflects the respective roles of HetN and patS in patterning. The involvement of two separate proteins with a similar functional motif, rather than one protein with two modes of expression, suggests that intrinsic differences in the mature

HetN- and PatS-dependent signals contribute to patterning. Mathematical models of heterocyst patterning with two inhibitors are consistent with this notion [26].

HetN and PatS share a further similarity within their amino acid sequence besides RGSGR. Both peptides share an ERGSGR sequence. A previous study reported that mutation of E12 in PatS increased the number of heterocyst doublets formed, indicating a contribution to PatS-dependent inhibitory activity [9]. Further work implicates the potential importance of E12 in PatS and E131 in HetN with the finding that synthetic ERGSGR binds to hetR with 30 times greater affinity than RGSGR and that the addition of further residues greatly decreases binding [11]. The current work examined the role of E131 of HetN with the production of three genetic mutants in which one or two nucleotides was mutated in the chromosome to produce strains encoding alanine at position 131, leucine at position 131, and glutamine at position 131 of HetN. When glutamate 131 in HetN was mutated to an alanine, E131A, or leucine, E131L, the resulting strains produced heterocysts in excess of the wild-type and filaments displayed an Mch phenotype after 48 h N-, consistent with the production of a protein with reduced function (Figure 7, Table 3). When glutamate 131 was mutated to glutamine, E131Q, the resulting strain produced a similar percentage of heterocyst as the wild-type and did not display an Mch phenotype at any time (Figure 7, Table 3). The discrepancy in phenotype of the three strains could be explained by the identity of the amino acids used to replace glutamine, a hydrophilic amino acid. Alanine and Leucine are both hydrophobic amino acids and are useful in determining if the relative size of the side chair present on a residue is important for protein function. Glutamine is a hydrophilic amino acid that could facilitate interactions that are vital to HetN function in a way more like glutamate

than alanine or leucine can. However, previous work showed no significant difference in the binding affinity between HetR and synthetic hexa-peptideds in which aspartate, lysine, or glycine replaced glutamine in ERGSGR [10]. The combined result suggests that E131 is likely present in the mature form of HetN that presumably moves from cell to cell and likely interacts with HetR during its role as an inhibitory morphogen responsible for heterocyst pattern maintenance.

References

1. Bauer, C.C., et al., *Subtracted cDNA libraries containing genes involved in heterocyst differentiation in the cyanobacterium Anabaena sp. strain PCC 7120.* to be submitted, 1995.
2. Black, T., A. and C.P. Wolk, *Analysis of a Het¯ mutation in Anabaena sp. strain PCC 7120 implicates a secondary metabolite in the regulation of heterocyst spacing.* J. Bacteriol., 1994. **176**: p. 2282-2292.
3. Borthakur, P.B., et al., *Inactivation of patS and hetN causes lethal levels of heterocyst differentiation in the filamentous cyanobacterium Anabaena sp. PCC 7120.* Mol. Microbiol., 2005. **57**: p. 111-123.
4. Buikema, W.J. and R. Haselkorn, *Characterization of a gene controlling heterocyst development in the cyanobacterium Anabaena 7120.* Genes Dev., 1991. **5**: p. 321-330.
5. Buikema, W.J. and R. Haselkorn, *Use of a copper-inducible promoter for the controlled expression of genes in the cyanobacterium Anabaena.* In preparation, 1995.
6. Buikema, W.J. and R. Haselkorn, *Expression of the Anabaena hetR gene from a copper-regulated promoter leads to heterocyst differentiation under repressing conditions.* Proc. Natl. Acad. Sci., U.S.A., 2001. **98**: p. 2729-2734.
7. Cai, Y. and C.P. Wolk, *Use of a conditionally lethal gene in Anabaena sp. strain PCC 7120 to select for double recombinants and to entrap insertion sequences.* J. Bacteriol., 1990. **172**: p. 3138-3145.
8. Callahan, S.M. and W.J. Buikema, *The role of HetN in maintenance of the heterocyst pattern in Anabaena sp. PCC 7120.* Mol. Microbiol., 2001. **40**: p. 941-950.
9. Corrales-Guerrero, L., et al., *Functional dissection and evidence for intercellular transfer of the heterocyst-differentiation PatS morphogen.* Mol. Microbiol., 2013. **88**(6): p. 1093-1105.
10. Feldman, E.A., et al., *Differential binding between PatS C-terminal peptide fragments and HetR from Anabaena sp. PCC 7120.* Biochemistry, 2012. **51**: p. 2436-2442.
11. Feldmann, E.A., et al., *Differential binding between PatS C-terminal peptide fragments and HetR from Anabaena sp. PCC 7120.* Biochemistry, 2012. **51**: p. 2436-2442.
12. Feldmann, E.A., et al., *Evidence for direct binding between HetR from Anabaena sp. PCC 7120 and PatS-5.* Biochemistry, 2011. **50**: p. 9212-9224.
13. Gerdtzen, Z.P., et al., *Modeling heterocyst pattern formation in cyanobacteria.* BMC Bioinformatics, 2009. **10**(Suppl 6): p. S16-S16.
14. Higa, K.C., et al., *The RGSGR amino acid motif of the intercellular signaling protein, HetN, is required for patterning of heterocysts in Anabaena sp. strain PCC 7120.* Mol. Microbiol., 2012. **83**: p. 682-693.
15. Higuchi, R., B. Krummel, and R.K. Saiki, *A general method of in vitro preparation and specific mutagenesis of DNA fragments: study of protein and DNA interactions.* Nucleic Acids Res., 1988. **16**: p. 7351-7367.

16. Huang, X., Y. Dong, and J. Zhao, *HetR homodimer is a DNA-binding protein required for heterocyst differentiation, and the DNA-binding activity is inhibited by PatS.* Proc. Natl. Acad. Sci. U.S.A., 2004. **101**(14): p. 4848-4853.
17. Li, B., X. Huang, and J. Zhao, *Expression of hetN during heterocyst differentiation and its inhibition of hetR up-regulation in the cyanobacterium Anabaena sp. PCC 7120.* FEBS Lett., 2002. **517**: p. 87-91.
18. Liu, J. and W.-L. Chen, *Characterization of HetN, a protein involved in heterocyst differentiation in the cyanobacterium Anabaena sp. strain PCC 7120.* FEMS microbiology letters, 2009. **297**(1): p. 17-23.
19. Liu, J. and W.L. Chen, *Characterization of HetN, a protein involved in heterocyst differentiation in the cyanobacterium Anabaena sp. strain PCC 7120.* FEMS Microbiol Lett, 2009. **297**(1): p. 17-23.
20. Rajagopalan, R. and S.M. Callahan, *Temporal and Spatial Regulation of the Four Transcription Start Sites of hetR from Anabaena sp. Strain PCC 7120.* J. Bacteriol., 2010. **192**(4): p. 1088-1096.
21. Risser, D.D. and S.M. Callahan, *Genetic and cytological evidence that heterocyst patterning is regulated by inhibitor gradients that promote activator decay.* Proc. Natl. Acad. Sci. USA, 2009. **106**(47): p. 19884-19888.
22. Wei, T.-F., R. Ramasubramanian, and J.W. Golden, *Anabaena sp. strain PCC 7120 ntcA gene required for growth on nitrate and heterocyst development.* J. Bacteriol., 1994. **176**: p. 4473-4482.
23. Wu, X., et al., *patS minigenes inhibit heterocyst development of Anabaena sp. strain PCC 7120.* J. Bacteriol., 2004. **186**: p. 6422-6429.
24. Yoon, H.-S. and J.W. Golden, *Heterocyst pattern formation controlled by a diffusible peptide.* Science, 1998. **282**: p. 935-938.
25. Yoon, H.-S. and J.W. Golden, *PatS and products of nitrogen fixation control heterocyst pattern.* J. Bacteriol., 2001. **183**: p. 2605-2613.
26. Zhu, M., S.M. Callahan, and J.A. Allen, *Maintenance of heterocyst patterning in a filamentous cyanobacterium.* J. Biol. Dyn., 2010. **4**: p. 621-633.

Chapter 3. The Subcellular Localization of HetN-YFP, its Ability to be Transported from Cell to Cell as a Full-Length Protein, and the Spatial Range of its Inhibitory Activity

Introduction

To better understand the localization of HetN and aid in determining the role of HetN as an inhibitory morphogen, fusions of HetN to yellow fluorescent protein (YFP) were expressed in cells of *Anabaena*. When grown with combined nitrogen, all cells of filaments have a low level of HetN in thylakoid and cytoplasmic membranes. Upon the removal of combined nitrogen, HetN is degraded [15], and after the formation of proheterocysts, expression of *hetN* is found in proheterocysts and heterocysts [4]. HetN contains a predicted signal sequence and predicted internal hydrophobic domain. The domains are consistent with the presence of HetN in both thylakoid and cytoplasmic membranes. The importance to inhibitory function of HetN's association to cellular membranes has not been defined.

To asses the viability of using a HetN-YFP fusion protein in further studies a 6-histadine tag was added to the C-terminus of HetN-YFP expressed in *Anabaena* and in *E. coli* strain BL 21 DE3, a strain designed for the expression of heterologous proteins lacking Lon and OmpT protease activity (New England BioLabs). Extracts from the two strains, and from wild-type *Anabaena*, were probed with an antibody specific to 6-histadines in order to ensure that a chimeric HetN-YFP protein was present within the *Anabaena* cells. Turbo YFP, the variant of YFP used here, is 234 aa with a molecular weight of 26 kDa. The size is comparable to that of HetN, being 287 aa with a molecular weight of 30.4 kDa. HetN-YFP(6-His) was imaged using laser scanning confocal microscopy to determine if the subcellular localization is consistent with that seen when

HetN-YFP, lacking the histadine tag, was expressed in *Anabaena*. The results indicated a stable HetN-YFP chimera was present in the *Anabaena* cells and determined the fusion protein is appropriate for use in further studies.

The localization of a protein within a cell can be used to elucidate the proteins function. To determine the subcellular localization of HetN a translational fusion using YFP was introduced into wild-type and UHM163, *hetR*(R250K), on a multi-copy plasmid. HetN-YFP was expressed from the *petE* promoter in both wild-type and UHM163, and from the native *hetN* promoter in UHM163. UHM163 is used here because this strain differentiates heterocysts in the presence of excess inhibitor. Cultures were grown in N+ and N- conditions, and the fluorescent signal from HetN-YFP was visualized using laser scanning confocal microscopy. The subcellular localization of HetN-YFP in both vegetative cells and heterocysts suggests a role in cell wall synthesis.

HetN has four predicted domains based on the hydrophobicity of HetN's amino acids. To determine the contribution of the domains to the subcellular localization of HetN, C-terminal translational fusions to YFP were constructed. The constructs were introduced on a multi-copy plasmid to wild-type and UHM163 before visualization of N+ and N- cultures under a laser scanning confocal microscope. The presence and localization of YFP within the two strains indicated that any truncation of HetN abrogates the localization or presence of detectable HetN-YFP.

HetN as an inhibitory morphogen implies that HetN be produced in source cell(s) and moves away from those cell(s) in order to determine the developmental fate of adjacent cells. This requirement as a function of HetN could be abrogated by the fusion of HetN to YFP. The fusion of PatS to green fluorescent protein (GFP) results in a

nonfunctional protein [29] that is potentially confined to source cells when proper patterning requires movement of the inhibitor into cells adjacent to the source [30]. In order to establish if HetN-YFP retains its function as an inhibitor fluorescence recovery after photobleaching (FRAP) and mosaic filament experiments were utilized.

The fluid mosaic nature of the cellular membrane allows for the movement of membrane associated proteins throughout the cell. The cellular membranes of the adjacent cells within *Anabaena* filaments are not contiguous so do not facilitate the transport of HetN between cells. However, HetN could move from cell to cell associated within the membrane present in an undefined vesicle transport system.

To determine if HetN-YFP associates with the cellular membranes and moves from cell to cell as a membrane associated protein a FRAP experiment was utilized. A small region of the cellular membrane of a single *Anabaena* cell expressing HetN-YFP was bleached and the ability of unbleached HetN-YFP to diffuse back into the bleached region was observed. It is expected that if HetN-YFP associates with the cellular membrane than protein should diffuse within the membrane of the cell and YFP fluorescence will be detected in the bleached region after a short period of time. To observe if full-length HetN-YFP moves from cell to cell an entire cell expressing HetN-YFP was bleached and the ability of HetN-YFP from adjacent cells to be transported to the bleached cell was observed.

To determine if full-length HetN-YFP expressed in source cells can move away from the source a mosaic filament was created. Cerulene fluorescent protein (CFP) and HetN-YFP were simultaneously expressed from a replicative plasmid in wild-type and viewed 72 hours post-conjugation. The predicted outcomes are that CFP fluorescence and

YFP fluorescence will be in the same cell(s), indicating that full-length HetN-YFP is confined to source cell(s), or that YFP fluorescence will be detected in cells lacking CFP fluorescence, indicating that full-length HetN-YFP is not confined to source cell(s) (Fig. 12A).

To determine if confinement of HetN-YFP to source cells also confines the HetN-dependent inhibitory signal a second mosaic filament was created. HetN-YFP was expressed from a replicative plasmid in strain UHM191, Δ*patA* Δ*hetF PpetE-hetR*-CFP, and viewed 72 hours post-conjugation. CFP fluorescence marked the presence of HetR in cells. A lack of CFP fluorescence indicated a lack of hetR, consistent with HetN-dependent inhibitory activity [24]. YFP fluorescence labeled the location of full-length HetN-YFP. The predicted outcomes are YFP fluorescence and CFP fluorescence will be detected in adjacent cells, indicating that no inhibitory signal is produced from HetN-YFP, or YFP fluorescence and CFP fluorescence will not be detected in adjacent cells, indicating that confinement of HetN-YFP does not confine the HetN-dependent inhibitory signal (Fig. 8). The non-fluorescing cells represent the range that was traveled by the inhibitor and is defined as the signal range (Fig. 8). The signal ranges produced by HetN and HetN-YFP were compared to determine any significant difference.

As a negative control YFP was expressed from a replicative plasmid in UHM191 and viewed 72 hours post-conjugation. The predicted result is that CFP fluorescence will be detected in all cells and YFP fluorescence will be detected in a subset of those same cells, indicating that the introduction of a plasmid expressing the YFP fluorophore alone does not change the pattern of CFP fluorescence present in UHM191.

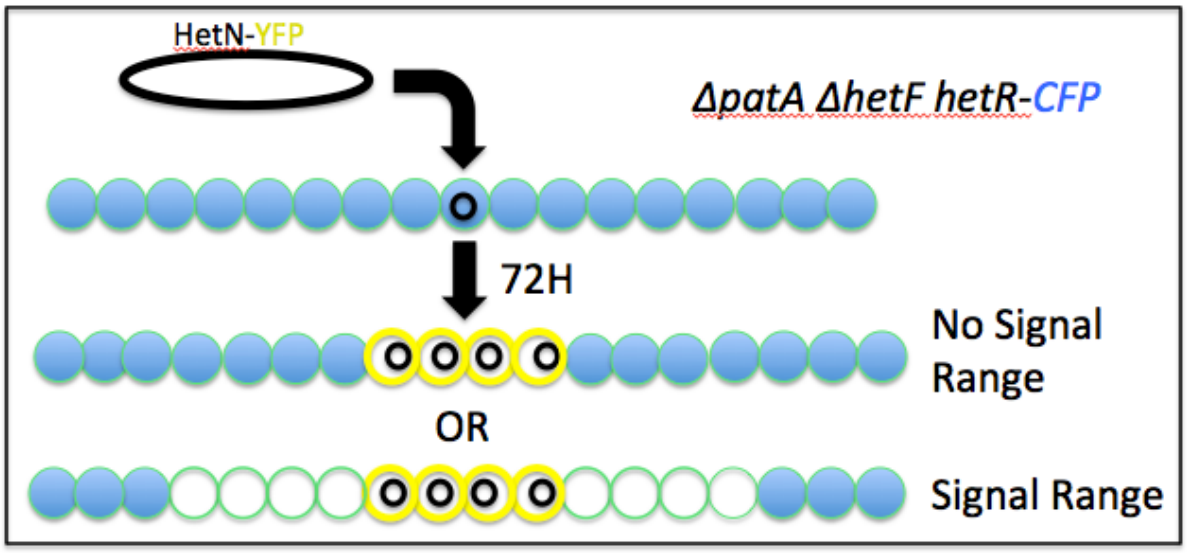

Figure 8: Determining the spatial range of HetN-YFP's inhibitory function. Schematic of the two expected outcomes when a plasmid carrying HetN-YFP is observed 72 hours after its introduction into UHM191, *ΔpatA ΔhetF hetR-CFP*, during a mosaic filament experiment. HetN-YFP could be confined to source cells, indicated by the presence of CFP in cells adjacent to those expressing HetN-YFP, producing no signal range, or HetN-YFP could produce a signal range while it's self being confined to source cells, indicated by a lack of CFP in cells adjacent to those expressing HetN-YFP.

Materials and Methods

Culture conditions. *Anabaena* sp. PCC 7120 and its derivatives were grown in BG-11 medium containing 17.6 mM nitrate as previously described [2]. Media were supplemented with neomycin at 45 μg ml^{-1} or spectinomycin and streptomycin at 2.5 μg ml^{-1} each as appropriate. *Escherichia coli* strains were grown in Luria-Bertani (LB) broth for liquid cultures and LB solidified with 15% agar for plate cultures. For selective growth, media were supplemented with 50 μg ml^{-1} kanamycin. To induce the copper inducible *petE* promoter, media were supplemented with 2 μM $CuSO_4$. Plasmids were conjugated from *E. coil* to *Anabaena* as previously described [8]. Genetic mosaic filaments were created as previously described [22].

Plasmid construction. Plasmids and oligonucleotide primers used in this study are described in Tables 5 and 6, respectively. Plasmids pCO115, pCO117, pCO118, and pCO121 are mobilizable shuttle vectors containing P_{petE}-*hetN*(Δ2-46), P_{petE}-*hetN*(Δ47-176) P_{petE}-*hetN*(Δ177-195), and P_{petE}-*hetN*(Δ47-128), respectively, translationally fused to YFP. The fragment used to make the mutant alleles of *hetN* were amplified via PCR using pCO105, pCO107, pCO108, and pCO113 as templates, respectively. The primers used to create the constructs were PpetE-BamHI-F and hetN-Sma1-R. The PCR products were cloned into pDR386 as *Bam*HI-*Sma*I fragments to generate fusions with YFP.

Plasmid pOR120 is a mobilazable shuttle vector containing P_{petE}-*hetN* translationally fused to YFP. The *hetN* coding region was amplified by PCR from chromosomal DNA with the primers hetN-EcoRI and hetN-BamHI-R, and the product was cloned as an *Eco*RI-*Bam*HI fragment into the same sites in pKH256 [14]. A fragment containing P_{petE}-*hetN* was amplified from this construct with the primers PpetE-BamHI-F and hetN-SmaI-R and was cloned as a *Bam*HI-*Sma*I fragment into the same sites in pDR386 [14] to create pOR120.

Plasmid pOR130 is a mobilizable shuttle vector containing P_{petE}-*hetN* translationally fused to YFP transcribed divergently from P_{nir}-*cfp*. The *nir* promoter was amplified by PCR using pSMC188 [21] as a template with the primers Pnir-BamHI-F and Pnir-CFP-R. The coding region of *cfp* was amplified using pSMC254 as a template with the primers CFP-Pnir-F and CFP-XhoI-R. The products were fused fused together by overlap extension PCR, cloned as a *Bam*HI-*Xho*I fragment into the *Bam*HI-*Sal*I sites of pOR120, and screened by PCR to determine directionality to create pOR130.

Plasmid pPJAV437 is a mobilizable shuttle vector containing P_{petE}-*hetN*-YFP-His6. A region containing P_{petE}-*hetN*-YFP-His6 was amplified by PCR using pPJAV440 as a template with the primers hetN-EcoRI and pET28B-BglII-R. The product was cloned as as *Eco*RI-*Bgl*II fragment into the *Eco*RI-*Bam*HI sites in pPJAV213 [27] to create pPJAV437.

Plasmid pPJAV440 is used to purify HetN-YFP tagged with a C-terminal His6 tag from the BL21(DE3) *E. coli* expression strain. A region containing *hetN-yfp* was amplified by PCR using pPJAV326 [25] as a template with the primers hetN-BsphI-F and YFP-XhoI-R. The product was cloned as a *Bsp*HI-*Xho*I fragment into the *Nco*I-*Xho*I sites of pET28a+*hetR* [9], which replaced the *hetR* coding region with *hetN-yfp*, to create pPJAV440.

Plasmid pRR159 and pPJAV155 are mobilizable shuttle vectors containing P_{hetN}-*hetN* and P_{hetN}-*hetN*(Δ193-287), respectively, translationally fused to YFP. The inserts were amplified via PCR using *Anabaena* chromosomal DNA as a template with the primers PhetN-BamHI-Fwd and hetN-SmaI-R for plasmid pRR159 and PhetN-BamHI-Fwd and HetN(1-192)-SmaI-R for plasmid pPJAV155. The PCR products was cloned as *Bam*HI-*Sma*I fragment into the same sites on pDR386 [14] to create pRR159 and pPJAV155.

The plasmids pRR163 and pRR167 are mobilizable shuttle vectors containing P_{petE}-*hetN* and P_{petE}-*hetN*(Δ193-287), respectively, translationally fused to YFP. The inserts were amplified via PCR using pDR320 as template with the primers PpetE-BamHI-F and hetN-SmaI-R for pRR163 and PpetE-BamHI-F and HetN(1-192)-SmaI-R

for pRR167. The PCR products were cloned into pDR386 [14] as *Bam*HI-*Sma*I fragments.

Plasmid pSMC254 is a suicide vector created to introduce the copper-inducible promoter of *petE* (P_{petE}) controlling the expression of *hetR* (P_{petE}-*hetR*) translationally fused to CFP into the native *Anabaena hetR* locus. CFP was amplified via PCR using EKAR (Harvey et al 2008) as a template with the primers Cer/Ven-Tnl-F and Cer-Tnl-R and cloned into the *Eco*RV site of pBlueScript SK+ (Stratagene). A *Bam*HI-*Sac*I fragment containing CFP was excised from this construct and was cloned into the same sites in pAM504 [28]. The P_{petE}-*hetR* insert was moved from pDR293 [22] as a *Bam*HI-*Sma*I fragment into the same sites in the previous construct upstream of CFP to create an inducible C-terminal CFP translational fusion to *hetR* in pAM504. This vector was used as a template to amplify P_{petE}-*hetR*-CFP via PCR with the primers PpetE-NcoI-F and CFP-SpeI-R and the product was cloned into the *Eco*RV site of pBlueScript SK+. The P_{petE}-*hetR*-CFP region was moved as a *Nco*I-*Spe*I fragment into the same sites of the suicide vector pDR325 [23] to create pSMC254.

Plasmid pSMC262 is a mobilizable shuttle vector containing P_{petE} transcriptionally fused to *hetN* transcribed divergently from the *nir* operon promoter (P_{nir}) transcriptionally fused to YFP. The coding region of YFP was amplified via PCR using pUC57-P_{S12}-yfp [19] as a template with the primers Turbo-NdeI-F and Turbo-PstI-R and the product was cloned into the *Eco*RV site of pBlueScript SK+. A *Nde*I-*Sal*I fragment from pDR324 [23] containing P_{nir} was cloned into the same sites upstream of YFP in pBlueScript SK+ to create a P_{nir}-YFP fusion in pSMC265 [14]. The P_{nir}-YFP fusion was moved as a *Sal*I-*Eco*RI fragment into the same sites of pDR320 [23] to create pSMC262.

Plasmid pSMC266 ia a mobilazable shuttle vector containing P_{nir}-YFP. The P_{nir}-YFP insert was moved as a *Sal*I-*Eco*RI fragment from pSMC265 [14] into the same sites of pAM504 to create pSMC266.

Strain construction. Table 5 lists the strains used in this study. Replacement of chromosomal DNA was done as previously described [1]. Strain UHM191 was created by the introduction of the suicide vector pSMC254 to UHM134 to create UHM191. PCR with primers that anneal outside of the region of *Anabaena* DNA used on pSMC254 for strain construction was performed. The size of the various PCR products was used to confirm the presence of the introduced construct.

Microscopy and determination of signal ranges. Cells were routinely viewed and imaged as previously described [1]. Confocal microscopy was completed using an Olympus Fluoview 1000 laser scanning confocal mounted on an IX81 motorized inverted microscope. Fluorescence from Turbo-YFP was detected with an excitation of 525 nm and an emission of 538 nm. Fluorescence from CFP was detected with an excitation of 436 nm and an emission of 485 nm. All images were processed in Adobe photophop CS2. To determine the signal range of the inhibitors produced in source cells, the peak pixel intensity along a line drawn through a cell perpendicular to the filament axis was determined for 20 cells adjacent to source cells using the plot profile function in ImageJ. The largest number of contiguous cells adjacent to the source that fell below a threshold value, twice the value measured in control cells without the fluorophore, was taken as the signal range measured in cell numbers.

Overexpression and purification of recombinant HetN-YFP(6-His). A 20 mL culture of *E. coil* BL21(DE3)(New England BioLabs) transformed with pPJAV440 was

grown to an optical density at 600 nm of 0.6 at 37^{o}C with aeration. After inducing protein expression overnight with the addition of 1 mM IPTG, the culture was pelleted by centrifugation at 10 000 *g* for 10 minutes. The pellet was re-suspended in 5 mL $T_{10}E_{25}$ (10 mM Tris, 25 mM EDTA, pH 8.0), 5 ml of 8% sodium dodecyl sulfate (SDS) was added, and the entire mixture was boiled for 12 minutes to solubilize the pellet. Once the solubilized pellet had cooled at room temperature for 10 minutes, 30 ml of membrane buffer (20 mM Tris-HCl, pH 8.0, 300 mM NaCl, 10% glycerol, 0.01% NaN_3) containing 5 mM imidazole, prepared as previously described [13] and 1 ml of Ni-NTA agarose (Quiagen) that had been washed twice with membrane buffer were added and the entire mixture was mixed on a rocking table for 2 h at room temperature. The Ni-NTA agarose was pelleted at 700 *g* for 5 minutes, washed with 20 ml of membrane buffer containing 5 mM imidazole and a final concentration of 1% SDS, pelleted, and the protein was eluted with the addition of 5 ml of membrane buffer containing 300 mM imidazole and a final concentration of 1% SDS.

Western Blot analysis. One hundred milliliter cultures of wild-type *Anabaena* harboring plasmids containing either HetN-YFP(6-His), pPJAV437, or the empty vector control, pPJAV213, were pelleted by centrifugation at 2000 *g* for 5 minutes and re-suspended in 30 ml of fresh BG-11 medium containing a cOmplete Protease Inhibitor Cocktail Tablet (Roche). The cultures were lysed by passage through a French pressure cell press at 20 000 psi. Protein concentrations were determined by NanoDrop analysis. *Anabaena* lysates containing about 3.5 μg of protein and 80 ng of purified recombinant HetN-YFP(6-His) were then subjected to SDS-polyacrylamide gel electrophoresis followed by electrophoretic transfer onto a polyvinylidene difluoride membrane. HetN-

YFP was detected with Penta-His antibodies (Quiagen) followed by chemiluminescence detection (Western Breeze; Invitrogen) and imaging with the GeneGenome BioImaging System (Syngene).

Table 5. Strains and Plasmids used in Chapter 3

Strain or Plasmid	Relevant Characteristic(s)*	Source or Reference
***Anabaena* sp. strains**		
PCC 7120	Wild-type	Pasteur Culture Collection
UHM134	Δ*patA* Δ*hetF* Δ*HetR*	[23]
UHM163	*hetR*(R250K)	[9]
UHM191	Δ*patA* Δ*hetF* P_{petE}-*hetR-cfp*	This study
***Eserichia coli* strains**		
BL21(DE3)	Recombinant protein expression	New England BioLabs
Plasmids		
pAM504	Shuttle vector for replication in *E. coli* and *Anabaena*; Km^r Nm^r	[28]
pRL277	Suicide vector; Sp^r/Sm^r	[3]
pUC57-P_{S12}-yfp	Plasmid used as template for YFP	[19]
pCO115	pAM504 with P_{petE}-*hetN*(Δ2-46)-YFP	This study
pCO117	pAM504 with P_{petE}-*hetN*(Δ47-176)-YFP	This study
pCO118	pAM504 with P_{petE}-*hetN* (Δ177-195)-YFP	This study
pCO121	pAM504 with P_{petE}-*hetN*(Δ47-128)-YFP	This study
pOR120	pAM504 with P_{hetN}-*hetN*-YFP	This study
pOR130	pAM504 with P_{hetN}-*hetN*-YFP transcribed divergently from P_{nir}-CFP	This study This study
pPJAV155	pAM504 with P_{hetN}-*hetN* (Δ193-287)-YFP	This study
pPJAV347	pAM504 with P_{petE}-*hetN-YFP*(His6)	This study
pPJAV440	pET28a with *hetN-YFP*(His6)	This study
pRR159	pAM504 with P_{hetN}-*hetN*-YFP	This study
pRR163	pAM504 with P_{petE}-*hetN*-YFP	This study
pRR167	pAM504 with P_{petE}-*hetN* (Δ193-287)-YFP	This study
pSMC254	pRL277 used to make UHM191	This study
pSMC262	pAM504 with P_{petE}-*hetN* and P_{nir}-YFP	This study
pSMC266	pAM504 with P_{nir}-YFP	This study

*Km, kanamycin; Nm, neomycin; Sm, streptomycin; Sp, spectinomycin

Table 6. Oligonucleotide primers used in Chapter 3

Oligonucleotide*	Sequence
Turbo-NdeI-F	TATATATATACATATGAGCAGCGGCGCCCTGCTGTTC
Turbo-PstI-R	CTGCAGTCAGCTGGTGTCTCCGGAACC
CFP-Pnir-F	GAACGAATTCATGGTGAGCAAGGGCGAGGAGC
CFP-XhoI-R	TATAATCTCGAGTTACTTGTACAGCTCGTCCATG
CFP-SpeI-R	AATAACTAGTTTACTTGTACAGCTCGTCCATGC
PpetE-NcoI-F	AATACCATGGGCTGAGGTACTGAGTACACAGC
Cer/Ven-Tnl-F	TTTGGATCCAATCCCGGGGATCGGCGTCAGCTGTGAG CAAGGGCGAGGAGCTGTTCA
Cer-Tnl-R	CCACAGAGCTCTTACTTGTACAGCTCGTCCATGCCGAG
HetN(1-192)-SmaI-R	ATTATCCCGGGACCCAGTTTGCGAGACATAGCC
PhetN-BamHI-Fwd	ATATAGGATCCAGGAGAAGACGCGATGAATC
hetN-SmaI-R	ATATACCCGGGATGAGCGATGAGACTCAACAG
hetN-BsphI-F	ATATATCATGACAACTCTTACAGGTAAGACAGTAC
YFP-XhoI-R	ATATACTCGAGGCTCATGGATGCGGAGCTGGTGTCTC CGGAACCGGCGTCGAAGTC
Pnir-BamHI-F	ATATAGGATCCAGCTACTCATTAGTTAAGTGTAATG
Pnir-CFP-R	TGCTCACCATGAATTCGTTCTCATAAAG
hetN-EcoRI	ATATAGAATTCTATGTGTAATCGCGTTAAGGCTGC
hetN-BamHI-R	ATATAGGATCCTCATGAGCGATGAGACTCAAC
pET28B-BglII-R	ATATAAGATCTCAGCGGTGGCAGCAGCCAACTCAGC
PpetE-BamHI-F	ATATAGGATCCCTGAGGTACTGAGTACACAG

*Oligonucleotides are shown in the 5' to 3' direction

Results

Identification of stable HetN-YFP within *Anabaena*. The localization of a protein within a living cell can be used to elucidate the function of the protein. In many cases the translational fusion of a protein being studied to a fluorescent protein, like green fluorescent protein (GFP), can be used to determine a protein's localization within living cells [5]. Proteins involved in cellular division like FtsZ [26], MinE [12], and MinD [20] have been examined using translational fusions to fluorophores and their localization has supported their hypothesized functions. During these types of studies it is important that the fusion of a specific protein to a fluorophore does not disrupt the organism in any way. The organism may be unable to survive, the localization of the protein within the cells may be effected, the protein may be degraded immediately after translation, or the protein may be rendered non-functional. In order to utilize a HetN-YFP fusion protein to further understand the function of HetN as a potential inhibitory morphogen it must first be shown that the HetN-YFP fusion protein has the same function as HetN alone.

When a HetN-YFP(6-His) fusion protein was expressed in *Anabaena* YFP fluorescence was detected in high levels localizing to the cytoplasmic membrane and in low levels localized to thylakoid membranes (Fig. 9B). To ensure that the YFP detected represents the localization of full-length HetN-YFP, extracts from *Anabaena* expressing HetN-YFP(6-His) were probed with a commercially available antibody specific to the 6-histadine tag. The full-length protein, including a 5 aa linker domain, is predicted to be 59 kDa. When the extracts from *Anabaena* were probed and compared to extracts from *E. coli* expressing the same HetN-YFP(6-His), full-length HetN-YFP was the primary protein identified by the western blot (Fig. 9C). There was a faint dimer of HetN-YFP(6-

His) detected in the extracts from *Anabaena* (Fig. 9C). This dimer was also present in the extracts from *E. coli* (Fig. 9C). There was no product smaller than full-length HetN-YFP(6-His) detected in the *Anabaena* extract. There was further no product identified in the *Anabaena* strain carrying the empty vector control (Fig. 9C). The results indicate that the antibody does not cross react with any other proteins within *Anabaena* and that the YFP signal detected within the *Anabaena* cells is consistent with the localization of full-length HetN-YFP.

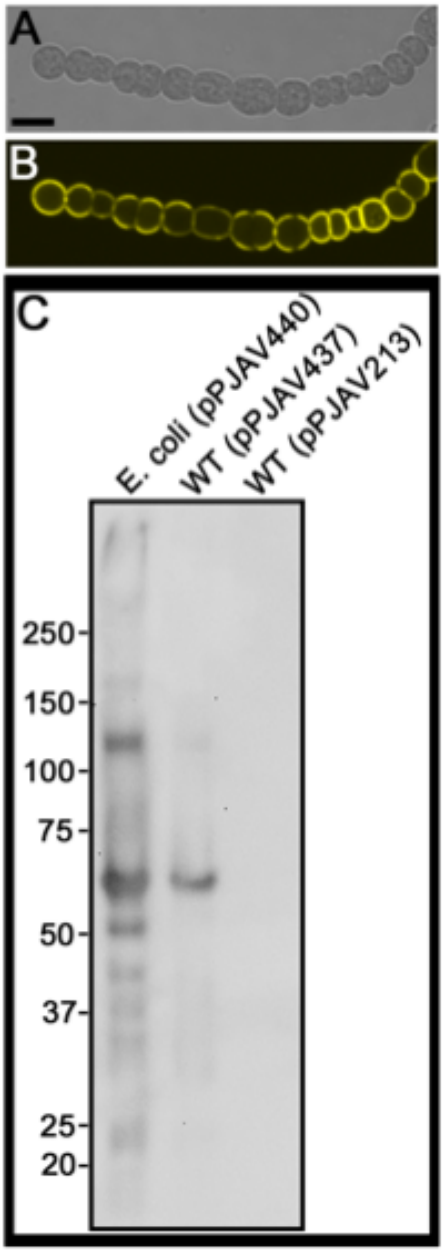

Figure 9. Western blot analysis of the fusion protein HetN-YFP expressed in *Anabaena* sp. PCC 7120 and Eserichia coli. Bright field confocal image of *Anabaena* containing pPJAV437, which encodes P_{petE}-*hetN*-*YFP*(6-histadine)(A). Yellow fluorescence channel from the image in panel A (B). Western blot analysis of HetN-YFP(6-His) using a commercial antibody against the hexa-histadine tag (C). Lane 1, from left, HetN-YFP(6-His) from *E. coli,* containing pPJAV440, which encodes HetN-YFP(6-His). Lane 2, HetN-YFP(6-His) from *Anabaena* containing, pPJAV437, which encodes HetN-YFP(6-His). The predicted size of HetN-YFP from the sequence is about 59 kDa. Lane 3, *Anabaena* containing pPJAV213, which is pAM504 carrying the *petE* promoter. Numbers at left indicate molecular size markers in kilodaltons. Scale bar in panel A equals 10 μm.

Subcellular localization of HetN-YFP. To ensure that the translational fusion of HetN to YFP does not disrupt the function of HetN a HetN-YFP fusion was examined in *Anabaena* and strain UHM163, which has a *hetR*(R250K) replacement and can form heterocysts in the presence of excess HetN. Fluorescence from full-length HetN fused at its C-terminus to YFP and driven by the *petE* promoter was observed primarily at the periphery of cells in filaments, consistent with localization to the plasma membrane (Fig. 10A). In addition, a more diffuse fluorescence signal was observed from the interior region of cells, consistent with the previous detection of HetN in thylakoid membranes (Fig. 10A). The fusion protein prevented the formation of heterocysts, so it was not possible to view the localization of HetN in heterocysts in a wild-type genetic background. The inhibition of heterocyst by HetN-YFP and the localization within the cells of filaments suggests that HetN-YFP is capable of functioning as an inhibitor.

To facilitate visualization of HetN-YFP in heterocysts, a plasmid borne *hetN-YFP* fusion was introduced into a derivative of *Anabaena* that continues to form heterocysts even when extra copies of *hetN* are introduced [9]. The strain, UHM163, has the wild-type copy of *hetR* replaced by an allele that encodes *hetR*(R250K). With transcription of *hetN-YFP* from either the native *hetN* promoter or the *petE* promoter, fluorescence from YFP was observed primarily at the periphery of heterocysts (Fig. 10B and C). With expression from the *petE* promoter, fluorescence was observed in both cell types, whereas with the native *hetN* promoter fluorescence was observed only in heterocysts, consistent with heterocyst specific expression of *hetN* (Fig. 10B and C)[4]. The pattern of YFP fluorescence indicates that HetN localizes primarily to the plasma membrane in both vegetative cells and heterocysts.

C-terminal translational fusions to YFP were also made with the following variants of HetN: HetN(Δ2-46), HetN(Δ47-128), HetN(Δ47-176), HetN(Δ177-195), and HetN(Δ193-287), where the numbers in parentheses represents a protein lacking the amino acids indicated. Heterocyst differentiation in a wild-type background was suppressed with all fusions in which the RGSGR motif was present. There was no observable YFP detected in wild-type from the *petE* promoter or in UHM163 from either the *petE* or *hetN* promoters from the translational YFP fusions to HetN(Δ2-46), HetN(Δ47-128), HetN(Δ47-176), or HetN(Δ177-195) (data not shown).

In filaments with the construct encoding HetN(Δ193-287)-YFP, which lacks the C-terminal domain of HetN, YFP fluorescence was observed primarily at cell junctions. In particular, rings of fluorescence were observed circumscribing cell septa (Fig. 10D). Fusions of HetN(Δ193-287) to YFP were made with expression from the native *hetN* promoter or the *petE* promoter, but fluorescence was observed only when the *petE* promoter was used. In a wild-type genetic background, the HetN(Δ193-287)-YFP fusion protein inhibited differentiation, so fluorescence could only be observed in vegetative cells (data not shown). In strain UHM163 rings of fluorescence were detected in vegetative cells but were absent from heterocysts (Fig. 10D).

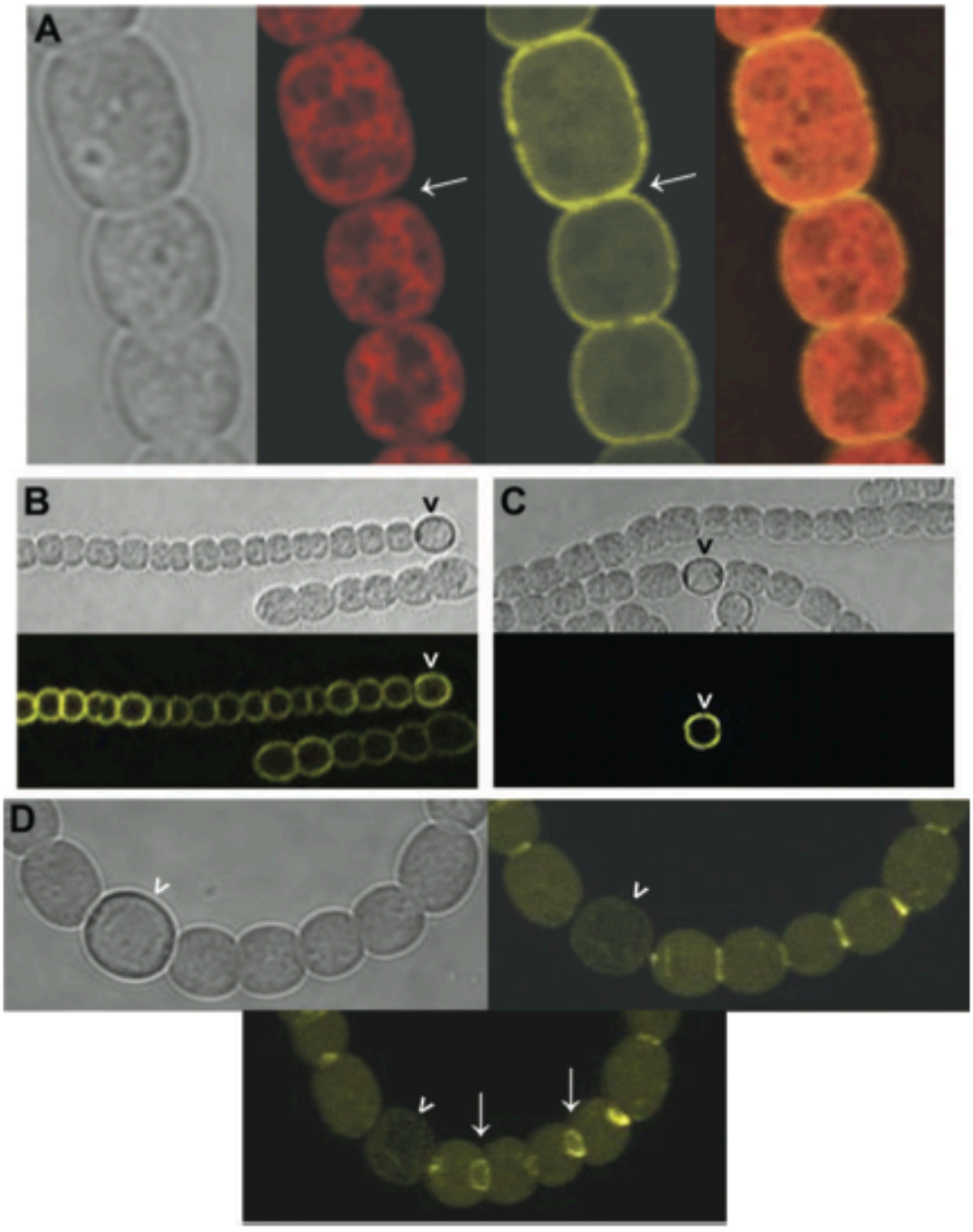
A
B
V
V
C
V
V
D

Figure 10: Subcellular localization of HetN-YFP. Confocal micrographs of *Anabaena* with a plasmid carrying P_{petE}-*hetN-YFP* (A). From left to right: bright-field, chlorophyll auto fluorescence, HetN-YFP fluorescence, and composite image. Arrows indicate areas showing the lack of overlap between autofluorescence and HetN-YFP at the periphery of cells. UHM163, a strain that forms heterocysts even when *hetN* is overexpressed from a multi-copy plasmid, with a plasmid carrying P_{petE}-*hetN-YFP* (B). UHM163 with a plasmid carrying P_{hetN}-*hetN-YFP* (C). Top panels are bright-field images and bottom panels are corresponding yellow fluorescent images, which represent a 0.2 µm section of the filament for (B) and (C). UHM163 with a plasmid carrying P_{petE}-*hetN*(Δ193-287)-*YFP* (D). Top-left: bright-field, top-right: yellow fluorescence, below center: rings of fluorescence indicated by arrows are apparent when the three-dimentional image at top-right is rotated 50 degrees horizontally. A 7x and 3x digital zoom on the confocal was used for (A) and (D) respectively. Carets indicate heterocysts.

Fluorescent recovery after photobleaching of HetN-YFP. The localization and function of HetN is preserved when HetN is translationally fused to YFP and overexpressed in all cells of filaments. The hypothesis that HetN functions as an inhibitory morphogen within the *Anabaena* system implies that the protein must move away from the source of production. The preserved inhibitory function of HetN-YFP suggests that the protein could move from cell to cell as a full-length protein and fulfill its role as an inhibitor. This movement could be achieved by the dispersal of membrane fragments similar to argosomes, which are known to facilitate the movement of morphogens within the *Drosophila melanogaster* developmental system [11]. These membrane rafts could disperse full-length HetN from its heterocyst source to the adjacent vegetative cells as a membrane associated protein.

The presence of full-length HetN-YFP within *Anabaena* cells and the localization of HetN-YFP being consistent with the finding that HetN associates with cellular membranes [15] indicate that the fusion protein should behave as a membrane protein, freely diffusing throughout the cell associated with the membranes. When a small region

of the cellular membrane on a single cell was bleached in a FRAP experiment considerable levels of YFP fluorescence were present within the bleached region 240 seconds after the bleaching event (Fig 11A). In contrast when an entire cell expressing HetN-YFP was bleached in a FRAP experiment very little YFP fluorescence was detected within 360 seconds of the bleaching event (Fig. 11B). The results indicate that full length HetN-YFP is associated with the cell membranes but is unlikely to move from cell to cell as a full-length fusion protein.

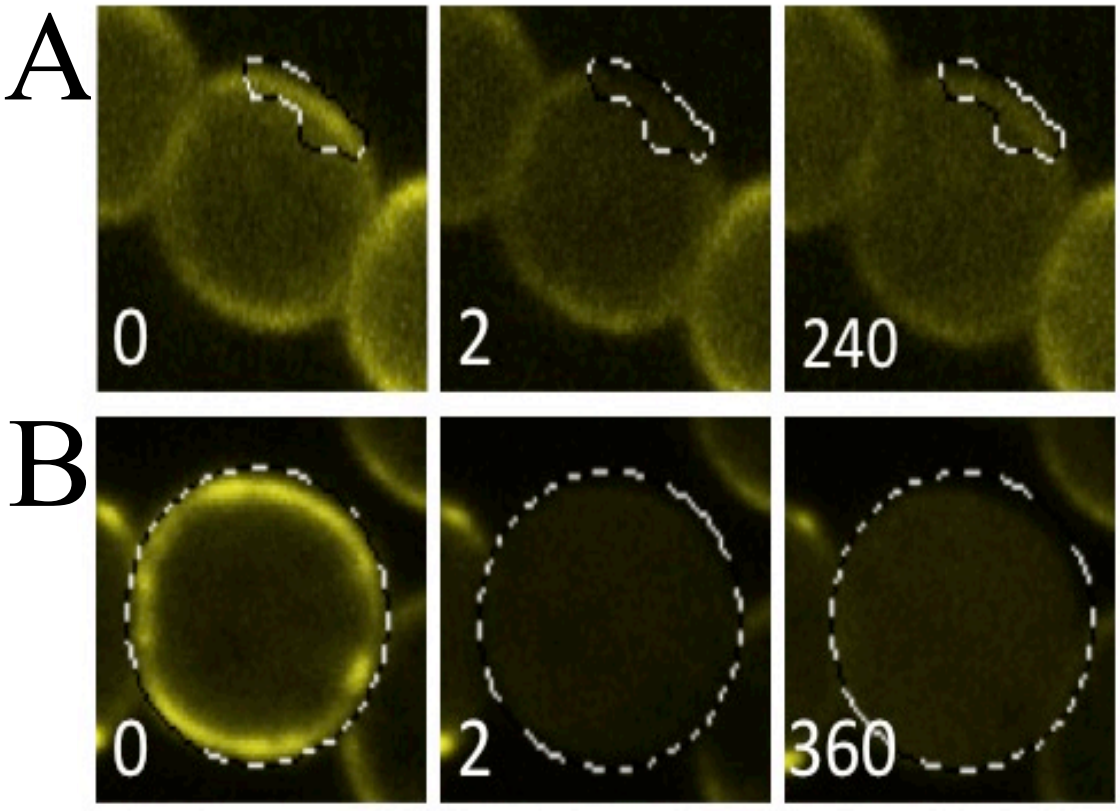

Figure 11: Determine if full length HetN-YFP can be transported within the membrane of a single cell or from cell to cell via a fluorescence recovery after photobleaching (FRAP) experiment. A region of membrane in a single *Anabaena* cell expressing *hetN-YFP*, time 0, was bleached, time 2 seconds, and the fluorescent recovery was observer for 240 seconds (A). An entire *Anabaena* cell expressing *hetN-YFP*, time 0, was bleached, time 2 seconds, and the fluorescent recovery was observer for 360 seconds (B).

Confinement of HetN-YFP to source cells. The signal range of HetN is approximately 10 cells when expressed from an inducible promoter in the engineered vegetative source cells of a mosaic filament [23]. To determine if the full-length HetN protein moves from source cells to target cells within the signal range, mosaic filaments with HetN-YFP produced in source cell(s) were created, and the location of the fluorescent fusion protein was observed. Plasmid pOR130, carrying P_{nir}-CFP and P_{petE}-*hetN-YFP*, was introduced into wild-type to create source cells of HetN-YFP. CFP marked source cells, and YFP indicated the location of HetN-YFP. Two potential outcomes were hypothesized. First, fluorescence from YFP could be limited to those cells that had CFP fluorescence (Fig. 12A). This outcome would be consistent with a lack of intercellular movement of HetN-YFP. Second, fluorescence from YFP could extend beyond those cells that had CFP fluorescence (Fig. 12A). This outcome would support the intercellular movement of full-length HetN protein. Figure 12B shows a mosaic filament in which fluorescence from HetN-YFP was limited to two contiguous cells. Fluorescence was primarily at the cell periphery, consistent with membrane association of HetN [14, 15]. Fluorescence from CFP was also observed in each of those two cells (Fig. 12B). For all filaments that were examined (n=12), cells that had robust YFP fluorescence also had CFP fluorescence. These results indicate that, at the level of detection afforded by the protein fluorophores and confocal microscopy, there was no evidence for intercellular movement of HetN-YFP between vegetative cells.

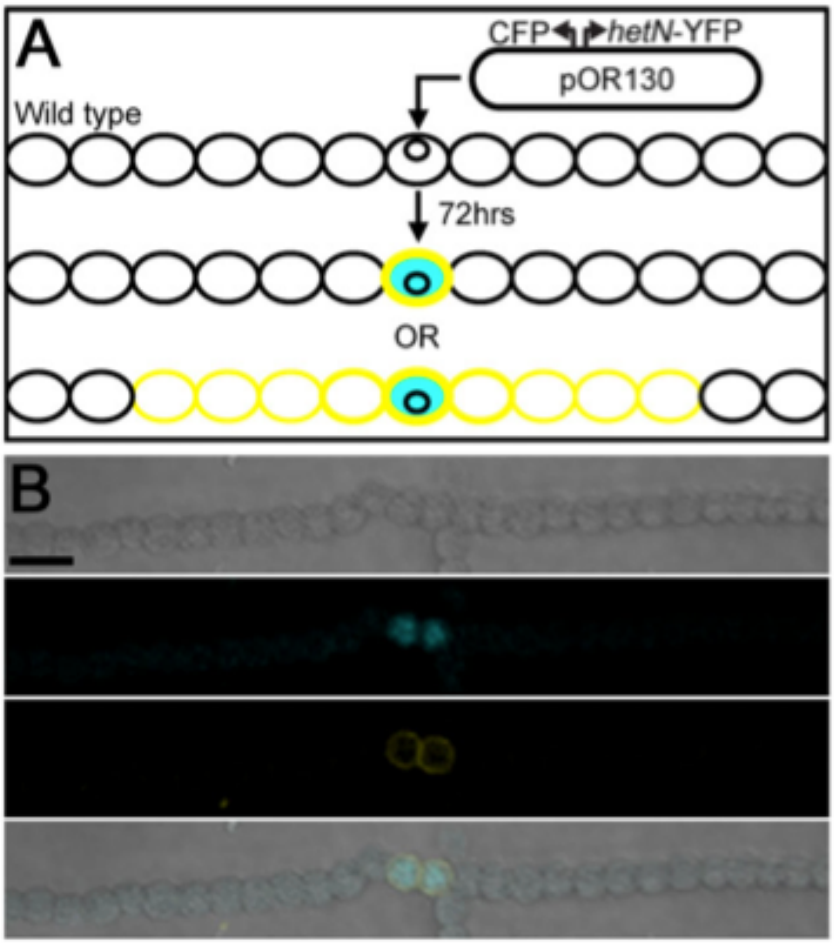

Figure 12: Determining if full length HetN-YFP can be transported from cell to cell in a mosaic filament experiment. Schematic of two possible outcomes in mosaic filaments created with pOR130, P_{petE}-*hetN-YFP* and P_{nir}-*CFP*, and wild-type. Yellow rings represents HetN-YFP localized to the periphery of cells, and blue represents CFP used to indicate source cells that have received plasmid pOR130 (A). Micrograph of the mosaic filament created with plasmid pOR130 and wild-type (B). From top to bottom: bright-field, blue fluorescence from CFP, yellow fluorescence from HetN-YFP, and a composite image. Scale bar, 10 μm.

Signal ranges produced by HetN and HetN-YFP. The confinement of full-length HetN-YFP to source cell suggests that the associated *hetN*-dependent inhibitory signal might also be confined to source cells. In order to determine if the *hetN*-dependent inhibitory signal of HetN-YFP is confined to source cells a mosaic filament was created. Plasmid pOR120, carrying P_{petE}-*hetN-YFP*, was introduced to strain UHM191, Δ*patA*

Δ*hetF* P_{petE}-*hetR*-CFP, and the presence or absence of a signal range was used to indicate if the *hetN*-dependent inhibitory signal is confined to source cells when HetN-YFP was the only inhibitor being expressed. The presence or absence of a signal range was determined using the plot profile function in ImageJ. The peak pixel intensity along a line drawn through a cell perpendicular to the filament axis was determined for 20 cells adjacent to source cells (Fig. 13C and D). The largest number of contiguous cells adjacent to the source that fell below a threshold value, twice the value measured in control cells without the fluorophore, was taken as the signal range measured in cell numbers (Fig. 13).

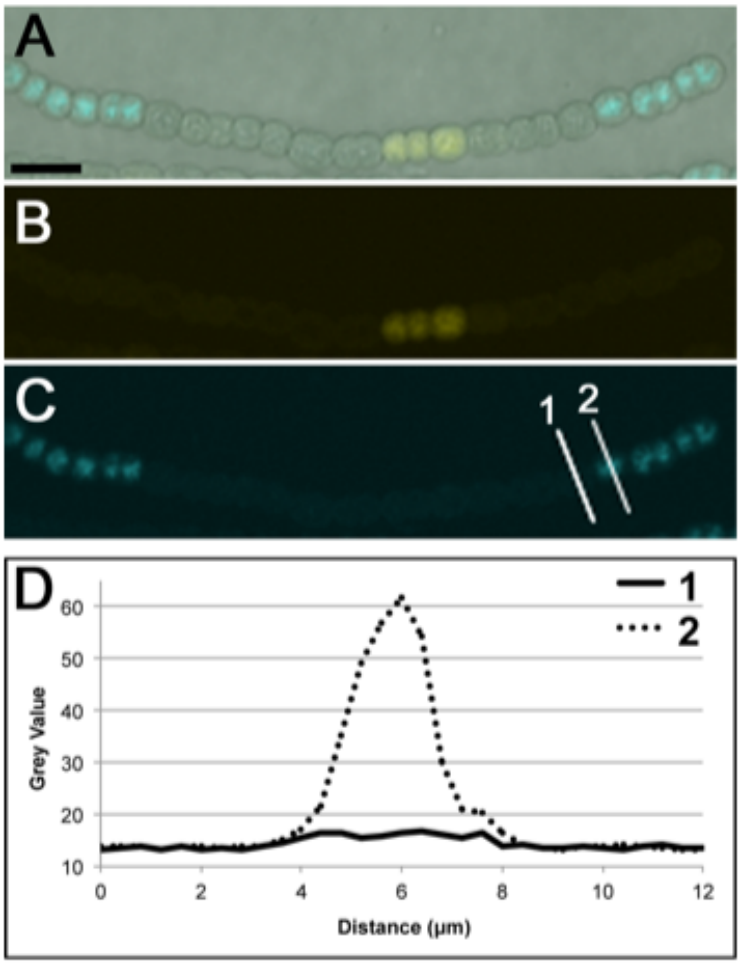

Figure 13: Quantification of HetR-CFP fluorescence in individual cells using the plot profile function of ImageJ. A merged confocal image of the bright-field, yellow channel, and blue channel of a mosaic filament with strain UHM191, which has the genotype Δ*patA* Δ*hetF* P_{petE}-*hetR-CFP*, and plasmid pSMC262, which encodes P_{nir}-*YFP* and P_{petE}-*hetN* (A). The psesence of YFP fluorescence indicates source cells carrying pSMC262 72 h after its introduction. Yellow channel of the merged image in panel A (B). Blue channel of the merged image in panel A (C). Plot profiles in panel D correspond to the cells indicated with lines 1 and 2. Graph of the grey scale intensity measured along the lines 1 (solid line) and 2 (dotted line) of the blue channel as seen in panel C (D). Scale bar in panel A equals 10 μm.

Early work with PatS used GFP or a hexa-histadine tag fused to the C-terminus of the peptide in an attempt to prevent intercellular transfer of the inhibitory signal and examine the effect on pattern formation [29]. If the full-length HetN protein serves as the intercellular inhibitory signal, confinement of HetN-YFP to source cells as described above should abolish the signal range of HetN-YFP produced in source cells. To determine if fusion of YFP to HetN influenced the movement of the HetN-dependent inhibitory signal, the signal ranges of HetN and HetN-YFP were compared in genetic mosaic filaments. Source cells of HetN were created by introduction of pSMC262, which carryies P_{petE}-*hetN* and P_{nir}-YFP. Transcription of both genes was driven by inducible promoters. YFP was used to mark cells that had received the plasmid. The background strain was UHM191, which lacks both the *patA* and *hetF* genes and has a gene encoding a HetR-CFP fusion transcribed from the copper inducible *petE* promoter in place of the native *hetR* gene. The mutations in *patA* and *hetF* facilitated observation of fluorescence from HetR-CFP as well as prevented heterocyst formation and induction of transcription of the chromosomal copies of *patS* and *hetN*; in strains lacking *hetF* and/or *patA*, an inactive form of HetR accumulates in cells but is still sensitive to *patS*- and *hetN*-

dependent degradation [23]. The absence of fluorescence from HetR-CFP was used to measure the signal range.

In figure 14A, cells adjacent to those expressing *hetN* from the plasmid, indicated by yellow fluorescence, lost observable HetR-CFP fluorescence, suggesting movement of the *hetN*-dependent signal from source cells to the adjacent cells. The average signal range was 8.3 ± 0.4 cells (n=30, Fig. 14A). Conversely, when the control plasmid pSMC266, which lacks *hetN*, was used to create yellow fluorescent cells in mosaic filaments with UHM191, no loss of HetR-CFP fluorescence was observed (Fig. 14B), indicating that the gene encoding HetN was required for the signal range.

When plasmid pOR120, which encodes the same HetN-YFP fusion used in figures 11 and 12, was used to create mosaic filaments with UHM191, a pattern of HetR-CFP fluorescence similar to that created by pSMC262 was observed (Fig. 14C). The average signal range was 8.8 ± 0.4 cells (n=15). YFP fluorescence was located primarily at the cell periphery, consistent with its fusion to HetN, and marked the source cells that received the plasmid and produced HetN-YFP (Fig. 14C). Analysis of the data sets collected with plasmids pSCM262 and pOR120 with a Levene's test yielded a value of 0.73, indicating that comparison with a *t*-test was appropriate. A value greater than 0.05 in a Levene's test is considered sufficient to justify use of a *t*-test to determine if the data sets are significantly different from one another. Comparison of the data sets collected with plasmids pSMC262 and pOR120 with a *t*-test yielded a *P*-value of 0.54, indicative of no significant difference between the signal ranges generated with genes encoding HetN or HetN-YFP. Despite lack of intercellular movement of HetN-YFP, the signal range of the gene encoding HetN-YFP was similar to that encoding HetN alone.

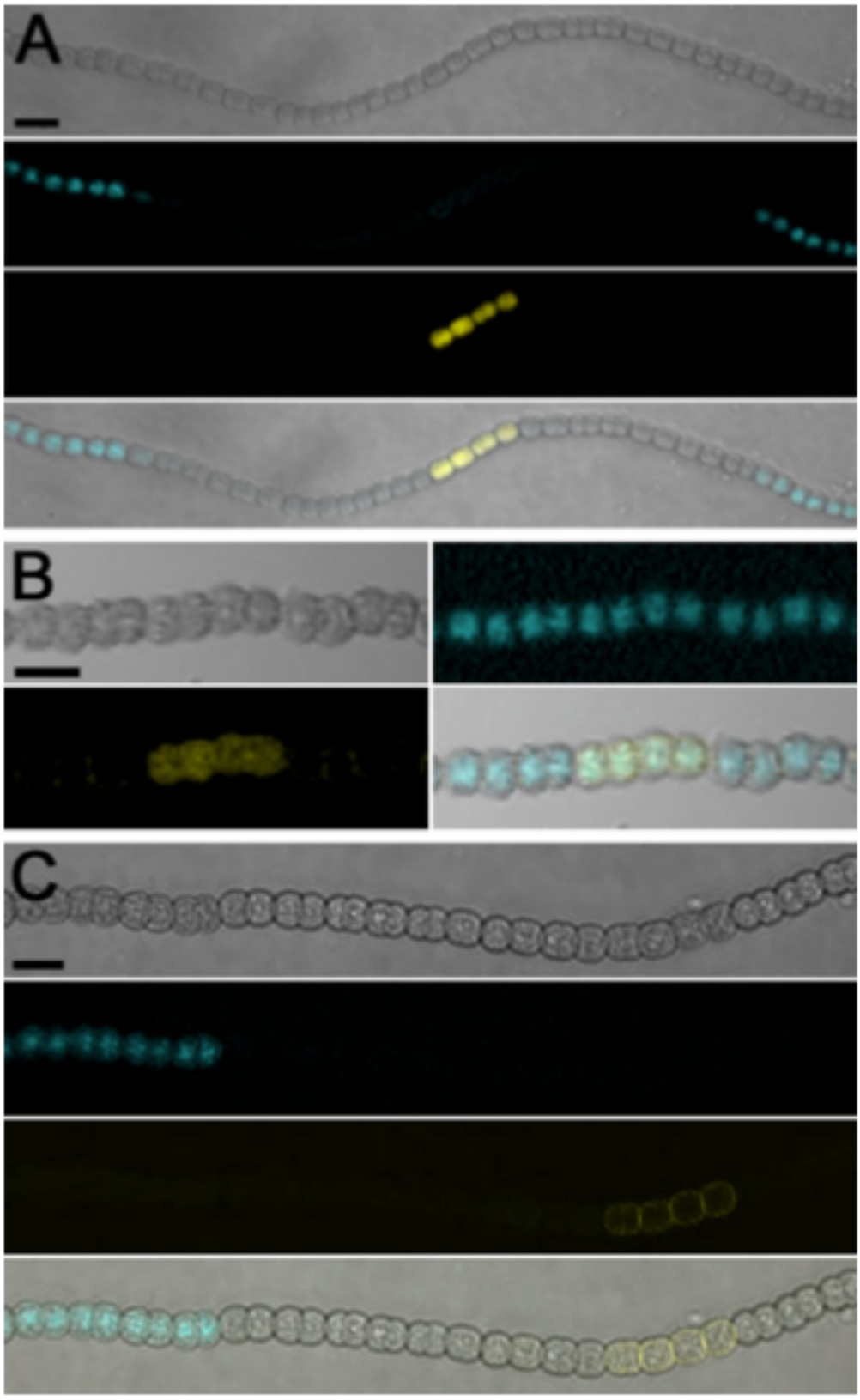
A
B
C

Figure 14. Expression of *hetN* produces similar signal ranges when expressed alone or as a HetN-YFP chimera. A mosaic filament of UHM191, which has *hetR-CFP* expressed from an inducible promoter, and plasmid pSMC262, which encodes HetN and YFP expressed separately from inducible promoters (average signal range of 8.3 ± 0.4 cells)(A). From top to bottom: bright-field, blue fluorescence from HetR-CFP, yellow fluorescence from YFP, and a composite image. A mosaic filament of UHM191 with plasmid pSMC266, which encodes YFP alone, serves as a control (average signal range 0)(B). Top left: bright-field, top right: blue fluorescence from HetR-CFP, bottom left: yellow fluorescence from YFP, bottom right: composite image. A mosaic filament of UHM191 with plasmid pOR120, which encodes HetN translationally fused to YFP, HetN-YFP (average signal range 8.8 ± 0.4 cells)(C). From top to bottom: bright-field, blue fluorescence from HetR-CFP, yellow fluorescence from HetN-YFP, and a composite image. Scale bar, 10μm.

Discussion

To determine if stable full-length HetN-YFP was produced in cells of *Anabaena* extracts from strains expressing HetN-YFP(6-His) were probed and compared to extracts from *E. coli* expressing the same HetN-YFP(6-His) protein. Full-length HetN-YFP was the primary protein identified by the western blot. The lack of a degradation product smaller than full-length HetN-YFP within *Anabaena* suggests that there is no protein processing site located in the N-terminal hydrophilic domain downstream of the RGSGR motif, amino acids 137-176, or that the c-terminal product of such a processing event is rapidly degraded as part of the processing. The presence of a protein processing site downstream of the RGSGR motif within amino acids 137-176 would be consistent with the findings that that amino acids 177-287 are not required for proper differentiation or patterning of heterocysts and that full-length HetN-YFP does not move from cell to cell while still producing a *hetN*-dependent inhibitory signal that does move from cell to cell.

HetN has been reported to be a membrane protein that resides in both cytoplasmic and thylakoid membranes [15]. In this study, fluorescence from HetN-YFP was observed

primarily in the cell envelope, presumably in the plasma membrane, with a more diffuse, lower level fluorescence from the interior of the cell, suggesting that the concentration of HetN is higher in the plasma membrane. HetN-YFP-dependent fluorescence intensity in the membrane was about twice that from the thylakoid membranes, but given the much larger surface area of the thylakoid membranes, the majority of HetN in a cell is likely to be in thylakoid membranes, consistent with earlier western blot analysis with cell fractions [15]. The only fusions to YFP in this study for which fluorescence was observed were those where YFP either replaced or was at the end of the C-terminal domain, suggesting that this domain of the protein is located in the cytoplasm. Proper folding of GFP requires the reducing environment present in the cytoplasm of bacterial cells, which has been used to map the topology of inner-membrane proteins [7]. The YFP used in the fusions is a derivative of GFP and would be expected to behave in a similar fashion. If the C-terminal domain is in the cytoplasm, the N-terminal hydrophilic domain, which contains that ERGSGR motif, may be located in the periplasm. However, it is difficult to interpret the lack of fluorescence with fusions to other parts of HetN, which could be explained by the creation of an unstable protein with a short half-life.

The deletion analysis, discussed in detail in chapter 2, of HetN has shown that removal of residues 2-46 or 177-287 of the 287 aa protein has no effect on differentiation or patterning of heterocysts [14]. In contrast, deletion of residues 47-176, which contains the ERGSGR sequence, has the same effect as deletion of the entire protein [6, 14], suggesting that functions required for movement between cells and inhibition of differentiation are contained within amino acids 47-176. Work here has shown that, at the level of detection afforded by the protein fluorophores and confocal microscopy, HetN-

YFP has intracellular movement within the membranes but there is no evidence for intercellular movement of the intact 287 aa protein. Fluorescence from a HetN-YFP fusion protein was observed only in cells of mosaic filaments that contained a plasmid encoding the fusion, yet the fusion protein produced a signal range similar to HetN alone. Because a C-terminal fusion was used, we conclude that the *hetN*-dependent signal that moves between cells does not include the C-terminal portion of the annotated HetN protein. Generation of an alternate C-terminus may result from post-translational processing, despite the lack of a possible C-terminal degradation product detected via western blot when HetN-YFP(6-His) was expressed in wild-type. Given that the N-terminal hydrophobic domain, amino acids 2-46, is not required for proper differentiation or pattern formation it is likely that this portion of HetN is not present in the intercellular inhibitory signal peptide which may be produced from HetN. Generation of an alternate N-terminal may result from production of a shorter peptide during translation.

Lateral inhibition implies the intercellular transfer of a signal that suppressed differentiation. Based on the deletion studies in chapter 2, the essential part of HetN that comprises the suppression signal appears to be little more than the ERGSGR motif. This raises the possibility that the signal that diffuses from cell to cell may be a peptide processed from a larger protein. Location of HetN in the cytoplasmic membrane suggests three potential routes of transfer between cells. First, the periplasm of cells in filaments is contiguous, and there is evidence both for and against the diffusion of proteins between cells via the periplasm [16, 31]. Processing of the N-terminal domain after insertion in the membrane could release a soluble fragment of HetN that contains the ERGSGR motif and diffuses through the contiguous periplasm. Uptake into the cytoplasm would be

necessary to allow interaction with HetR. Inhibition of heterocyst differentiation by addition of synthetic RGSGR peptide to the medium [30] suggests that transport into the cytoplasm is possible for such a molecule or that it can act from the periplasm. The second potential route of transfer is direct exchange between the membranes of adjacent cells. Although the plasma membranes at cell septa are not shared by adjacent cells and so are not continuous between cells, they are in close proximity [10], and could be bridged by an as yet uncharacterized intermembrane transport system. Results from this work suggest that the HetN-dependent inhibitory signal does not travel from cell to cell via one of these two potential routs because localization of HetN to the membrane is not required for proper patterning of heterocysts and there is no evidence for the intercellular exchange of full-length HetN. Therefore, the most likely route of transfer is via inter-cytoplasmic exchange or periplasmic exchange that does not rely on a signal sequence. The former route of transfer could be mediated by channel forming proteins SepJ, FraC, or FraD [17, 18], whereas the latter could be facilitated by an ABC-type transporter.

References

1. Borthakur, P.B., et al., *Inactivation of patS and hetN causes lethal levels of heterocyst differentiation in the filamentous cyanobacterium Anabaena sp. PCC 7120.* Mol. Microbiol., 2005. **57**: p. 111-123.
2. Buikema, W.J. and R. Haselkorn, *Characterization of a gene controlling heterocyst development in the cyanobacterium Anabaena 7120.* Genes Dev., 1991. **5**: p. 321-330.
3. Cai, Y. and C.P. Wolk, *Use of a conditionally lethal gene in Anabaena sp. strain PCC 7120 to select for double recombinants and to entrap insertion sequences.* J. Bacteriol., 1990. **172**: p. 3138-3145.
4. Callahan, S.M. and W.J. Buikema, *The role of HetN in maintenance of the heterocyst pattern in Anabaena sp. PCC 7120.* Mol. Microbiol., 2001. **40**: p. 941-950.
5. Chalfie, M., et al., *Green fluorescent protein as a marker for gene expression.* Science, 1994. **263**(5148): p. 802-5.
6. Corrales-Guerrero, L., et al., *Functional dissection and evidence for intercellular transfer of the heterocyst-differentiation PatS morphogen.* Mol. Microbiol., 2013. **88**(6): p. 1093-1105.
7. Drew, D., et al., *Rapid topology mapping of Escherichia coli inner-membrane proteins by prediction and PhoA/GFP fusion analysis.* Proc Natl Acad Sci U S A, 2002. **99**(5): p. 2690-5.
8. Elhai, J. and C.P. Wolk, *Conjugal transfer of DNA to cyanobacteria.* Methods Enzymol., 1988. **167**: p. 747-754.
9. Feldmann, E.A., et al., *Evidence for direct binding between HetR from Anabaena sp. PCC 7120 and PatS-5.* Biochemistry, 2011. **50**: p. 9212-9224.
10. Flores, E., et al., *Is the periplasm continuous in filamentous multicellular cyanobacteria?* Trends Microbiol., 2006. **14**: p. 439-443.
11. Greco, V., M. Hannus, and S. Eaton, *Argosomes: a potential vehicle for the spread of morphogens through epithelia.* Cell, 2001. **106**(5): p. 633-45.
12. Hale, C.A., H. Meinhardt, and P.A.J. de Boer, *Dynamic localization cycle of the cell division regulator MinE in Escherichia coli.* EMBO J, 2001. **20**(7): p. 1563-72.
13. Harder, D. and D. Fotiadis, *Purification of His-tagged membrane proteins from detergent-solubilized membranes.* Protocol Exchange, 2012: p. doi:10.1038/protex.2012.034.
14. Higa, K.C., et al., *The RGSGR amino acid motif of the intercellular signaling protein, HetN, is required for patterning of heterocysts in Anabaena sp. strain PCC 7120.* Mol. Microbiol., 2012. **83**: p. 682-693.
15. Li, B., X. Huang, and J. Zhao, *Expression of hetN during heterocyst differentiation and its inhibition of hetR up-regulation in the cyanobacterium Anabaena sp. PCC 7120.* FEBS Lett., 2002. **517**: p. 87-91.
16. Mariscal, V., A. Herrero, and E. Flores, *Continuous periplasm in a filamentous, heterocyst-forming cyanobacterium.* Mol. Microbiol., 2007. **65**: p. 1139-1145.

17. Merino-Puerto, V., et al., *Fra proteins influencing filament integrity, diazotrophy and localization of septal protein SepJ in the heterocyst-forming cyanobacterium Anabaena sp.* Mol. Microbiol., 2010. **75**: p. 1159-1170.
18. Mullineaux, C.W., et al., *Mechanism of intercellular molecular exchange in heterocyst-forming cyanobacteria.* EMBO J, 2008. **27**: p. 1299-1308.
19. Norris, M.H., et al., *Stable site-specific fluorescent tagging constructs optimized for Burkholderia species.* Appl. Env. Microbiol., 2010. **76**: p. 7635-7640.
20. Raskin, D.M. and P.A.J. de Boer, *Rapid pole-to-pole oscillation of a protein required for directing division to the middle of Escherichia coli.* Proc Natl Acad Sci U S A, 1999. **96**(9): p. 4971-6.
21. Risser, D.D. and S.M. Callahan, *Mutagenesis of hetR reveals amino acids necessary for HetR function in the heterocystous cyanobacterium Anabaena sp. strain PCC 7120.* J. Bacteriol., 2007. **189**: p. 2460-2467.
22. Risser, D.D. and S.M. Callahan, *HetF and PatA control levels of HetR in Anabaena sp. strain PCC 7120.* J. Bacteriol., 2008. **190**: p. 7645-7654.
23. Risser, D.D. and S.M. Callahan, *Genetic and cytological evidence that heterocyst patterning is regulated by inhibitor gradients that promote activator decay.* Proc. Natl. Acad. Sci. USA, 2009. **106**(47): p. 19884-19888.
24. Risser, D.D. and S.M. Callahan, *Genetic and cytological evidence that heterocyst patterning is regulated by inhibitor gradients that promote activator decay.* Proceedings of the National Academy of Sciences, 2009. **106**(47): p. 19884-19888.
25. Rivers, O.S., P. Videau, and S.M. Callahan, *Mutation of sepJ reduces the intercellular signal range of a hetN-dependent paracrine signal, but not of a patS-dependent signal, in the filamentous cyanobacterium Anabaena sp. strain PCC 7120.* Mol. Microbiol., 2014. **94**(6): p. 1260-1271.
26. Sun, Q. and W. Margolin, *FtsZ Dynamics during the Division Cycle of Live Escherichia coli Cells.* J Bacteriol, 1998. **180**(8): p. 2050-6.
27. Videau, P., et al., *Transcriptional dynamics of developmental genes assessed with an FMN-dependent fluorophore in mature heterocysts of Anabaena sp. strain PCC 7120.* Microbiol., 2014. **160**(9): p. 1874-1881.
28. Wei, T.-F., R. Ramasubramanian, and J.W. Golden, *Anabaena sp. strain PCC 7120 ntcA gene required for growth on nitrate and heterocyst development.* J. Bacteriol., 1994. **176**: p. 4473-4482.
29. Wu, X., et al., *patS minigenes inhibit heterocyst development of Anabaena sp. strain PCC 7120.* J. Bacteriol., 2004. **186**: p. 6422-6429.
30. Yoon, H.-S. and J.W. Golden, *Heterocyst pattern formation controlled by a diffusible peptide.* Science, 1998. **282**: p. 935-938.
31. Zhang, L.-C., et al., *Existence of periplasmic barriers preventing green fluorescent protein diffusion from cell to cell in the cyanobacterium Anabaena sp. strain PCC 7120.* Mol. Microbiol., 2008. **70**: p. 814-823.

Chapter 4. HetN, But Not PatS, is Transported From Cell to Cell Via SepJ-Dependent Intercellular Protein Channels

Introduction

The components of many signaling systems are known, but less is understood about the delivery of signaling molecules to target cells [36]. This is particularly true for developmental signals that govern the formation and maintenance of patterns of cellular differentiation. Morphogens are developmental signaling molecules that satisfy two criteria: they act at a distance from their source of production, and they influence the developmental fate of target cells in a concentration-dependent manner [35, 37]. When the spatial scale of developmental patterns is considered, the first criterion implies that most morphogens are paracrine signals; however, there are exceptions [1]. The second criterion is often manifested in the creation of a concentration gradient of signal emanating from source cells. The signal molecule effects different developmental fates on target cells based on their position within the gradient and, consequently, on distance from the source. In both cases, distribution of the morphogen signal is critical.

Several transport mechanisms are used in eukaryotic organisms. Proteinaceous paracrine signals move by diffusion through extracellular spaces, cell membranes, gap junctions in animals and plasmodesmata in plants [24]. Active transport occurs by transcytosis, the uptake of a signal by endocytosis on one side of a cell followed by its release by exocytosis on another, and by cytonemes, which are filopodia specialized for the transfer of signaling molecules [23]. Developmental signals dispersed by these various transport mechanisms pattern multicellular organisms that have capabilities not available to single cells.

Intercellular signaling regulates a variety of processes in bacteria, most notably as part of quorum-sensing systems. In quorum sensing, individual cells communicate with short peptides or other small molecules that are secreted into the surrounding medium to coordinate the behavior of multiple cells (Reviewed in, [28]). As a counterpoint to quorum sensing, signaling between cells in direct physical contact allows signals to pass directly between cells, without an intermediate extracellular stage. Examples include signaling during the formation of transient multicellular structures, such as the development of spores in *Bacillus subtilis* and in the fruiting bodies elaborated by *Myxococcus xanthus*, or in bacteria that grow as multicellular organisms, such as filamentous streptomycetes and cyanobacteria. In the latter of these examples, inhibitors of cellular differentiation in filamentous cyanobacteria are thought to move from cell to cell and govern the periodic patterning of heterocysts that form in response to deprivation of fixed nitrogen.

The ability to pass developmental signals from their source to the adjacent cells or tissues can be achieved in several ways depending on the organism. The filamentous cellular arrangement of *Anabaena* affords three potential routes for developmental signals to pass from cell to cell. The filaments of *Anabaena* have a Gram-negative cell wall arrangement were the cytoplasmic membranes of different cells are separate, but the outer membrane is contiguous, enclosing the entire filament. The periplasmic space produced by such an arrangement of cells is also contiguous and there is evidence both for and against the diffusion of proteins between cells via the periplasmic space [18, 41, 42]. If the predicted signal sequence of HetN functions to insert the protein into the cytoplasmic membrane than it is possible for the N-terminal hydrophilic domain,

containing the ERGSGR sequence, to be present in the contiguous periplasm where it could be released and allowed to move from cell to cell via the periplasm. This would be consistent with the finding that exogenous RGSGR peptide added to the medium inhibits the formation of heterocysts in N- conditions [40], suggesting that once present in the periplasmic space a system to import the peptide into the cytoplasm is present. A second potential route of transfer is direct exchange between the membranes of adjacent cells. This transport could be achieved by the dispersal of membrane fragments and could be similar to the movement of morphogens via argosomes within *D. melanogaster* [12]. The third potential route of transfer between cells is direct movement from the cytoplasm of the source cell(s) to the cytoplasm of adjacent cells. Protein channels are present at the junctions between vegetative cells and at the junctions between vegetative cells and heterocysts in cyanobacteria closely related to *Anabaena* [10]. Visualization using electron microscopy has identified the presence of multiple different sized channels connecting the cytoplasms of adjacent vegetative cells and connecting vegetative cells to heterocysts [30, 39].

The protein channels effectively allow for exchange from one cytoplasm to the next along the filaments. Proteins like SepJ, FraC, and FraD have been found to comprise some portion of these intercellular protein channels [21, 25]. The protein SepJ has three domains: an N-terminal coiled-coil domain, a central linker, and a C-terminal permease domain, consistent with proteins involved in channel formation [19]. Mutants in which *sepJ* was deleted from the chromosome were impaired in the ability to differentiate heterocysts and to transport calcein, a 624 kDa fluorescent dye, from cell to cell [8, 26, 27]. The Δ*sepJ* strain maintained the ability to transport fluorescein, a 354 kDa

fluorescent dye, indicating that a *sepJ* mutation only partially disrupts channel formation [22]. Mutants in which *fraD* or *fraC* were deleted from the chromosome were impaired in the ability to differentiate heterocysts, transport calcein, and transport fluorescein [21]. Localization of SepJ was also impaired in *fraC* or *fraD* mutants [20]. The findings indicate that the filaments have multiple different channels, which could be used for the movement of different sized molecules. Collectively the proteins involved in the formation of proteinacious channels connecting the cytoplasms of adjacent cells has been termed the septosome within *Anabaena* filaments [39].

To determine if the inhibitory signals produced by *hetN* and *patS* utilize SepJ-dependent protein channels for movement, a mutant strain was created. Strain UHM197, Δ*patA* Δ*sepJ* P_{petE}-*hetR*-GFP, was grown in N- medium and the presence or absence of HetR-GFP fluorescence in cells adjacent to proheterocysts indicated the presence or absence of PatS or HetN-dependent inhibition. Proheterocysts were identified with alcian blue staining and fluorescence microscopy to ensure the presence of autofluorescence. Alcian blue is a stain that identifies heterocyst-specific exopolysaccharide produced in proheterocysts before morphogenesis occurs. The presence of autofluorescence within a proheterocyst stained with alcian blue indicated that the cell is undergoing differentiation but is not yet a fully mature heterocyst. Identification and utilization of proheterocysts was required due to the fragmentation phenotype present in strains lacking functional *sepJ* [9, 27]. The average signal range produced by proheterocysts in UHM197 was compared to the average signal range produced by Δ*patA* P_{petE}-*hetR*-GFP. The comparison indicated that SepJ contributes to the intercellular movement of a *patS*- or *hetN*-dependent inhibitory signal.

To individually assess the contribution of SepJ to the movement of the inhibitory signals dependent on HetN or PatS a mosaic filament experiment was utilized. Replicative vectors expressing *hetN* and YFP, or *patS* and YFP were introduced into strain UHM218, Δ*patA* Δ*hetF* Δ*sepJ* P_{petE}-*hetR*-CFP, and viewed 72 hours post-conjugation. The average signal ranges produced in UHM218 and UHM191, Δ*patA* Δ*hetF* P_{petE}-*hetR*-CFP, by either of the inhibitors were compared to determine any significant difference.

As a negative control, mosaic filaments of strain UHM218 containing a plasmid expressing YFP alone were observed. The expected result is that CFP fluorescence will be detected in all cells and YFP fluorescence will be detected in a subset of those same cells, indicating that the introduction of a plasmid expressing the YFP fluorophore alone does not change the pattern of fluorescence present in UHM218.

The presence of multiple different sized protein channels suggests that developmental signals may move from cell to cell through channels specific to each signal being passed. To determine if the absence of SepJ and FraD-dependent protein channels prevents movement of the inhibitory signal produced by HetN, mosaic filament experiment was utilized. Replicative vectors expressing *hetN* and YFP were introduced into strain UHM265, Δ*patA* Δ*hetF* Δ*sepJ* Δ*fraD* P_{petE}-*hetR*-CFP, and viewed 72 hours post-conjugation. The presence or absence of a signal range in the resulting mosaic filaments determined if SepJ and FraD are required for the intercellular exchange of the HetN-dependent inhibitory signal.

Materials and Methods

Culture conditions. *Anabaena* sp. PCC 7120 and its derivatives were grown in BG-11 medium containing 17.6 mM nitrate as previously described [4]. Media were supplemented with neomycin at 45 μg ml^{-1} or spectinomycin and streptomycin at 2.5 μg ml^{-1} each as appropriate. *Escherichia coli* strains were grown in Luria-Bertani (LB) broth for liquid cultures and LB solidified with 15% agar for plate cultures. For selective growth, media were supplemented with 50 μg ml^{-1} kanamycin. To induce the copper inducible *petE* promoter, media were supplemented with 2 μM $CuSO_4$. Plasmids were conjugated from *E. coil* to *Anabaena* as previously described [7]. Genetic mosaic filaments were created as previously described [32].

Plasmid construction. Plasmids and oligonucleotide primers used in this study are described in Tables 7 and 8, respectively. Plasmid pSMC249 is a mobilizable shuttle vector based on pBBR1MCS [17] containing a cassette conferring resistance to spectinomycin and streptomycin. The spectinomycin and streptomycin resistance cassette was excised as a *Hind*III fragment from pDW9 [11], blunt-ended, and cloned into the blunt-ended *Nco*I-*Aat*II sites of pBBR1MCS [17] to create pSMC249.

Plasmid pSMC262 is a mobilizable shuttle vector containing P_{petE} transcriptionally fused to *hetN* transcribed divergently from the *nir* operon promoter (P_{nir}) transcriptionally fused to YFP. The coding region of YFP was amplified via PCR using pUC57-P_{S12}-yfp [29] as a template with the primers Turbo-NdeI-F and Turbo-PstI-R and the product was cloned into the *Eco*RV site of pBlueScript SK+. A *Nde*I-*Sal*I fragment from pDR324 [33] containing P_{nir} was cloned into the same sites upstream of YFP in

pBlueScript SK+ to create a P_{nir}-YFP fusion in pSMC265 [15]. The P_{nir}-YFP fusion was moved as a *Sal*I-*Eco*RI fragment into the same sites of pDR320 [33] to create pSMC262.

Plasmid pSMC266 ia a mobilazable shuttle vector containing P_{nir}-YFP. The P_{nir}-YFP insert was moved as a *Sal*I-*Eco*RI fragment from pSMC265 [15] into the same sites of pAM504 to create pSMC266.

Plasmid pST314 is a mobilizable shuttle vector containing P_{nir}-*YFP* transcribed divergently from the *petE* promoter. A *Bam*HI-*Sac*I fragment containing P_{petE}-*patS* was excised from pDR211 [33] and cloned into the same sites in pSMC249 to create pST242. The *nir* promoter was amplified by PCR using pSMC188 [31] as a template with the primers Pnir-BamHI-F and Pnir-Venus-R and fused by overlap extension PCR to the coding region of YFP, which was amplified cytoplasmic EKAR [13] with the primers Pnir-Venus-F and Venus-ApaI-R. The productwas cloned into the *Eco*RV site of pBlueScript SK+ (Stratagene) generating pST250 and moved as a *Bam*HI-*Apa*I fragment into the same sites in pST242 to create pST244. A *Sac*I-*Apa*I fragment containing P_{nir}-*YFP* was excised from pST244 and cloned into the same sites in pBBR1MCS-2 [16] to create pST259. The *petE* promoter was amplified by PCR using pDR211 [33] as a template with the primers PpetE-BamHI-F and PpetE-SacI-SmaI-R and cloned into the *Eco*RV site of pBlueScript SK+ to create pST262. A fragment containing P_{nir}-*YFP* and P_{petE} was amplified from pST262 with the primers Venus-EcoRI-R and PpetE-SacI-SmaI-R and cloned as a *Sac*I-*Eco*RI fragment into the same sites in pAM504 to create pST314.

Plasmid pTM148 is a mobilizable shuttle vector containing P_{PetE}-*patS* transcribed divergently from P_{nir}-*YFP*. The primers M475L-patS17-F and M475L-PatS17-R containing the coding region of *patS* and a 3' *Sac*I overhandwere annealed together and

cloned into the *Sma*I-*Sac*I sites of pST314. A *Sal*I-*Eco*RI fragment containing P_{PetE}-*patS* was excised and cloned into the same sites in pAM504 to create pTM137. A *Sal*I-*Eco*RI fragment containing P_{nir}-*YFP* was excised from pSMC266 and cloned into the same sites in pTM137 to create pTM148.

Plasmid pPJAV173 is a suicide vector used to cleanly delete the *fraD* coding region by allelic replacement. Regions upstream and downstream of the *fraD* coding region were amplified by PCR from chromosomal DNA with the primer sets fraD-up-F and fraD-up-R and fraD-down-F and fraD-down-R, respectively. These fragments were amplified by overlap extension PCR and the product was cloned into the *Eco*RV site in pBlueScript SK+. The entire insert, comprised of both upstream and downstream regions, was cloned as a *Bam*HI-*Sac*I fragment into the same the sites on pRL278 [2] to create pPJAV173.

Strain construction. Table 7 lists the strains used in this study. Replacement of chromosomal DNA was done as previously described [3]. Strains UHM197 and UHM218 were created by the introduction of the suicide vector pAN120 [27] to Δ*patA* P_{petE}-*hetR-GFP* [33] and UHM191 to create UHM197 (Δ*patA* Δ*sepJ* P_{petE}-*hetR-GFP*) and UHM218 (Δ*patA* Δ*hetF* Δ*sepJ* P_{petE}-*hetR-CFP*), respectively. Strain UHM265 was created by the introduction of the suicide vector pPJAV173 to UHM218 to create UHM265 (Δ*patA* Δ*hetF* Δ*sepJ* Δ*fraD* P_{petE}-*hetR-CFP*). PCR with primers that anneal outside of the regions of *Anabaena* DNA used on pAN120 or pPJAV173 for strain construction was performed individually. The size of the various PCR products was used to confirm the presence of the introduced constructs, respectively.

Microscopy and determination of signal ranges. Cells were routinely viewed and imaged as previously described [3]. Confocal microscopy was completed using an Olympus Fluoview 1000 laser scanning confocal mounted on an IX81 motorized inverted microscope. Fluorescence from Turbo-YFP was detected with an excitation of 525 nm and an emission of 538 nm. Fluorescence from CFP was detected with an excitation of 436 nm and an emission of 485 nm. All images were processed in Adobe Photoshop CS2. To determine the signal range of the inhibitors produced in source cells, the peak pixel intensity along a line drawn through a cell perpendicular to the filament axis was determined for 20 cells adjacent to source cells using the plot profile function in ImageJ. The largest number of contiguous cells adjacent to the source that fell below a threshold value, twice the value measured in control cells without the fluorophore, was taken as the signal range measured in cell numbers.

Alcian blue staining. Heterocyst-specific exopolysaccharide was stained with alcian blue as previously described [14].

Table 7. Strains and Plasmids used in Chapter 4

Strain or Plasmid	**Relevant Characteristic(s)***	**Source or Reference**
***Anabaena* sp. strains**		
PCC 7120	Wild-type	Pasteur Culture Collection
Δ*patA* P_{petE}-*hetR-GFP*	*patA*-deletion strain with chromosomal P_{hetR}-*hetR* replaced by P_{petE}-*hetR-GFP*	[33]
UHM191	Δ*patA* Δ*hetF* P_{petE}-*hetR-CFP*	This study
UHM197	Δ*patA* Δ*sepJ* P_{petE}-*hetR-GFP*	This study
UHM218	Δ*patA* Δ*hetF* Δ*sepJ* P_{petE}-*hetR-CFP*	This study
UHM265	Δ*patA* Δ*hetF* Δ*sepJ* Δ*fraD* P_{petE}-*hetR-CFP*	This study
Plasmids		
pAM504	Shuttle vector for replication in *E. coli* and *Anabaena*; Km^r Nm^r	[38]
pRL277	Suicide vector; Sp^r Sm^r	[5]
pRL278	Suicide vector; Km^r Nm^r	[5]
pAN120	pRL277 used to mutate *sepJ*	[27]
pUC57-PS12-yfp	Plasmid used as template for YFP	[29]
pSMC249	pBBR1MCS broad-host range cloning vector; Sp^r Sm^r	This study
pST314	pAM504 with P_{nir}-YFP transcribed divergently from P_{petE}	This study
pPJAV173	pRL278 used to delete *fraD*	This study
pTM148	pAM504 with P_{petE}-*patS* transcribed divergently from P_{nir}-YFP	This study
pSMC262	pAM504 with P_{petE}-hetN and P_{nir}-YFP	This study
pSMC266	pAM504 with P_{nir}-YFP	This study

*Km, kanamycin; Nm, neomycin; Sm, streptomycin; Sp, spectinomycin

Table 8. Oligonucleotide primers used in Chapter 4

Oligonucleotide*	Sequence
Turbo-NdeI-F	TATATATATACATATGAGCAGCGGCGCCCTGCTGTTC
Turbo-PstI-R	CTGCAGTCAGCTGGTGTCTCCGGAACC
Pnir-BamHI-F	ATATAGGATCCAGCTACTCATTAGTTAAGTGTAATG
Pnir-Venus-R	CCTTGCTCACCATGTTCTCATAAAGTTTTTTTGCTCA AG
Pnir-Venus-F	CTTTATGAGAACATGGTGAGCAAGGGCGAGGAGCTG
Venus-ApaI-R	ATATAGGGCCCCTCGTCCATGCCGAGAGTGATC
PpetE-BamHI-F	ATATAGGATCCCTGAGGTACTGAGTACACAG
PpetE-SacI-SmaI-R	ATATAGAGCTCCCCGGGGTTCTCCTAACCTGTAGTTT TATTTTTC
Venus-EcoRI-R	GAATTCTCACTCGTCCATGCCGAGAGTGATCCC
M475L-patS17-F	ATGAAGGCAATTATGTTAGTGAATTTCTGTGATGAGC GCGGTAGTGGTAGATAGGAGCT
M475L-PatS17-R	CCTATCTACCACTACCGCGCTCATCACAGAAATTCAC TAACATAATTGCCTTCAT
fraD-up-F	GGATCCCTTACACCCGTTCTCAACAGAAAATCTG
fraD-up-R	CCTGAGAACCCGGGTCCGAAAAGGTCTTTAAATAATA AATTCACAAG
fraD-down-F	TTTTCGGACCCGGGTTCTCAGGTGCAGCGCCACCGCA GCAG
fraD-down-R	GAGCTCCCATAGACAGCATTACCCATGAGTG

*Oligonucleotides are shown in the 5' to 3' direction

Results

SepJ and movement of developmental signals away from proheterocysts.

SepJ-dependent intercellular channels represent a potential route of transfer of the inhibitory signals between cells within *Anabaena* filaments. To examine the involvement of SepJ in the intercellular transfer of the inhibitory signals produced by *hetN* and *patS* proheterocysts were examined in Δ*patA* P_{petE}-*hetR-GFP* and UHM197 (Δ*patA* Δ*sepJ* P_{petE}-*hetR-GFP*) between 14 and 17 hours after the induction of differentiation. Proheterocysts in Δ*patA* P_{petE}-*hetR-GFP* produced an average signal range of 6.25 ± 0.4 cells (n=28) (Fig. 15A). Proheterocysts in UHM197 produced an average signal range of 4.62 ± 0.39 cells (n=27) (Fig. 15B). The presence of a signal range in UHM197 suggests that SepJ is not required for the intercellular transfer of inhibitory signals within *Anabaena*. Comparison of the two data sets with a Levene's test yielded a value of 0.049, which is significant, indicating that the data sets do not have equal variances and a Students t-test should not be used for comparisons. Comparison of the two data sets with a Welchs t-test, a statistical comparison that does not require equal variance in the data sets, yielded a p-value of 0.005, indicating a significant difference in the two data sets. The results suggest that mutation of *sepJ* influences the movement of one or both of the inhibitory signals within the *Anabaena* developmental system.

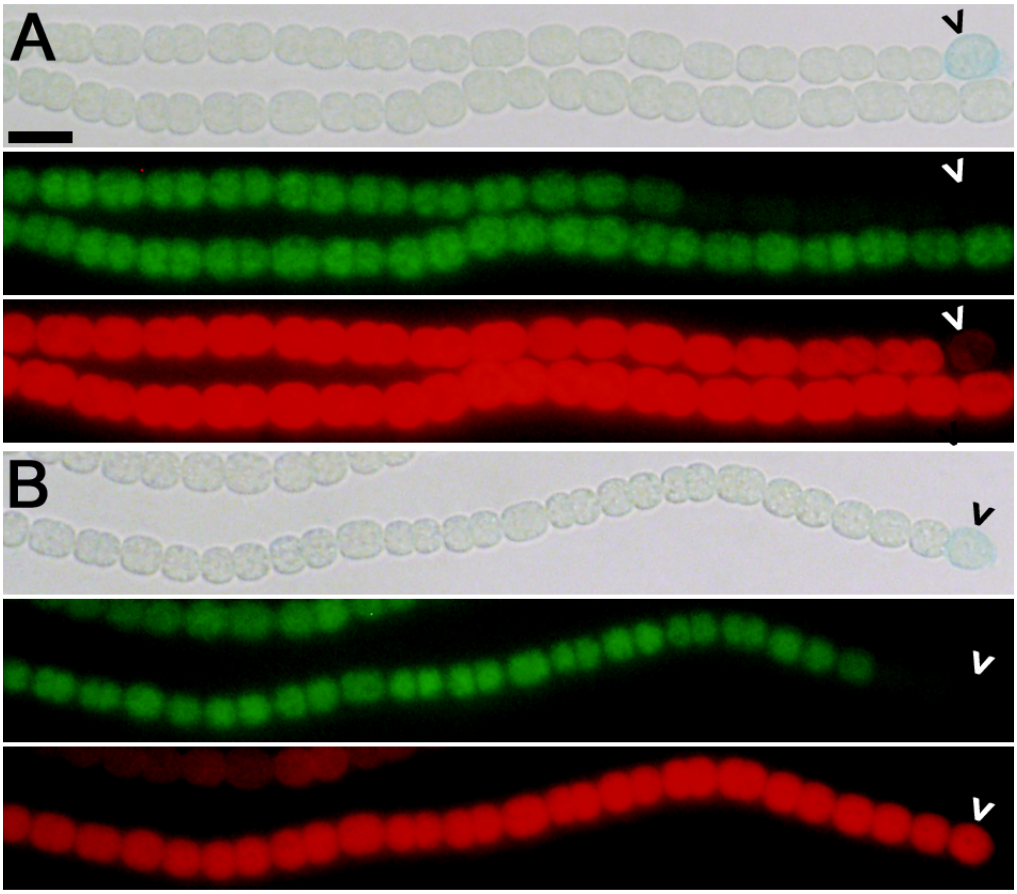

Figure 15. The inhibitory signal range emanating from proheterocysts is reduced in a strain lacking a functional *sepJ* gene. A filament of Δ*patA* P_{petE}-*hetR-GFP* stained with alcian blue 14-17 hours after the induction of differentiation (average signal range 6.25 ± 0.4 cells; A). A filament of UHM197, Δ*patA* Δ*sepJ* P_{petE}-*hetR-GFP*, which was created by mutation of *sepJ* in strain Δ*patA* P_{petE}-*hetR-GFP*, stained with alcian blue 14-17 hours after the induction of differentiation (average signal range of 4.62 ± 0.39; B). From top to bottom: bright-field, green fluorescence from HetR-GFP, red

SepJ and movement of the *hetN*-dependent signal between vegetative cells.

To examine the involvement of SepJ in the intercellular transfer of the *hetN*-dependent signal, a mosaic filament was created by introduction of plasmid pSMC262, which encodes the genes for HetN and YFP, into strain UHM218, which has *sepJ* inactivated. UHM218 was created from strain UHM191 by replacement of a portion of *sepJ* with an

Ω interposon. When strain UHM191, which has *sepJ* intact, and plasmid pSMC262 were used in chapter 3, an average signal range of 8.3 ± 0.4 cells was observed for HetN produced in vegetative cells. In contrast, the average signal range of HetN produced in vegetative cells of the *sepJ* strain UHM218 was 3.7 ± 0.5 cells (n=30; Fig. 16A)[34]. Comparison of the data sets collected from the strains with (UHM191) and without (UHM218) *sepJ* intact with a Levene's test yielded a value of 0.28, indicating that comparison of the data sets with a Students *t*-test was appropriate. Comparison with a Students *t*-test yielded a *P*-value of <0.001, indicative of a significant difference between the two data sets. The control plasmid pSMC266, which lacks *hetN*, was used to create a mosaic filament in strain UHM218, and no loss of HetR-CFP was observed (Fig. 16B)[34]. These results indicate that deletion of *sepJ* reduced the number of cells to which the HetN-dependent inhibitory signal was transferred from vegetative source cells.

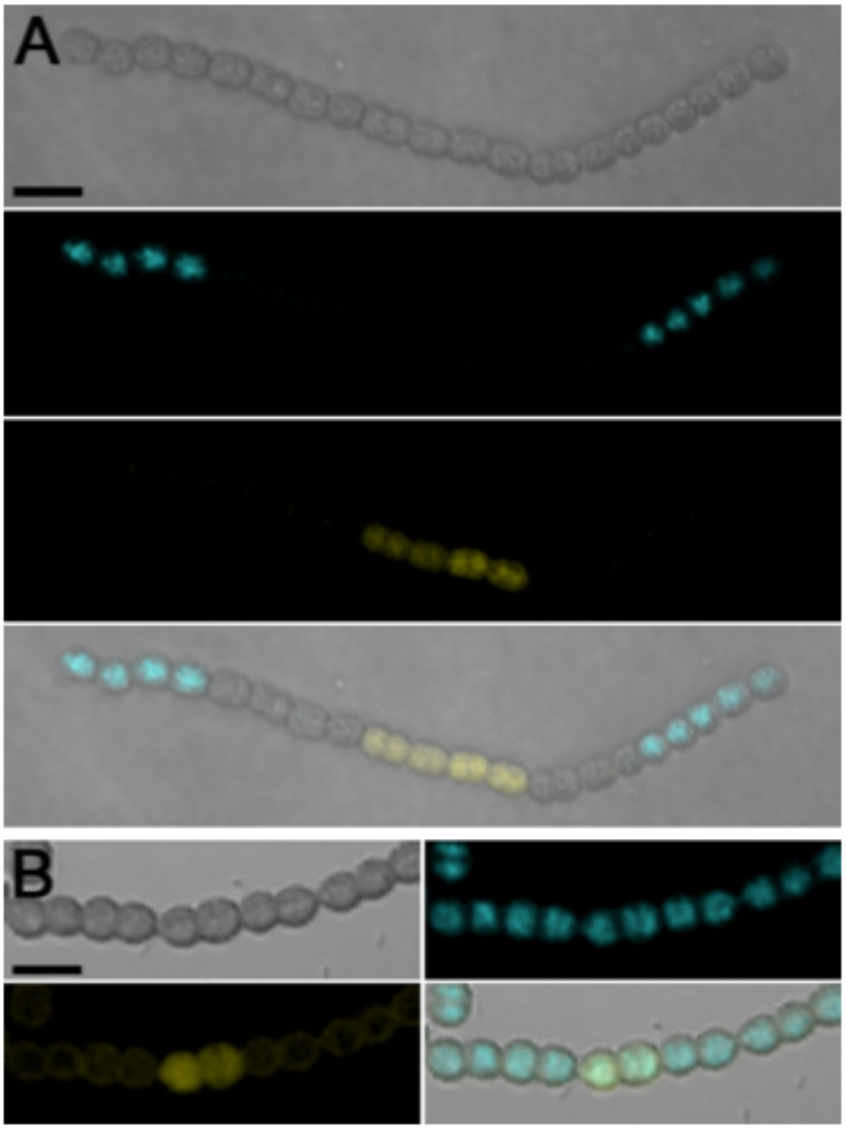

Figure 16. The hetN-dependent signal range is reduced in a strain lacking a functional *sepJ* gene. A mosaic filament of UHM218, which was created by mutation of *sepJ* in strain UHM191, with plasmid pSMC262, which encodes HetN and YFP (average signal range of 3.7 ± 0.5 cells; A). From top to bottom: bright-field, blue fluorescence from HetR-CFP, yellow fluorescence from YFP, and a composite image. A mosaic filament of UHM218 with plasmid pSMC266, which encodes YFP alone as a control (average signal range of 0 cells; B). Top left: bright-field; top right: blue fluorescence from HetR-CFP; bottom left: YFP; bottom right: composite image. Scale bar, 10 μm.

SepJ and movement of the *patS*-dependent signal between vegetative cells.

To examine the potential involvement of SepJ in the intercellular transfer of the PatS-dependent developmental signal, introduction of plasmid pTM148, which includes the genes encoding PatS and YFP, was used to make mosaic filaments with strains UHM191 and UHM218. The average signal ranges from vegetative source cells expressing *patS* in the two strains, which differ only by lack of SepJ in the latter, were compared. When *patS* was expressed in vegetative source cells of strain UHM191, the average signal range was 13.3 ± 0.96 (n = 10; Fig. 17A). When UHM218 was used as the background strain, the average signal range was 14 ± 1.1 (n = 17; Fig. 17B)[34]. Comparison of the data sets collected from strains with (UHM191) and without (UHM218) *sepJ* intact with a Students *t*-test yielded a *P*-value of 0.67 (Levene's test = 1.95), indicative of no significant difference between the two data sets. As with strain UHM191, introduction of control plasmid pSCM266, which lacks *patS* but has the gene encoding YFP, to strain UHM218 resulted in a signal range of 0 (Fig. 16B)[34]. Because the average signal ranges of vegetative cells expressing *patS* in strains UHM191 and UHM218 were similar, we conclude that the presence or absence of SepJ did not influence transfer of the *patS*-dependent signal between vegetative cells.

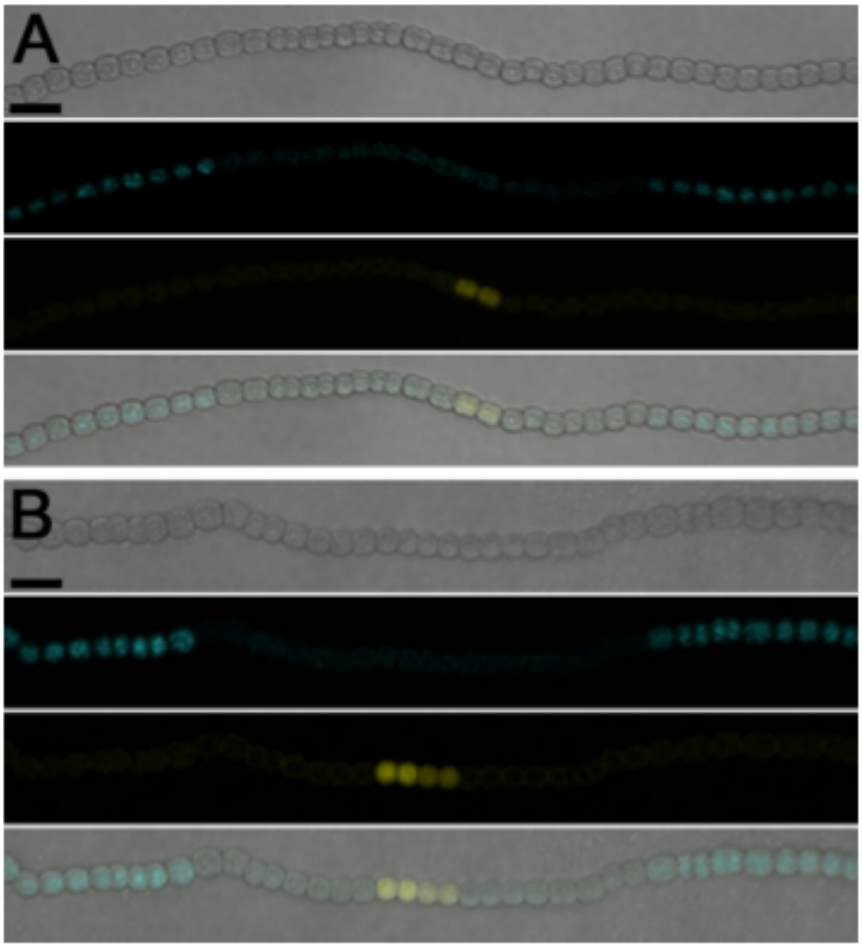

Figure 17. The *patS*-dependent signal range is unaffected in a strain lacking a functional *sepJ* gene. A mosaic filament of UHM191, which has an intact *sepJ* gene (average signal range of 13.1 ± 0.96 cells; A), or UHM218, which has a mutated *sepJ* gene (average signal range of 14 ± 1.1 cells; B), using plasmid pTM148, which encodes PatS and YFP. From top to bottom: bright-field, blue fluorescence from HetR-CFP, yellow fluorescence from YFP, and a composite image. Scale bars, 10 μm.

FraD and movement of the *hetN*-dependent signal between vegetative cells.

FraD-dependent intercellular channels represent a second potential route of transfer of the inhibitory signals between cells of *Anabaena* filaments. To examine the involvement of FraD in the intercellular transfer of the *hetN*-dependent signal, a mosaic filament was created by introduction of plasmid pSMC262, which encodes the genes for HetN and YFP, into strain UHM265, which has *fraD* deleted from the chromosome. UHM265 was

created from strain UHM218 by deletion of a majority of *fraD*. The resulting strain lacks both *fraD* and *sepJ*. When strain UHM265 and plasmid pSMC262 were used in a mosaic filament, a signal range greater than one cell was observed for HetN produced in vegetative source cells (Fig. 18). The result suggests that neither FraD nor SepJ are absolutely required for the intercellular transfer of the hetN-dependent developmental signal between vegetative cells. The lack of a sufficient number of replicate mosaic filaments to produce an average signal range when pSMC262 was used in a mosaic filament experiment with strain UHM265 does not allow for statistical comparison, and thus the contribution of FraD to the transfer of the HetN-dependent signal is inconclusive.

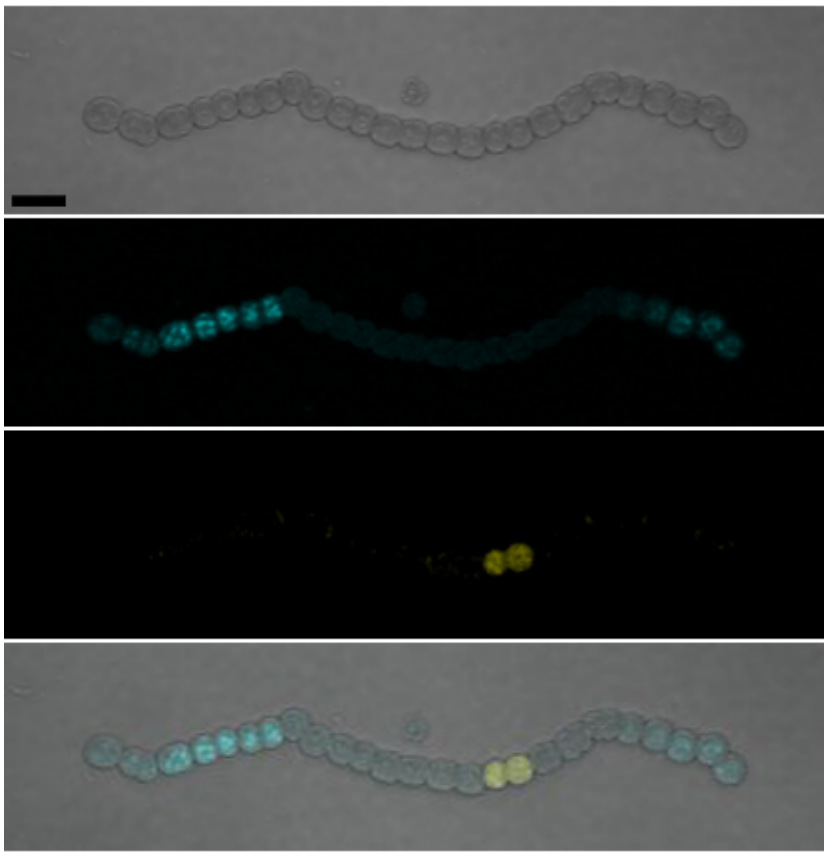

Figure 18. A hetN-dependent signal range is produced in a strain lacking *sepJ* and *fraD* function. A mosaic filament of UHM265, which was created by mutation of *fraD* in strain UHM218, with plasmid pSMC262, which encodes HetN and YFP (signal range >0). From top to bottom: bright-field, blue fluorescence from HetR-CFP, yellow fluorescence from YFP, and a composite image. Scale bar, 10 μm.

Discussion

Direct transfer from the cytoplasm of one cell to the cytoplasm of an adjacent cell via plasmodesmata in plants is referred to as symplastic transport. Movement of substances via proteinacious SepJ, FraD, or FraC channels would be the cyanobacterial equivalent of symplastic transport. The mutation of *sepJ* reduced the inhibitory signal range emanating from proheterocyst source cells within filaments of *Anabaena*. Proheterocysts were examined due to the fragmentation, resulting from mutation of *sepJ*, before the formation of morphologically distinct heterocysts. Therefore the reduction in signal range cannot be attributed to the interruption of the movement of HetN or PatS individually within a *sepJ* mutant.

When *sepJ* was mutated, the signal range of the *hetN*-dependent inhibitory signal produced in vegetative cells was reduced. The signal range of the *patS*-dependent inhibitory signal produced in vegetative cells was not reduced by the mutation of *sepJ*. This suggests PatS and HetN-dependent signals use different mechanisms of distribution between vegetative cells. Because the signal range of the *hetN*-dependent signal was not 0, mutation of *sepJ* may have only partially inactivated a single route of transfer or completely inactivated one of the multiple potential routes [21, 30]. Strains lacking SepJ are more prone to fragmentation [9, 27], so indirect effects of destabilization of cell septa cannot be ruled out as a possible explanation for the reduced signaling range. However,

the signal range of PatS was not affected by mutation of *sepJ*, suggesting that filament integrity was not significantly impaired. Because PatS is thought to be the primary regulator of initial pattern formation, the lack of an effect of mutation of *sepJ* on the *patS*-dependent signal range is consistent with the formation of a wild-type initial periodic pattern of proheterocysts in a *sepJ*-deletion strain [27]. In contrast, the *hetN*-dependent signal produced in heterocysts is thought to regulate maintenance of the periodic pattern as division of vegetative cells increases filament length and distance between existing heterocysts [6]. Movement of the inhibitors from heterocysts to vegetative cells may involve a different mechanism of transport than that used between vegetative cells. Unfortunately, the excessive fragmentation of strains lacking a functional copy of *sepJ* after induction of differentiation but prior to the production of mature heterocysts precluded examination of the effect of mutation of *sepJ* on movement of the inhibitors from heterocyst source cells. The signal range of the *hetN*-dependent inhibitor is greater than one, implying both the movement from a heterocyst to a vegetative cell and between several vegetative cells. The presence of multiple channels of different sizes connecting heterocysts to vegetative cells and connecting vegetative cells to one another [30], suggests there may be individual channels for the movement of specific molecules or that there are many different non-specific channels, which facilitate the movement of molecules between cells. Individual channels may be specific to certain sized molecules while the removal of one non-specific channel would only disrupt the movement of a class of molecules between cells. This is consistent with the reduced signal range of HetN in a *sepJ* mutant, were the *hetN*-dependent inhibitory signal could

be restricted to passage through a reduced number of non-specific channels, resulting in a reduced signal range.

The presence of a reduced signal range produced by HetN within a *sepJ* mutant implies that SepJ is not required for the movement of the *hetN*-dependent inhibitory signal between vegetative cells, but the impact on the signals range suggests that proteinacious channels may be involved in the transfer and movement of the *hetN*-dependent inhibitory signal. Proteinacious FraD channels would also be consistent with symplastic transport in cyanobacteria. When *fraD* and *sepJ* were mutated in combination the resulting strain, UHM265, was difficult to work with, fragmenting under normal N+ growth conditions. This fragmentation made it impossible to collect a large enough data set to compare the strain statistically to any other. However, there was evidence that a signal range greater than one was produced in the *fraD*/*sepJ* double mutant, suggesting that neither SepJ nor FraD are required for the movement of the *hetN*-dependent inhibitory signal between vegetative cells. In order to determine the role of protienacous channels in the movement of developmental signals within the *Anabaena* system a more complete study, mutating different predicted protienacous channel forming proteins and mutating combinations of these proteins, is necessary.

References

1. Andersson, E.R., R. Sandberg, and U. Lendahl, *Notch signaling: simplicity in design, versatility in function.* Development, 2011. **138**(17): p. 3593-612.
2. Black, T.A., Y. Cai, and C.P. Wolk, *Spatial expression and autoregulation of hetR, a gene involved in the control of heterocyst development in Anabaena.* Mol. Microbiol., 1993. **9**: p. 77-84.
3. Borthakur, P.B., et al., *Inactivation of patS and hetN causes lethal levels of heterocyst differentiation in the filamentous cyanobacterium Anabaena sp. PCC 7120.* Mol. Microbiol., 2005. **57**: p. 111-123.
4. Buikema, W.J. and R. Haselkorn, *Characterization of a gene controlling heterocyst development in the cyanobacterium Anabaena 7120.* Genes Dev., 1991. **5**: p. 321-330.
5. Cai, Y. and C.P. Wolk, *Use of a conditionally lethal gene in Anabaena sp. strain PCC 7120 to select for double recombinants and to entrap insertion sequences.* J. Bacteriol., 1990. **172**: p. 3138-3145.
6. Callahan, S.M. and W.J. Buikema, *The role of HetN in maintenance of the heterocyst pattern in Anabaena sp. PCC 7120.* Mol. Microbiol., 2001. **40**: p. 941-950.
7. Elhai, J. and C.P. Wolk, *Conjugal transfer of DNA to cyanobacteria.* Methods Enzymol., 1988. **167**: p. 747-754.
8. Flores, E., et al., *Septum-localized protein required for filament integrity and diazotrophy in the heterocyst-forming cyanobacterium Anabaena sp. strain PCC 7120.* Journal of bacteriology, 2007. **189**(10): p. 3884-3890.
9. Flores, E., et al., *Septum-localized protein required for filament integrity and diazotrophy in the heterocyst-forming cyanobacterium Anabaena sp. strain PCC 7120.* J. Bacteriol., 2007. **189**(10): p. 3884-3890.
10. Giddings, T.H. and L.A. Staehelin, *Observation of microplasmodesmata in both heterocyst-forming and non-heterocyst forming filamentous cyanobacteria by freeze-fracture electron microscopy.* Archives of Microbiology, 1981. **129**(4): p. 295-298.
11. Golden, J.W. and D.R. Wiest, *Genome rearrangement and nitrogen fixation in Anabaena blocked by inactivation of xisA gene.* Science, 1988. **242**(4884): p. 1421-1423.
12. Greco, V., M. Hannus, and S. Eaton, *Argosomes: a potential vehicle for the spread of morphogens through epithelia.* Cell, 2001. **106**(5): p. 633-45.
13. Harvey, C.D., et al., *A genetically encoded fluorescent sensor of ERK activity.* Proc. Natl. Acad. Sci. USA, 2008. **105**: p. 19264-19269.
14. Higa, K.C. and S.M. Callahan, *Ectopic expression of hetP can partially bypass the need for hetR in heterocyst differentiation by Anabaena sp strain PCC 7120.* Mol. Microbiol., 2010. **77**: p. 562-574.
15. Higa, K.C., et al., *The RGSGR amino acid motif of the intercellular signaling protein, HetN, is required for patterning of heterocysts in Anabaena sp. strain PCC 7120.* Mol. Microbiol., 2012. **83**: p. 682-693.

16. Kovach, M.E., et al., *Four new derivatives of the broad-host-range cloning vector pBBR1MCS, carrying different antibiotic-resistance cassettes.* Gene, 1995. **166**(1): p. 175-176.
17. Kovach, M.E., et al., *pBBR1MCS: a broad-host-range cloning vector.* BioTechniques, 1994. **16**: p. 800-802.
18. Mariscal, V., A. Herrero, and E. Flores, *Continuous periplasm in a filamentous, heterocyst-forming cyanobacterium.* Mol. Microbiol., 2007. **65**: p. 1139-1145.
19. Mariscal, V., et al., *Functional dissection of the three-domain SepJ protein joining the cells in cyanobacterial trichomes.* Mol Microbiol, 2011. **79**(4): p. 1077-88.
20. Merino-Puerto, V., et al., *Fra proteins influencing filament integrity, diazotrophy and localization of septal protein SepJ in the heterocyst-forming cyanobacterium Anabaena sp.* Mol Microbiol, 2010. **75**(5): p. 1159-70.
21. Merino-Puerto, V., et al., *FraC/FraD-dependent intercellular molecular exchange in the filaments of a heterocyst-forming cyanobacterium, Anabaena sp.* Mol. Microbiol., 2011. **82**: p. 87-98.
22. Merino-Puerto, V., et al., *FraC/FraD-dependent intercellular molecular exchange in the filaments of a heterocyst-forming cyanobacterium, Anabaena sp.* Molecular microbiology, 2011. **82**(1): p. 87-98.
23. Muller, P., et al., *Morphogen transport.* Development, 2013. **140**(8): p. 1621-38.
24. Müller, P. and Alexander F. Schier, *Extracellular Movement of Signaling Molecules.* Developmental Cell. **21**(1): p. 145-158.
25. Mullineaux, C.W., et al., *Mechanism of intercellular molecular exchange in heterocyst-forming cyanobacteria.* EMBO J, 2008. **27**: p. 1299-1308.
26. Mullineaux, C.W., et al., *Mechanism of intercellular molecular exchange in heterocyst-forming cyanobacteria.* The EMBO journal, 2008. **27**(9): p. 1299-1308.
27. Nayar, A.S., et al., *FraG is necessary for filament integrity and heterocyst maturation in the cyanobacterium Anabaena sp. strain PCC 7120.* Microbiology, 2007. **153**: p. 601-607.
28. Ng, W.L. and B.L. Bassler, *Bacterial Quorum-Sensing Network Architectures*, in *Annual Review of Genetics*. 2009. p. 197-222.
29. Norris, M.H., et al., *Stable site-specific fluorescent tagging constructs optimized for Burkholderia species.* Appl. Env. Microbiol., 2010. **76**: p. 7635-7640.
30. Omairi-Nasser, A., R. Haselkorn, and J. Austin, 2nd, *Visualization of channels connecting cells in filamentous nitrogen-fixing cyanobacteria.* FASEB J, 2014. **28**(7): p. 3016-22.
31. Risser, D.D. and S.M. Callahan, *Mutagenesis of hetR reveals amino acids necessary for HetR function in the heterocystous cyanobacterium Anabaena sp. strain PCC 7120.* J. Bacteriol., 2007. **189**: p. 2460-2467.
32. Risser, D.D. and S.M. Callahan, *HetF and PatA control levels of HetR in Anabaena sp. strain PCC 7120.* J. Bacteriol., 2008. **190**: p. 7645-7654.
33. Risser, D.D. and S.M. Callahan, *Genetic and cytological evidence that heterocyst patterning is regulated by inhibitor gradients that promote activator decay.* Proc. Natl. Acad. Sci. USA, 2009. **106**(47): p. 19884-19888.

34. Rivers, O.S., P. Videau, and S.M. Callahan, *Mutation of sepJ reduces the intercellular signal range of a hetN-dependent paracrine signal, but not of a patS-dependent signal, in the filamentous cyanobacterium Anabaena sp. strain PCC 7120.* Mol. Microbiol., 2014. **94**(6): p. 1260-1271.
35. Rogers, K.W. and A.F. Schier, *Morphogen gradients: from generation to interpretation.* Annu Rev Cell Dev Biol, 2011. **27**: p. 377-407.
36. Tabata, T. and Y. Takei, *Morphogens, their identification and regulation.* Development, 2004. **131**: p. 703-712.
37. Teleman, A.A., M. Strigini, and S.M. Cohen, *Shaping morphogen gradients.* Cell, 2001. **105**(5): p. 559-62.
38. Wei, T.-F., R. Ramasubramanian, and J.W. Golden, *Anabaena sp. strain PCC 7120 ntcA gene required for growth on nitrate and heterocyst development.* J. Bacteriol., 1994. **176**: p. 4473-4482.
39. Wilk, L., et al., *Outer membrane continuity and septosome formation between vegetative cells in the filaments of Anabaena sp. PCC 7120.* Cell Microbiol, 2011. **13**(11): p. 1744-54.
40. Yoon, H.-S. and J.W. Golden, *Heterocyst pattern formation controlled by a diffusible peptide.* Science, 1998. **282**: p. 935-938.
41. Zhang, L.-C., et al., *Existence of periplasmic barriers preventing green fluorescent protein diffusion from cell to cell in the cyanobacterium Anabaena sp. strain PCC 7120.* Mol. Microbiol., 2008. **70**: p. 814-823.
42. Zhang, L.C., et al., *Exploring the size limit of protein diffusion through the periplasm in cyanobacterium Anabaena sp. PCC 7120 using the 13 kDa iLOV fluorescent protein.* Res Microbiol, 2013. **164**(7): p. 710-7.

Chapter 5. *hetN* Encodes a Signal That Influences Differentiation at a Distance From Source Cells

Introduction

In multi-cellular organisms, communication between cells involves the exchange of signals that convey information over various distances. Juxtacrine signals travel exclusively between direct neighbors; paracrine signals travel over several cell diameters; and endocrine signals travel long distances, sometimes throughout an entire organism. The information in these signals is used to coordinate physiological processes on both spatial and temporal scales. Both proteins and small molecules can serve as intercellular signals. Their signaling range, the distance from the source at which a response is observed, is determined by their activity, mobility, stability, and rate of release from the source [10]. Morphogens are developmental signals produced in source cell(s) that move away from source cell(s) to determine the developmental fate of cells adjacent to the source. As morphogens move away from their source cell(s) they are communicating with cell(s) that are not producing the morphogen signal but maintain the genetic material for the production of the morphogen. Defining a protein or molecule as a morphogen thus requires the utilization of genetic mutants that are capable of reporting the presence of the morphogen signal but are incapable of morphogen production [9].

To determine if a *hetN*-dependent signal is acting as a paracrine type morphogen, a genetic mosaic filament was created. The strain used in the experiment, UHM337, has both *patS* and *hetN* cleanly deleted from the chromosome and has P_{petE}-*hetR(S179N)-CFP* at the native *hetR* locus. Cells of this strain that did not receive the plasmid described below were unable to form heterocysts and unable to propagate an inhibitory

signal through the up-regulation of *patS* or *hetN* in cells adjacent to the source. The plasmid introduced carries P_{petE}-*hetR(R250K)* to induce differentiation of all ex-conjugant cells and P_{hetN}-*hetN-YFP* to mark cells producing HetN-YFP. The native *hetN* promoter limited the production of HetN-YFP to mature heterocysts.

The experiment tested the ability of HetN-YFP to produce an inhibitory signal when expressed in a heterocyst, its normal site of production. Signal ranges of 0, 1, or >1 were predicted as possible results (Fig. 19). First, confinement of the inhibitory signal to the source heterocysts would have resulted in a signal range of 0 (Fig. 19). Second, a signal range of 1 would have been consistent with a juxtacrine signal that requires the genetic elements *patS* and/or *hetN* in cells adjacent to the source for the creation of the signal range (Fig. 19). Third, a signal range of >1 would have been indicative of a mechanism of signal movement that is independent of *patS* and *hetN* in cells adjacent to the source and consistent with a paracrine signal (Fig. 19). Results were obtained consistent with the production of a paracrine signal.

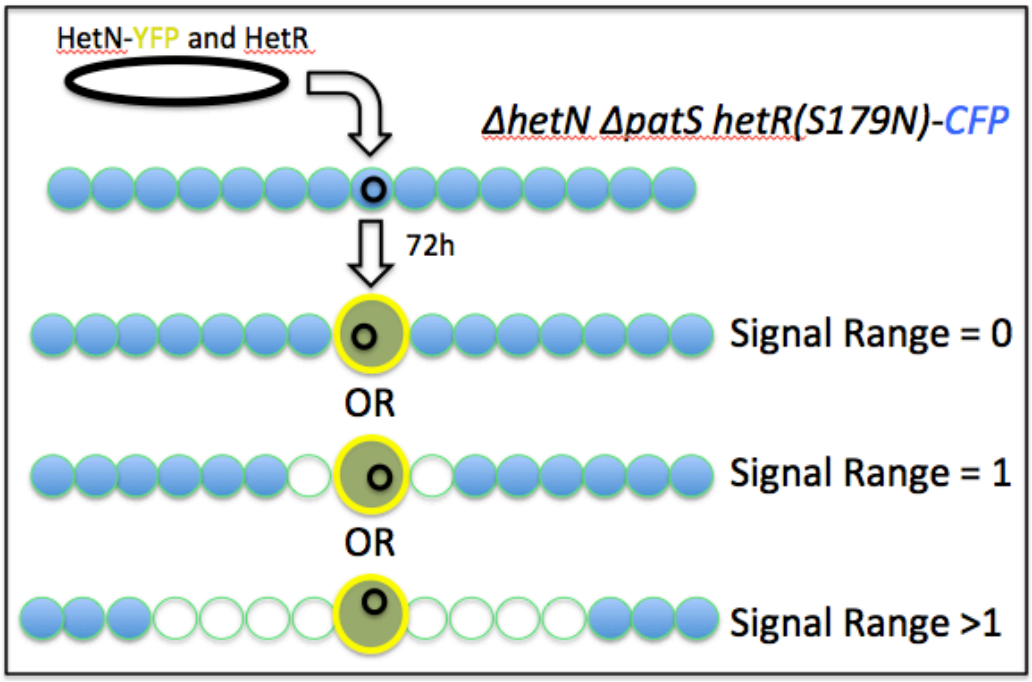

Figure 19: Determining if *hetN* encodes a signal that influences differentiation at a distance from source cells. Schematic of the three possible outcomes when a plasmid carrying HetN-YFP and HetR(R250K) is observed 72 hours after its introduction into *ΔpatS ΔhetN hetR(S179N)-CFP* during a mosaic filament experiment. Confinement of the inhibitory signal to the source heterocysts will result in a signal range of 0. A signal range of 1 would be consistent with a juxtacrine signal that requires the genetic elements *patS* and/or *hetN* in cells adjacent to the source. A signal range of >1 would be indicative of a mechanism of signal movement that is independent of *patS* and *hetN* in cells adjacent to the source and is consistent with a paracrine signal.

As a negative control a mosaic filament of strain UHM337 containing a plasmid carrying P_{petE}-*hetR(R250K)* and P_{hetN}-*hetN(R132K)-YFP,* an inactive allele of *hetN*, was observed. The expected result was that YFP and CFP would be detected in all the heterocysts that form, and CFP would be detected in all vegetative cells, indicating that neither differentiation nor the presence of an inactive form of HetN-YFP produces an inhibitory signal in cells adjacent to source heterocysts in this strain background.

Materials and Methods

Culture conditions. UHM337, *ΔpatS ΔhetN hetR(S179N)-CFP*, was grown in BG-11 medium containing 17.6 mM nitrate as previously described [3]. *Escherichia coli* strains were grown in Luria-Bertani (LB) broth for liquid cultures and LB solidified with 15% agar for plate cultures. For selective growth, media were supplemented with 50 μg ml^{-1} kanamycin. To induce the copper inducible *petE* promoter, media were supplemented with 2 μM $CuSO_4$. Plasmids were conjugated from *E. coil* to *Anabaena* as previously described [6]. Genetic mosaic filaments were created as previously described [13].

Plasmid construction. Plasmids and oligonucleotide primers used in this study are described in Tables 9 and 10, respectively. Plasmid pST201 is a mobilizable shuttle vector containing P_{petE}-*hetR*(R250K) translationally fused to GFP. The fragments used to introduce the base substitution in *hetR* were amplified via PCR using pDR293 [13] as template with the primer sets PpetE-BamHI-F and hetRR250K-R and hetRR250K-F and hetR-SmaI-R. The products were fused together by overlap extension PCR and cloned as a *Bam*HI-*Sma*I fragment into the same sites in pSMC232 [13] to create pST201.

Plasmid pPJAV153 is a mobilizable shuttle vector for constructing C-terminal translational fusions with YFP expressed from the *petE* promoter. The *petE* promoter was amplified via PCR from *Anabaena* chromosomal DNA with the primers PpetE-XhoI-F and PpetE-Cterm-OEX-R. The coding region of YFP was amplified via PCR from pUC57-P_{S12}-yfp [11] with the primers PpetE-Cterm-OEX-F and TurboYFP-CtermR-SacI. The products were fused together by overlap extension PCR and cloned as a *Xho*I-*Sac*I fragment into the *Sal*I-*Sac*I sites of pPJAV123, which is pAM504 that has the *Nde*I

site removed by digestion with *Nde*I and blunt-ending with T4 DNA polymerase followed by ligation, to create pPJAV153.

Plasmid pPJAV181 is a mobilizable shuttle vector for constructing C-terminal translational fusions with CFP expressed from the *petE* promoter. The *petE* promoter was amplified via PCR from *Anabaena* chromosomal DNA with the primers PpetE-XhoI-F and CCFP-OEX-R. The coding region of CFP was amplified via PCR from pSMC254 with the primers CCFP-OEX-F and CFP-SacI-R. The products were fused together by overlap extension PCR and cloned as a *Xho*I-*Sac*I fragment into the *Sal*I-*Sac*I sites of pPJAV123 to create pPJAV181.

Plasmid pPJAV325 is a mobilizable shuttle vector containing P_{petE}-*hetR*(R250K). A fragment containing P_{petE}-*hetR*(R250K) was amplified by PCR using pST201as a template with the primers PpetE-XhoI-F and hetR-BglII-R. The product was cloned into the *Sma*I site of pAM504 and screened by PCR to determine directionality to create pPJAV325.

Plasmid pPJAV326 is a mobilizable shuttle vector containing the promoter of *hetN* (P_{hetN}) transcriptionally fused to *hetN-YFP* transcribed divergently from P_{petE}-hetR(R250K). A fragment containing P_{hetN}-*hetN-YFP* was amplified via PCR using pRR159 [8] as a template with the primers PhetN-MunI-F and YFP-MunI-R and was cloned into the *Eco*RV site of pBlueScript SK+ (Stratagene). The P_{hetN}-*hetN-YFP* insert was moved as a *Mun*I fragment into the *Eco*RI site of pPJAV325 and screened for directionality by PCR to create pPJAV326.

Plasmid pPJAV387 is a mobilizable shuttle vector containing P_{petE}-*hetR*(S179N)-*CFP*. The coding region of *hetR*(S179N) was amplified via PCR from pDR145 [12] with

the primers HetR-F-NdeI-express and hetR-Tln-BamHI-R. The product was cloned as a *Nde*I-*Bam*HI fragment into the same sites in pPJAV181 to create pPJAV387.

Plasmid pPJAV398 is a mobilizable shuttle vector containing P_{hetN}-*hetN*(R132K)-*YFP* transcribed divergently from P_{petE}-hetR(R250K). A fragment containing P_{hetN}-*hetN*(R132K) was amplified via PCR using pDR387 [8] as a template with the primers PhetN-MunI-F and hetN-Tln-BglII-R, digested with *Bgl*II, and cloned into the *Sma*I-*Bam*HI sites in pPJAV153. P_{hetN}–*hetN*(R132K)-*YFP* was amplified via PCR from this construct with the primers PhetN-MunI-F and YFP-MunI-R. the product was cloned as a *Mun*I fragment into the *Eco*RI site in pPJAV325. This was screened for directionality by PCR to create pPJAV398.

Plasmid pOR100 is a suicide vector based on pRL277 [1] that was used to introduce P_{petE}-*hetR*(S179N) translationally fused to CFP into the native *hetR* locus. A fragment containing P_{petE}-*hetR*(S179N)-*CFP* was amplified via PCR using pPJAV387 as a template with the primers PpetE-NcoI-F and CFP-SpeI-R. The product was cloned as a *Nco*I-*Spe*I fragment into the same sites in pDR325 [14] to create pOR100.

Strain construction. Table 9 lists the strains used in this study. Replacement of chromosomal DNA was done as previously described [2]. Strain UHM337 was created by the introduction of the suicide vector pOR100 to UHM144 to create UHM337 (Δ*patS* Δ*hetN* P_{petE}-*hetR*(S179N)-*CFP*).

Microscopy and determination of signal ranges. Cells were routinely viewed and imaged as previously described [2]. Confocal microscopy was completed using an Olympus Fluoview 1000 laser scanning confocal mounted on an IX81 motorized inverted microscope. Fluorescence from Turbo-YFP was detected with an excitation of 525 nm

and an emission of 538 nm. Fluorescence from CFP was detected with an excitation of 436 nm and an emission of 485 nm. All images were processed in Adobe Photoshop CS2. To determine the signal range of the inhibitors produced in source cells, the peak pixel intensity along a line drawn through a cell perpendicular to the filament axis was determined for 20 cells adjacent to source cells using the plot profile function in ImageJ. The largest number of contiguous cells adjacent to the source that fell below a threshold value, twice the value measured in control cells without the fluorophore, was taken as the signal range measured in cell numbers.

Table 9. Strains and Plasmids used in Chapter 5

Strain or Plasmid	Relevant Characteristic(s)*	Source or Reference
***Anabaena* sp. strains**		
UHM144	Δ*patS* Δ*hetN* Δ*hetR*	[14]
UHM337	Δ*patS* Δ*hetN* P_{petE}-*hetR*(S179N)-*CFP*	This study
Plasmids		
pAM504	Shuttle vector for replication in *E. coli* and *Anabaena*; Km^r Nm^r	[16]
pRL277	Suicide vector; Sp^r/Sm^r	[4]
pUC57-PS12-yfp	Plasmid used as template for YFP	[11]
pOR100	pRL277 used to create UHM337	This study
pPJAV123	pAM504 with the NdeI site removed	This study
pPJAV153	pAM504 with P_{petE}-YFP	
pPJAV181	pAM504 with P_{petE}-CFP	This study
pPJAV325	pAM504 with P_{petE}-*hetR*(R250K)	This study
pPJAV326	pAM504 with P_{petE}-*hetR*(R250K) transcribed divergently from P_{hetN}-*hetN*-YFP	This study
pPJAV387	pAM504 with P_{petE}-*hetR*(S179N)-CFP	This study
pPJAV398	pAM504 with P_{petE}-*hetR*(R250K) transcribed divergently from P_{hetN}-*hetN*(R132K)-YFP	This study
pST201	pAM504 with P_{petE}-*hetR*(R250K)-GFP	This study

*Km, kanamycin; Nm, neomycin; Sm, streptomycin; Sp, spectinomycin

Table 10. Oligonucleotide primers used in Chapter 5

Oligonucleotide*	Sequence
PpetE-BamHI-F	ATATAGGATCCCTGAGGTACTGAGTACACAG
hetRR250K-R	CTTCTAAGGCCTTCATAGCGTTTGGC
hetRR250K-F	CAAACGCTATGAAGGCCATAGAAGAA
hetR-SmaI-R	ATATACCCGGGAATCTTCTTTTCTACCAAACACC
PpetE-XhoI-F	TATATCTCGAGGCTGAGGTACTGAGTACACAGC
PpetE-Cterm-OEX-R	ATCCGCGGGAGGATCCCCCGGGCATATGGTTCTCCTAACCTGTAGTTTTATTTTTCT
PpetE-Cterm-OEX-F	GGGATCCTCCCGCGGATCGGCGTCAGCTATGAGCAGCGGCGCCCTGCTGTTC
TurboYFP-CtermR-SacI	GAGCTCTCAGCTGGTGTCTCCGGAACCGG
PpetE-XhoI-F	TATATCTCGAGGCTGAGGTACTGAGTACACAGC
CCFP-OEX-R	CCCGGGGGATCCCGCGGATCGTCAGCTGTGAGCAAGGGCGAGGAGCTGTTC
CCFP-OEX-F	CGATCCGCGGGATCCCCCGGGCATATGGTTCTCCTAACCTGTAGTT
CFP-SacI-R	GAGCTCTTACTTGTACAGCTCGTCCATG
hetR-BglII-R	ATATAAGATCTTTAATCTTCTTTTCTACCAAACACCATTTG
PhetN-MunI-F	ATATACAATTGAGGAGAAGACGCGATGAATC
YFP-MunI-R	ATATACAATTGTCAGCTGGTGTCTCCGGAAC
HetR-F-NdeI-express	ATCGATCGCATATGAGTAACGACATCGATCTGATC
hetR-Tln-BamHI-R	GGATCCATCTTCTTTTCTACCAAACACCATTTG
hetN-Tln-BglII-R	AGATCTTGAGCGATGAGACTCAACAGCTACATAGC
PpetE-NcoI-F	AATACCATGGGCTGAGGTACTGAGTACACAGC
CFP-SpeI-R	AATAACTAGTTTACTTGTACAGCTCGTCCATGC

*Oligonucleotides are shown in the 5' to 3' direction

Results

HetN-dependent paracrine type inhibitory morphogen. Defining a protein as a paracrine type inhibitory morphogen requires rigorous experimental evidence establishing that any perceived signal range of the protein in question is not a cell-autonomous response to a second, unidentified molecule that is, in fact, the actual paracrine signal. In developmental biology this is often accomplished by creation of a group of engineered source cells within a field of cells incapable of producing the putative signal molecule being tested [15]. A response to the signal in cells distant from the source is indicative of direct action over a distance, or paracrine signaling, because the cells within the signal range are incapable of producing the signal. To determine if the HetN-dependent inhibitory signal acts in a paracrine fashion, a background strain incapable of producing HetN, PatS, and functional HetR was used to look for the presence or absence of a signal range when HetN was produced only in engineered source heterocysts. Genetic mosaic filaments were created by introduction of plasmid pPJAV326, which encodes HetN-YFP and HetR(R250K), into strain UHM337, which has *hetN* and *patS* deleted from the chromosome and P_{petE}-HetR(S179N)-CFP replacing HetR at the native *hetR* locus. Source cells were indicated by fluorescence from HetN-YFP, expression of which was from the native *hetN* promoter. Because *hetN* is expressed in proheterocysts and heterocysts in wild-type *Anabaena*, HetR(R250K), a form of HetR that is insensitive to inhibition by PatS or HetN, was used to promote the differentiation of source cells [7]. The presence or absence of fluorescence from HetR(S179N)-CFP was used to measure the signal range of HetN-YFP. An allele of *hetR* encoding an S179N substitution, rendering the protein unable to promote differentiation, was used in this case

to prevent the excessive differentiation of heterocysts seen in strains lacking PatS and HetN [2]. HetR(S179N)-GFP has been shown previously to be an efficient reporter of *patS*- and *hetN*-dependent signal ranges [14]. Figure 20 shows a representative genetic mosaic filament in which expression of *hetN*-YFP from a heterocyst source cell created a clearly discernable signal range greater that one cell. The average signal range was 13.3 ± 0.6 cells (n = 29). In contrast, when plasmid pPJAV398, which has the inactive *hetN*(R132K) allele in place of *hetN* [8], was used instead of plasmid pPJAV326, there was no detectable signal range in cells adjacent to heterocyst source cells (Fig. 20). In addition, all cells that had detectable fluorescence from YFP were heterocysts. This control demonstrated that the signal range observed with plasmid pPJAV326 was dependent on a functional copy of *hetN*. These results suggest that the *hetN*-dependent inhibitory signal produced in heterocysts acts in a paracrine fashion.

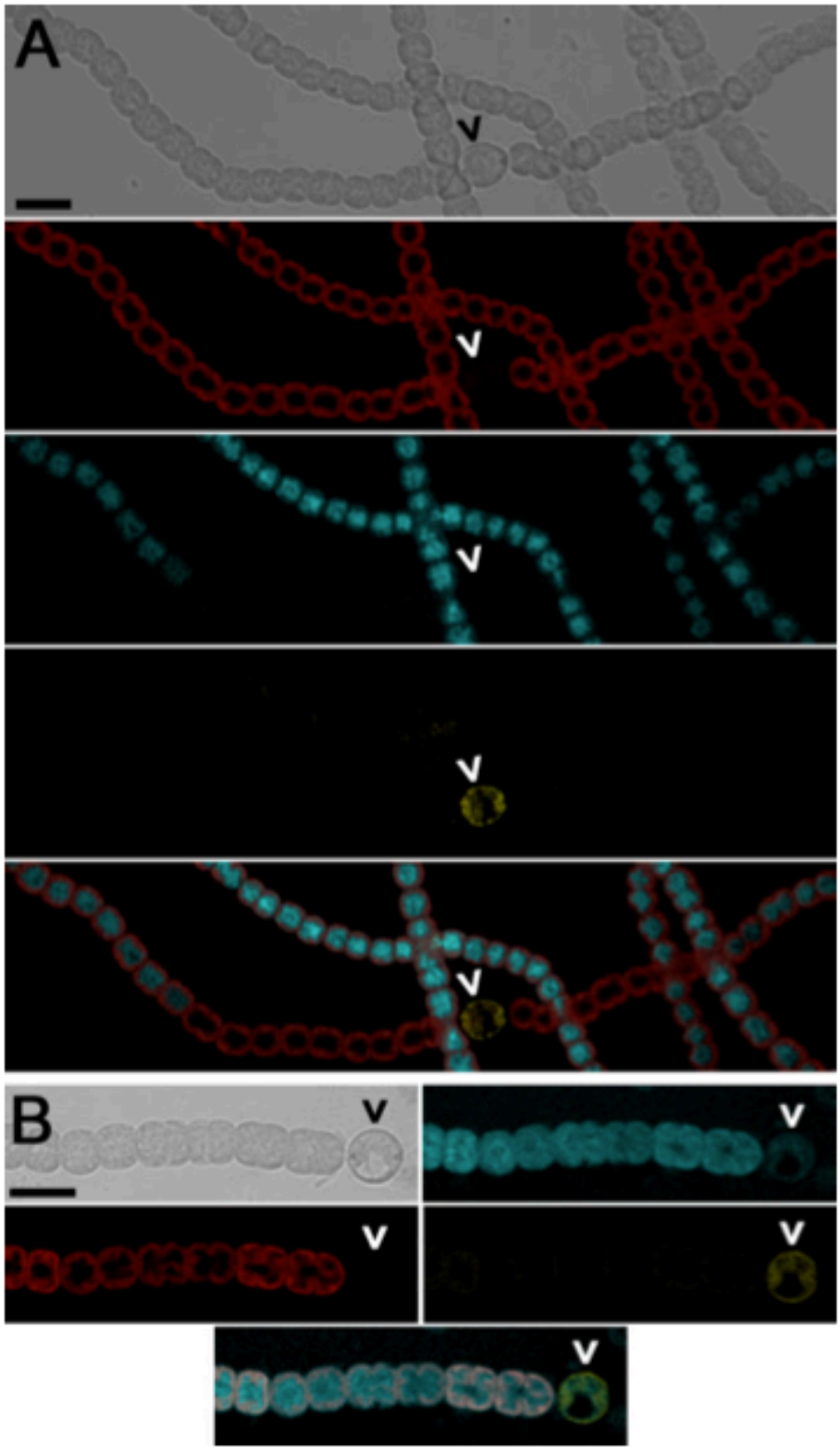
A
V
V
V
V
V
B
V
V
V
V
V

Figure 20. The HetN-dependent signal range extends over cells lacking *hetN* and *patS*. A mosaic filament of UHM337, which is Δ*hetN* Δ*patS* P_{petE}-*hetR*(*S179N*)-CFP, with plasmid pPJAV326, which encodes P_{petE}-*hetR*(*R250K*) and P_{hetN}-*hetN*-YFP (average signal range of 13.3 ± 0.6 cells; A). From top to bottom: bright-field, red autofluorescence, blue fluorescence from HetR(S179N)-CFP, yellow fluorescence from HetN-YFP, and a composite image. A mosaic filament of UHM337 with plasmid pPJAV398, which encodes P_{petE}-*hetR*(*R250K*) and P_{hetN}-*hetN*(*R132K*)-YFP as a control (average signal range of 0 cells; B). Top left: bright-field; top right: blue fluorescence from HetR(S179N)-CFP; middle left: red autofluorescence; middle right: yellow fluorescence from HetN(R132K)-YFP; bottom: composite image. Scale bars, 10 μm.

Discussion

Detection of a signaling molecule or its activity is essential for characterization of intercellular transfer. Work done to demonstrate intercellular transfer of PatS utilized an antibody directed against the amino acid sequence RGSGR, which is present in four proteins in *Anabaena* including PatS and HetN [17], to visualize levels of a PatS-dependent peptide in cells adjacent to source cells [5]. In contrast, the system described here detected the activity of the *hetN*-dependent signal, which was visualized as a loss of HetR-CFP in an area adjacent to source cells. Expression of *patS* or *hetN* was shown earlier to be both necessary and sufficient for this activity when HetR-GFP was used as the reporter [14]. The number of cells with a discernable reduction in fluorescence constituted the signal range of the inhibitor under the conditions employed. Replacement of GFP with CFP allowed a second fluorophore, in this case YFP, to be used simultaneously to indicate source cells that were engineered to produce HetN. This system was used to demonstrate inhibitory paracrine signaling by HetN.

Rigorous demonstration of paracrine signaling is complicated by the need to conclusively show that the effect of a given molecule cannot be explained by cell autonomous activity. Since its discovery in 1998, PatS has been regarded as an

intercellular signaling molecule that regulates the patterning of heterocyst differentiation [18]. The evidence for paracrine signaling by a PatS-dependent inhibitory signal is extensive but not definitive. First, inhibition of differentiation by exogenous addition of RGSGR peptide is consistent with action of the peptide at a distance from its source [18]. Second, restoration of a normal pattern of heterocysts to a *patS* mutant only when expression was from a developmentally regulated promoter suggests that production in proheterocyst source cells followed by intercellular transfer was necessary for patterning [18]. Third, work demonstrating a concentration gradient of an RGSGR-containing peptide in cells adjacent to proheterocysts is also consistent with inhibitory paracrine activity by a PatS signal [5]. However, none of these studies specifically excluded cell-autonomous activity of PatS. In the second and third examples, all cells of the filaments had functional copies of *patS*, and in the third, transcription of *patS* was from the native promoter, which is known to be induced in vegetative cells at the stage of differentiation examined [5]. Consequently, accumulation of a cell-autonomous PatS inhibitory signal in response to another unknown paracrine signal could not be ruled out. To avoid the ambiguity inherent in these previous studies, the strain used to test paracrine signaling of HetN in the work described here had both *patS* and *hetN* deleted from the chromosome, and *hetN* was added back on a plasmid to only a small number of cells in a filament. Because the signal range from cells expressing *hetN* extended over an average of 13 cells, all of which lacked the ability to produce both inhibitors, we conclude that a *hetN*-dependent inhibitory signal produced in source heterocysts was transferred from cell to cell to effect paracrine signaling.

With the demonstration of paracrine signaling for a *hetN*-dependent inhibitory signal and mounting evidence for the same with a *patS*-dependent inhibitory signal, it might seem appropriate to refer to these inhibitory signals as morphogens, and in the case of PatS, this has already been done [5]. The number of cells in filaments that differentiate has been shown to correlate with expression levels of *patS* and *hetN* as well as with concentrations of RGSGR peptide [2, 18], the functional domain of both signals, seemingly satisfies the first criterion of a morphogen: determination of developmental fate in a concentration-dependent manner. Paracrine signaling would seem to satisfy the second criterion of a morphogen: action at a distance from the source of production. However, reference to a signal molecule as a morphogen implies that the identity of the molecule is known, and this is true for neither PatS nor HetN, rendering use of the term morphogen ambiguous at the current time. For the sake of clarity, we suggest that the terms *patS*-dependent and *hetN*-dependent inhibitory paracrine signals be used to more accurately reflect the state of knowledge regarding the putative peptide inhibitors until the physical nature of each is determined.

References

1. Black, T.A., Y. Cai, and C.P. Wolk, *Spatial expression and autoregulation of hetR, a gene involved in the control of heterocyst development in Anabaena.* Mol. Microbiol., 1993. **9**: p. 77-84.
2. Borthakur, P.B., et al., *Inactivation of patS and hetN causes lethal levels of heterocyst differentiation in the filamentous cyanobacterium Anabaena sp. PCC 7120.* Mol. Microbiol., 2005. **57**: p. 111-123.
3. Buikema, W.J. and R. Haselkorn, *Characterization of a gene controlling heterocyst development in the cyanobacterium Anabaena 7120.* Genes Dev., 1991. **5**: p. 321-330.
4. Cai, Y. and C.P. Wolk, *Use of a conditionally lethal gene in Anabaena sp. strain PCC 7120 to select for double recombinants and to entrap insertion sequences.* J. Bacteriol., 1990. **172**: p. 3138-3145.
5. Corrales-Guerrero, L., et al., *Functional dissection and evidence for intercellular transfer of the heterocyst-differentiation PatS morphogen.* Mol. Microbiol., 2013. **88**(6): p. 1093-1105.
6. Elhai, J. and C.P. Wolk, *Conjugal transfer of DNA to cyanobacteria.* Methods Enzymol., 1988. **167**: p. 747-754.
7. Feldmann, E.A., et al., *Evidence for direct binding between HetR from Anabaena sp. PCC 7120 and PatS-5.* Biochemistry, 2011. **50**: p. 9212-9224.
8. Higa, K.C., et al., *The RGSGR amino acid motif of the intercellular signaling protein, HetN, is required for patterning of heterocysts in Anabaena sp. strain PCC 7120.* Mol. Microbiol., 2012. **83**: p. 682-693.
9. Muller, P., et al., *Morphogen transport.* Development, 2013. **140**(8): p. 1621-38.
10. Müller, P. and Alexander F. Schier, *Extracellular Movement of Signaling Molecules.* Developmental Cell. **21**(1): p. 145-158.
11. Norris, M.H., et al., *Stable site-specific fluorescent tagging constructs optimized for Burkholderia species.* Appl. Env. Microbiol., 2010. **76**: p. 7635-7640.
12. Risser, D.D. and S.M. Callahan, *Mutagenesis of hetR reveals amino acids necessary for HetR function in the heterocystous cyanobacterium Anabaena sp. strain PCC 7120.* J. Bacteriol., 2007. **189**: p. 2460-2467.
13. Risser, D.D. and S.M. Callahan, *HetF and PatA control levels of HetR in Anabaena sp. strain PCC 7120.* J. Bacteriol., 2008. **190**: p. 7645-7654.
14. Risser, D.D. and S.M. Callahan, *Genetic and cytological evidence that heterocyst patterning is regulated by inhibitor gradients that promote activator decay.* Proc. Natl. Acad. Sci. USA, 2009. **106**(47): p. 19884-19888.
15. Teleman, A.A., M. Strigini, and S.M. Cohen, *Shaping morphogen gradients.* Cell, 2001. **105**(5): p. 559-62.
16. Wei, T.-F., R. Ramasubramanian, and J.W. Golden, *Anabaena sp. strain PCC 7120 ntcA gene required for growth on nitrate and heterocyst development.* J. Bacteriol., 1994. **176**: p. 4473-4482.
17. Wu, X., et al., *patS minigenes inhibit heterocyst development of Anabaena sp. strain PCC 7120.* J. Bacteriol., 2004. **186**: p. 6422-6429.

18. Yoon, H.-S. and J.W. Golden, *Heterocyst pattern formation controlled by a diffusible peptide.* Science, 1998. **282**: p. 935-938.

Chapter 6. Translation of HetN From a Methionine Internal to the Annotated Start Codon.

Introduction

The regulation of protein production is a complex process within biological organisms. In some cases, multiple translation start sites are used to produce different proteins from a single genetic locus. For example, depending on growth conditions, the cyanobacterium *Synechocystis* sp. strain PCC6803 translates two isoforms of ferredoxin:NADP oxidoreductase from methionines 1 and 113 [15]. Products derived from alternative translation initiation sites are also known to produce protein products that are targeted to different regions of the cell. Examples include human fibroblast growth factor 2, which uses four separate initiation sites to produce proteins destined for both nuclear and cytoplasmic functions. In addition, Serum- and glucocorticoid-induced kinase 1 produces two isoforms that are present in either the ER or nucleus and cytoplasm [1, 21]. Alternative translational initiation sites are important to consider when investigating a protein with an undetermined structure and/or function.

There is evidence of a HetN-dependent paracrine type inhibitory morphogen within *Anabaena*, but the exact nature of the signal has not yet been clearly defined. The presence of HetN-dependent inhibitory activity within cells that are unable to produce HetN implies action at a distance that is not dependent on *hetN* expression. The *hetN* domain deletion analysis reported in Chapter 2 indicates the HetN-dependent inhibitory signal is likely not the full-length HetN protein but could be derived from full-length HetN. Both PatS and HetN contain the hexa-peptide sequence ERGSGR, which is known to bind directly to HetR [12] and results in the abrogation of HetR DNA binding activity

[9], suggesting that some portion of HetN containing the ERGSGR sequence is the active *hetN*-dependent inhibitory morphogen. If the HetN-dependent inhibitory signal is some portion of the full-length HetN protein there are a number of ways the inhibitor could be produced. The inhibitory signal could be released via protease processing, which could cleave both upstream and downstream of the ERGSGR motif. Alternatively, the inhibitory protein could be translated from a methionine internal to the annotated start codon followed by protease processing somewhere downstream of the ERGSGR motif.

There are four methionine residues, including the annotated start codon, as well as one GTG potential translation initiation site, present upstream of the ERGSGR motif in HetN. In order to assess the potential of HetN to be translated from a methionine other than the annotated start codon, seven mutant strains were created. Each strain had one, or a combination, of the four methionines found at positions 1, 119, 129, and 130 mutated to leucines to create mutant strains. Methionines 129 and 130 were always mutated in combination due to their proximity to one another. The strains were created by the reintroduction of the mutant *hetN* alleles into UHM150, Δ*hetN*. The combined phenotypes of the seven strains compared to those of wild-type and UHM150 were then used to determine if HetN might be translated from a methionine internal to the annotated start codon.

Translation is known to be initiated at the valine codon GTG in some cases [17]. In order to determine if the GTG codon found upstream of the ERGSGR motif in HetN is used as a translation initiation site, this codon was mutated from GTG to GTT, a codon commonly used by *Anabaena* to code for valine but not known to initiate translation, in a genetic background in which M1, M129, and M130 were mutated to leucines. The

mutation did not change the amino acid, which is predicted to be coded for at position 64, but only removed the potential translation initiation site. The resulting strain, UHM362, had M119 as the only potential translation initiation site remaining for the production of HetN protein.

To differentiate between two potential causes of mutation phenotypes, namely inactivation of a translational start site or destabilization of structure followed by rapid degradation of the full-length protein, N-terminal YFP fusions were made to the allele(s) with single mutations used above that lacked proper heterocyst patterning.

Materials and Methods

Culture conditions. The growth of *Escherichia coli* and wild-type *Anabaena* sp. strain PCC 7120 and its derivatives, concentrations of antibiotics, and the induction of heterocysts in media lacking a source of combined nitrogen were as previously described [2, 9]. Growth medium containing 6 mM ammonia as a nitrogen source was prepared as previously described and used to grow strains prior to the induction of heterocyst differentiation [14]. Heterocyst percentages, frequency of single, double, and higher numbers of contiguous heterocysts, and the mean vegetative cell interval between heterocysts were determined as previously described [23]. Expression from the copper-inducible *petE* promoter was induced with the addition of copper to a final concentration of 2 μM [3]. Plasmids were introduced into *Anabaena* strains by conjugation from *E. coli* as previously described [7].

Plasmid construction. Plasmids and oligonucleotide primers used in this study are described in Tables 11 and 12, respectively. The integrity of all PCR-derived constructs was verified by sequencing. Plasmids pAD120, pAD121, pAD122, pAD123,

pAD124, pAD125, pAD126, and pAD127 are mobilizable shuttle vectors based on pAM504 [24] containing P_{hetN}-*hetN*(*M1L*)-YFP, P_{hetN}-*hetN*(*M119L*)-YFP, P_{hetN}-*hetN*(*M129L*/*M130L*)-YFP, P_{hetN}-*hetN*(*M1L*, *M119L*)-YFP, P_{hetN}-*hetN*(*M1L*, *M129L*/*M130L*)-YFP, P_{hetN}-*hetN*(*M1L*, *M119L*, *M129L*/*M130L*)-YFP, and P_{hetN}-*hetN*-YFP, respectively. P_{hetN}-*hetN*(*M1L*), P_{hetN}-*hetN*(*M119L*), P_{hetN}-*hetN*(*M129L*/*M130L*), P_{hetN}-*hetN*(*M1L*, *M119L*), P_{hetN}-*hetN*(*M1L*, *M129L*/*M130L*), P_{hetN}-*hetN*(*M1L*, *M119L*, *M129L*/*M130L*), or P_{hetN}-*hetN* were amplified by PCR with the primers PhetN-MunI-F and hetN-Tln-BglII-R from the plasmids pOR101, pOR102, pOR103, pOR104, pOR105, pOR106, pOR107, and pDR382 [10], respectively, digested with *Mun*I-*Bgl*II, and individually cloned into the *Eco*RI-*Bam*HI sites of pPJAV153 [19] to create pAD120, pAD121, pAD122, pAD123, pAD124, pAD125, pAD126, and pAD127.

Plasmids pAD128, pAD129, pAD130, pAD131, pAD132, pAD133, pAD134, and pAD135 are mobilizable shuttle vectors based on pAM504 containing P_{petE}-*hetN*(*M1L*)-YFP, P_{petE}-*hetN*(*M119L*)-YFP, P_{petE}-*hetN*(*M129L*/*M130L*)-YFP, P_{petE}-*hetN*(*M1L*, *M119L*)-YFP, P_{petE}-*hetN*(*M1L*, *M129L*/*M130L*)-YFP, P_{petE}-*hetN*(*M1L*, *M119L*, *M129L*/*M130L*)-YFP, and P_{petE}-*hetN*-YFP, respectively. P_{petE}-*hetN*(*M1L*), P_{petE}-*hetN*(*M119L*), P_{petE}-*hetN*(*M129L*/*M130L*), P_{petE}-*hetN*(*M1L*, *M119L*), P_{petE}-*hetN*(*M1L*, *M129L*/*M130L*), P_{petE}-*hetN*(*M1L*, *M119L*, *M129L*/*M130L*), and P_{petE}-*hetN* were amplified by PCR with the primers PpetE-MunI-F and hetN-Tln-BglII-R from the plasmids pOR108, pOR109, pOR110, pOR111, pOR112, pOR113, pOR114 and pDR320 [18], respectively, digested with *Mun*I-*Bgl*II, and individually cloned into the *Eco*RI-*Bam*HI sites of pPJAV153 to create pAD128, pAD129, pAD130, pAD131, pAD132, pAD133, pAD134, and pAD135.

Plasmid pAHB174 is a suicide vector based on pRL277 [4] to introduce *hetN*(*M1L*, *M129L*/*M130L*) with a point mutation at +192 to change the codon for V64 from a GTG to a GTT at the native locus. The plasmid pOR105 was amplified by PCR with the primers HetN-GTG-to-GTT-QC-F and HetN-GTG-to-GTT-QC-R and QuickChange was done to create pAHB174.

Plasmid pOR101 is a suicide vector based on pRL277 to introduce *hetN*(*M1L*) at the native locus. Regions up- and downstream of the HetN start codon were amplified from pDR382 with the primer pairs PhetN-Bam-F and hetN Mod-M1 R and hetN Mod-M1 F and HetN-SacI-R, respectively. The products harboring the mutation were fused by overlap extension PCR [11], digested with *Spe*I-*Sac*I, and cloned into the same sites of pDR382 replacing the native allele to create pOR101.

Plasmid pOR102 is a suicide vector based on pRL277 to introduce *hetN*(*M119L*) at the native locus. The plasmid pDR382 was amplified by PCR with the primers HetN-Mod-M2-QC-F and HetN-Mod-M2-QC-R and QuickChange was done to create pOR102.

Plasmid pOR103 is a suicide vector based on pRL277 to introduce *hetN*(*M129L*/*M130L*) at the native locus. Regions up- and downstream of *hetN*(*M129*/*M130*) were amplified from pDR382 with the primer pairs PhetN-Bam-F and MMERGSGR-Sub Met-R2 and MMERGSGR-Sub Met-F2 and HetN-SacI-R, respectively. The products harboring the mutation were fused by overlap extension PCR, digested with *Spe*I-*Sac*I, and cloned into the same sites of pDR382 replacing the native allele to create pOR103.

Plasmid pOR104 is a suicide vector based on pRL277 to introduce *hetN*(*M1L*, *M119L*) at the native locus. The plasmid pOR101 was amplified by PCR with the primers

HetN-Mod-M2-QC-F and HetN-Mod-M2-QC-R and QuickChange was done to create pOR104.

Plasmids pOR105, pOR106, and pOR107 are suicide vectors based on pRL277 to introduce *hetN*(*M1L*, *M129L*/*M130L*), *hetN*(*M119L*, *M129L*/*M130L*), and *hetN*(*M1L*, *M119L*, *M129L*/*M130L*), respectively, at the native locus. Regions up- and downstream were amplified from pOR101, pOR102, and pOR104, respectively, with the primer pairs PhetN-Bam-F and MMERGSGR-Sub Met-R2 and MMERGSGR-Sub Met-F2 and HetN-SacI-R, respectively. The products harboring the mutation were fused by overlap extension PCR, digested with *Spe*I-*Sac*I, and cloned into the same sites of pDR382 replacing the native allele to create pOR105, pOR106, and pOR107.

Plasmids pOR108, pOR111, pOR112, and pOR114 are mobilizable shuttle vectors based on pAM504 containing P_{petE}-*hetN*(*M1L*), P_{petE}-*hetN*(*M1L*, *M119L*), P_{petE}-*hetN*(*M1L*, *M129L*/*M130L*), and P_{petE}-*hetN*(*M1L*, *M119L*, *M129L*/*M130L*), respectively. The *hetN*(*M1L*), *hetN*(*M1L*, *M119L*), *hetN*(*M1L*, *M129L*/*M130L*), and *hetN*(*M1L*, *M119L*, *M129L*/*M130L*) alleles were amplified by PCR from pOR101, pOR104, pOR105, and pOR107, respectively, with the primers HetN(M1L)-EcoRI-F and hetN-BamHI-R. The products were digested with *Eco*RI-*Bam*HI and cloned into the same sites in pPJAV213 to create pOR108, pOR111, pOR112, and pOR114.

Plasmids pOR109, pOR110, and pOR113 are mobilizable shuttle vectors based on pAM504 containing P_{petE}-*hetN*(*M119L*), P_{petE}-*hetN*(*M129L*/*M130L*), and P_{petE}-*hetN*(*M119L*, *M129L*/*M130L*), respectively. The *hetN*(*M119L*), *hetN*(*M129L*/*M130L*), and *hetN*(*M119L*, *M129L*/*M130L*) alleles were amplified by PCR from pOR102, pOR103, and pOR106, respectively, with the primers HetN-EcoRI-F-petE and hetN-

BamHI-R. The products were digested with *Eco*RI-*Bam*HI and cloned into the same sites in pPJAV213 to create pOR109, pOR110, and pOR113.

Strain construction. Table 11 lists the strains used in this study. Replacement of the coding region of *hetN* with different *hetN* alleles was accomplished by allelic exchange as previously described [2, 5, 16]. The following plasmids were used to introduce altered *hetN* alleles at the native *hetN* locus in UHM150: pOR101 for UHM328; pOR102 for UHM345; pOR103 for UHM346; pOR104 for UHM356; pOR105 for UHM347; pOR106 for UHM348; pOR107 for UHM349; pOR115 for UHM352; pOR116 for UHM353; and pPJAV369 for UHM354. Strains with mutations in *hetN* were verified by PCR with the primers up-hetN-F and down-hetN-R, which anneal outside of the region used to make the mutations.

Statistical analysis. Multiple phenotypes were compared to one another using a one-way analysis of variance (one-way ANOVA). Groups of phenotypes with significant variance of the means were analyzed with a post-hoc Tukey test in order to identify individual mean pairs, which are significantly different from one another.

Microscopy. Cells were routinely viewed and imaged as previously described [2]. Confocal microscopy was performed as previously described [10].

Table 11. Strains and Plasmids used in Chapter 6.

Strain or Plasmid	Relevant Characteristic(s)*	Source or Reference
***Anabaena* sp. strains**		
PCC 7120	Wild-type	Pasteur Culture Collection
UHM150	Δ*hetN*	[10]
UHM163	*hetR*(*R250K*)	[8]
UHM328	*hetN*(*M1L*)	This study
UHM345	*hetN*(*M119L*)	This study
UHM346	*hetN*(*M129L*/*M130L*)	This study
UHM347	*hetN*(*M1L*, *M129L*/*M130L*)	This study
UHM348	*hetN*(*M119L*, *M129L*/*M130L*)	This study
UHM349	*hetN*(*M1L*, *M119L*, *M129L*/*M130L*)	This study
UHM356	*hetN*(*M1L*, *M119L*)	This study
UHM362	*hetN*(*M1L*, V64V, *M129L*/*M130L*)	
Plasmids		
pAM504	Shuttle vector for replication in *E. coli* and *Anabaena*; Km^r Nm^r	[24]
pRL277	Suicide vector; Sp^r/Sm^r	[4]
pDR320	pAM504 with P_{petE}-*hetN*	[18]
pDR382	pRL277 to introduce *hetN* into the native locus	[10]
pPJAV153	pAM504 with P_{petE}-YFP	[19]
pPJAV213	pAM504 with P_{petE}	[22]
pAD120	pAM504 with P_{hetN}-*hetN*(M1L)-YFP	This study
pAD121	pAM504 with P_{hetN}-*hetN*(M119L)-YFP	This study
pAD122	pAM504 with P_{hetN}-*hetN* (M129L/M130L)-YFP	This study
pAD123	pAM504 with P_{hetN}-*hetN* (M1L, M119L)-YFP	This study
pAD124	pAM504 with P_{hetN}-*hetN* (M1L, M129L/M130L)-YFP	This study
pAD125	pAM504 with P_{hetN}-*hetN* (M119L, M129L/M130L)-YFP	This study
pAD126	pAM504 with P_{hetN}-*hetN* (M1L, M119L, M129L/M130L)-YFP	This study
pAD127	pAM504 with P_{hetN}-*hetN*-YFP	This study
pAD128	pAM504 with P_{petE}-*hetN*(M1L)-YFP	
pAD129	pAM504 with P_{petE}-*hetN*(M119L)-YFP	This study
pAD130	pAM504 with P_{petE}-*hetN* (M129L/M130L)-YFP	This study
pAD131	pAM504 with P_{petE}-*hetN* (M1L, M119L)-YFP	This study
pAD132	pAM504 with P_{petE}-*hetN*	This study

Table 11 continued.

	(M1L, M129L/M130L)-YFP	
pAD133	pAM504 with P_{petE}-*hetN* (M119L, M129L/M130L)-YFP	This study
pAD134	pAM504 with P_{petE}-*hetN* (M1L, M119L, M129L/M130L)-YFP	This study
pAD135	pAM504 with P_{petE}-*hetN*-YFP	This study
pAHB174	pRL277 to make UHM362	This study
pOR101	pRL277 to make UHM328	This study
pOR102	pRL277 to make UHM345	This study
pOR103	pRL277 to make UHM346	This study
pOR104	pRL277 to make UHM356	This study
pOR105	pRL277 to make UHM347	This study
pOR106	pRL277 to make UHM348	This study
pOR107	pRL277 to make UHM349	This study
pOR108	pAM504 with P_{petE}-*hetN*(M1L)	This study
pOR109	pAM504 with P_{petE}-*hetN*(M119L)	This study
pOR110	pAM504 with P_{petE}-*hetN* (M129L/M130L)	This study
pOR111	pAM504 with P_{petE}-*hetN*(M1L, M119L)	This study
pOR112	pAM504 with P_{petE}-*hetN* (M1L, M129L/M130L)	This study
pOR113	pAM504 with P_{petE}-*hetN* (M119L, M129L/M130L)	This study
pOR114	pAM504 with P_{petE}-*hetN* (M1L, M119L, M129L/M130L)	This study

*Km, kanamycin; Nm, neomycin; Sp, spectinomycin; Sm, streptomycin.

Table 12. Oligonucleotide primers used in Chapter 6.

Oligonucleotide*	Sequence
PhetN-MunI-F	ATATACAATTGAGGAGAAGACGCGATGAATC
hetN-Tln-BglII-R	AGATCTTGAGCGATGAGACTCAACAGCTACATAGC
PpetE-MunI-F-	TATATCAATTGGCTGAGGTACTGAGTACACAGC
HetN-GTG-to-GTT-QC-F	GCGATCGCTATTCCTTTTGATGTTAGGAACACATCA CAATTATCG
HetN-GTG-to-GTT-QC-R	CGATAATTGTGATGTGTTCCTAACATCAAAAGGAAT AGCGATCGC
PhetN-Bam-F	ATATAGGATCCAGGAGAAGACGCGATGAATC
hetN Mod-M1 R	CCTGTAAGAGTTGTGAGTGTAACCTGCTAGT
hetN Mod-M1 F	ACTAGCAGGTTACACTCACAACTCTTACAGG
HetN-SacI-R	CGCCGAGCTCGCTGCTATTAACCTTGCAAAGTTC
HetN-Mod-M2-QC-F	CACTAATCTATTGGCTGCTCTCGAATTAACAC GTTTGTTAC
HetN-Mod-M2-QC-R	GTAACAAACGTGTTAATTCGAGAGCAGCCAAT AGATTAGTG
MMERGSGR-Sub Met-R2	CTACCCAGCTTGTTGGAACGCGGTAGTGGTCGG
MMERGSGR-Sub Met-F2	ACCGCGTTCCAACAAGCTGGGTAGTAACAAACGTGT TAATTC
HetN(M1L)-EcoRI-F	ATATAGAATTCCTCACAACTCTTACAGGTAAG
hetN-BamHI-R	ATATAGGATCCTCATGAGCGATGAGACTCAAC
HetN-EcoRI-F-petE	ATATAGAATTCATGACAACTCTTACAGGTAAG
up-hetN-F	GAGCTCGGCAAGCAGAGTTAATC
down-hetN-R	GGATCCGCCCATTAATATAAGTCTC

*Oligonucleotides are shown in the 5' to 3' direction

Results

M119 is a potential translational start site in HetN. To determine which translational start site(s) are required to produce HetN-dependent inhibitory activity, each possible start codon in the N-terminal hydrophilic domain was inactivated and the alleles were assessed for their ability to maintain a proper pattern of heterocysts when reintroduced into the native *hetN* locus. Each methionine was mutated to leucine in every possible combination, except that M129/M130 were always mutated together as they are directly upstream of ERGSGR in HetN. After 48 h N-, UHM328 (*hetN*(*M1L*)), UHM346 (*hetN*(*M129L*/*M130L*)), UHM347 (*hetN*(*M1L*, *M129L*/*M130L*)), and UHM362 (*hetN*(*M1L*, *V64V(GTG to GTT)*, *M129L*/*M130L*)) differentiated 9.3 % ± 0.23, 10.0 ± 0.06, 10.0 % ± 0.31, and 10.1 % ± 0.31 heterocysts respectively (Figure 21 and Table 13). When compared to the wild-type (9.5% ± 0.31) and the *hetN* mutant, UHM150 (16.2% ± 0.2), the heterocyst percentages produced by UHM328, UHM346, and UHM347 were not significantly different from the wild-type but were significantly different from UHM150 (Table 14). UHM328, UHM346, and UHM347 also did not produce an MCH phenotype (Table 13). The heterocyst percentage produced by UHM362 was not significantly different from the wild-type and did not yield an Mch phenotype (Table 13 and 14). These results suggest that the M1, M129, M130, and V64 residues are not required for HetN-dependent inhibitory function.

In contrast to the above mutants, after 48 h N-, UHM345 (*hetN*(*M119L*)), UHM348 (*hetN*(*M119L*, *M129L*/*M130L*)), UHM349 (*hetN*(*M1L*, *M119L*, *M129L*/*M130L*)), and UHM356 (*hetN*(*M1L*, *M119L*)) differentiated 14.3 % ± 0.31, 15.7 % ± 1.01, 16.8 % ± 0.72, and 15.2 % ± 1.06 heterocysts, respectively (Figure 21 and

Table 13). When compared to the wild-type and UHM150, the heterocyst percentages produced by UHM348, UHM349, and UHM356 were significantly different from the wild-type but were not significantly different from UHM150 (Table 14). While the heterocyst percentage produced by UHM345 was significantly different from both the wild-type and UHM150, it was more similar to UHM150 than the wild-type. All four mutant strains, UHM345, UHM348, UHM349, and UHM356, produced an Mch phenotype (Figure 21 and Table 13). The one characteristic that all of these strains share is the absence of M119. Taken together, these results suggest that M119 is required for proper HetN function and may represent a translational start site.

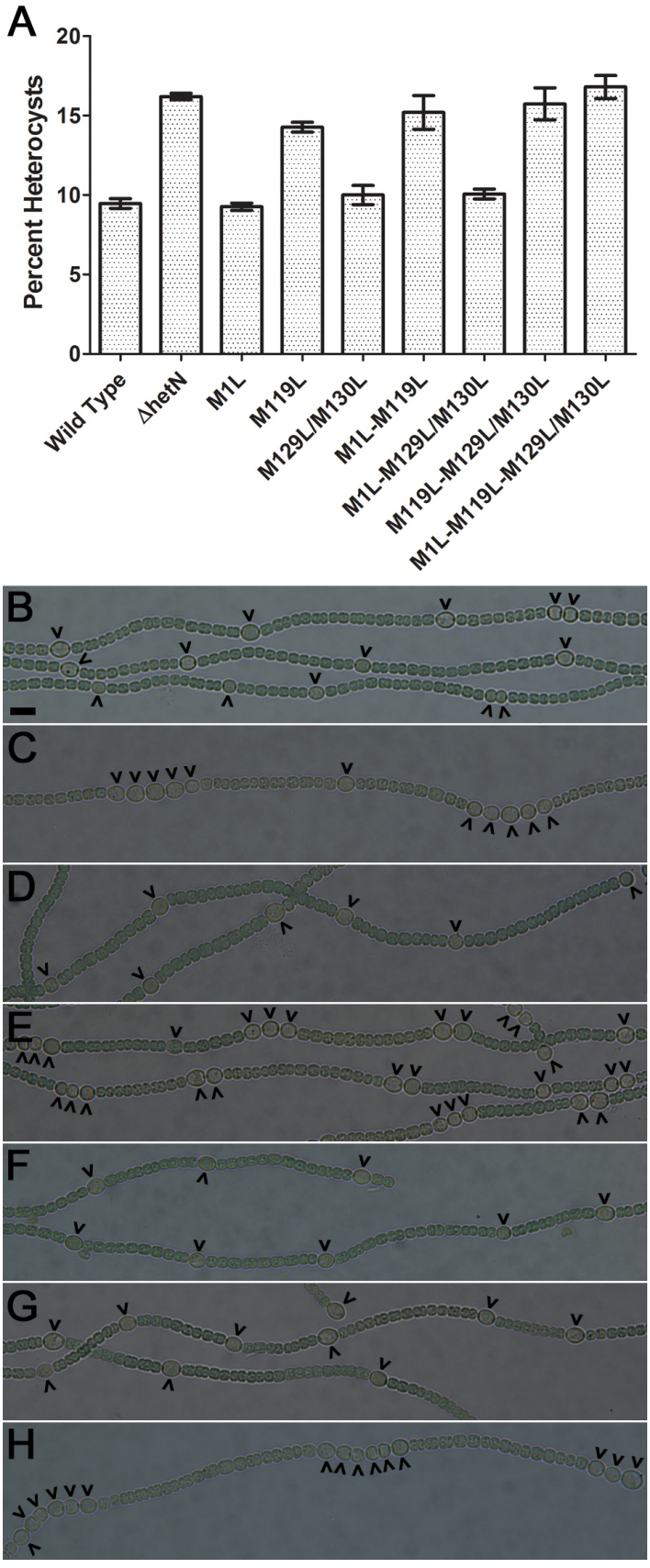
A
Percent Heterocysts
20
15
10
5
0
Wild Type
ΔhetN
M1L
M119L
M129L/M130L
M1L-M119L
M1L-M129L/M130L
M119L-M129L/M130L
M1L-M119L-M129L/M130L
B
C
D
E
F
G
H

Figure 21. Alleles of *hetN* encoding M119L substitutions result in an Mch phenotype similar to a Δ*hetN* strain. Heterocyst percentages for the wild-type and Δ*hetN* strains, as well as strains with the indicated chromosomal mutations (A). Bright-field images of the wild-type (B), UHM150, which is Δ*hetN* (C), UHM328, which is *hetN*(M1L) (D), UHM345, which is *hetN*(M119L) (E), UHM346, which is *hetN*(M129L/M130L) (F), UHM347, which is *hetN*(M1L, M129L/M130L) (G), UHM349, which is *hetN*(M1L, M119L, M129L/M130L) (H). Micrographs were taken 48 h after the removal of combined nitrogen. Carets indicate heterocysts. Bar, 10 μm.

Table 13. Patterns of heterocysts produced by strains of *Anabaena*.

Strain (Genotype)	**Hours N-**	**Heterocyst Percentage**	**Mean Vegetative Cell Interval**	**Heterocyst Occurrence**
Wild-type	24	9.07 ± 0.31	10.3 ± 0.46	96 ± 1.73; 4 ± 1.73
	48	9.47 ± 0.31	11.5 ± 0.31	96.67 ± 1.53; 3.33 ± 1.53
	72	8.93 ± 0.23	12.7 ± 0.38	95.33 ± 0.58; 6.67 ± 0.58
UHM150 (Δ*hetN*)	24	9.47 ± 0.5	10.4 ± 0.32	88.33 ± 3.79; 10.67 ± 2.08 1 ± 1.73
	48	16.2 ± 0.2	5.9 ± 0.17	41.67 ± 2.08; 33.33 ± 4.04; 25 ± 4.36
	72	16.07 ± 0.12	6.1 ± 0.45	29 ± 1; 29.11 ± 2.08; 42 ± 2.52
UHM328 (Δ*hetN*(*M1L*))	24	9.67 ± 0.23	10.6 ± 1.2	93.33 ± 1.53; 6.67 ± 1.53
	48	9.27 ± 0.23	11.6 ± 0.11	94.33 ± 2.08; 5.34 ± 1.53; 0.33 ± 0.58
	72	9.27 ± 0.42	11.3 ± 0.26	95 ± 1.73; 5 ± 1.73
UHM345 (Δ*hetN*(*M119L*))	24	10 ± 0.2	8.8 ± 0.4	82 ± 1; 14 ± 1; 4 ± 1
	48	14.27 ± 0.31	7 ± 0.45	70.67 ± 3.06; 20.33 ± 2.31; 9 ± 3.46
	72	15.33 ± 0.64	6.4 ± 0.15	70 ± 1; 19.67 ± 3.51; 10.33 ± 3.06

UHM346 (Δ*hetN*(*M129L*/ *M130L*))	24	10.2 ± 0.2	9.2 ± 0.32	95 ± 1.73; 5 ± 1.73
	48	10 ± 0.6	9.7 ± 0.14	91 ± 0.58; 8.67 ± 0.58; 0.33 ± 1
	72	9.93 ± 0.5	10.5 ± 0.47	93 ± 1; 7 ± 1
UHM356 (Δ*hetN*(*M1L*, *M119L*))	24	9.2 ± 0.92	11.2 ± 0.67	93.33 ± 2.52; 6.67 ± 2.52
	48	15.2 ± 1.06	6.2 ± 0.04	50.33 ± 3.79; 36.67 ± 3.21; 13 ± 2.65
	72	15.01 ± 0.61	6.4 ± 0.15	49.67 ± 3.51; 36.33 ± 4.62; 14 ± 2.65
UHM347 (Δ*hetN*(*M1L*, *M129L*/*M130L*))	24	10.3 ± 0.31	8.7 ± 0.23	95.33 ± 0.58; 4.67 ± 0.58
	48	10.07 ± 0.31	9.4 ± 0.53	93 ± 1; 7 ± 1
	72	10.2 ± 0.35	10 ± 0.27	94 ± 1; 5.67 ± 1.15; 0.33 ± 0.58
UHM348 (Δ*hetN*(*M119L*, *M129L*/*M130L*))	24	10.6 ± 0.2	9.4 ± 0.47	86.67 ± 3.51; 12 ± 2.65; 1.33 ± 1.15
	48	15.73 ± 1.01	6.4 ± 0.19	61.33 ± 3.21; 26.67 ± 0.58; 12 ± 3.61
	72	16.67 ± 1.14	6.5 ± 0.44	49 ± 7; 30 ± 2; 21 ± 5.19
UHM349 (Δ*hetN*(*M1L*, *M119L*, *M129L*/*M130L*))	24	10.87 ± 0.23	9.6 ± 0.08	82.33 ± 2.08; 14.67 ± 1.53; 3 ± 1
	48	16.8 ± 0.72	5.9 ± 0.52	39 ± 3; 34.67 ± 6.11; 26.33 ± 4.73
	72	17.67 ± 0.46	5 ± 0.48	39.67 ± 2.08; 29.33 ± 3.79; 31 ± 4.58
UHM362 (Δ*hetN*(*M1L*, *V64V(GTG to GTT)*, *M129L*/*M130L*))	24	9.33 ± 0.12	10.9 ± 0.29	97.67 ± 1.15 2.33 ± 1.15
	48	10.13 ± 0.31	9.1 ± 0.34	94.67 ± 2.08 5.33 ± 2.08
	72	9.6 ± 0.2	9.2 ± 0.26	93 ± 1.73 7 ± 1.73

At the indicated times following nitrogen stepdown, 500 cells were counted in triplicate and total heterocysts are presented as the mean ± the standard deviation. The presence of single (top line), double (second line), or multiple contiguous heterocysts (third line) was determined for 300 heterocyst occurrences in triplicate and are presented as the average percent ± the standard deviation. The number of vegetative cell between heterocysts was counted for 300 intervals and is presented as the mean ± the standard deviation of the mean.

Table 14. Statistical analysis of UHM328, UHM345, UHM346, UHM347, UHM348, UHM349, UHM356, and UHM362.

	Wild-type	Δ*hetN*
ANOVA p-value	$3.04 * 10^{-12}$	$2.17 * 10^{-12}$
Strain:	post-hoc Tukey HSD p-value	post-hoc Tukey HSD p-value
UHM328 (*hetN*(M1L))	0.001	0.001
UHM345 (*hetN*(M119L))	0.001	0.024
UHM346 (*hetN*(M129L/M130L))	0.899	0.001
UHM356 (*hetN*(M1L, M119L))	0.001	0.557
UHM347 (*hetN*(M1L, M129L/M130L))	0.899	0.001
UHM348 (*hetN*(M119L, M129L/M130L))	0.001	0.899
UHM349 (*hetN*(M1L, M119L, M129L/M130L))	0.001	0.899
UHM362 (*hetN*(M1L, V64V(GTG to GTT), M129L/M130L))	0.899	0.001

One-way ANOVA with post-hoc Tukey HDS test comparing UHM352, UHM353, and UHM354 to the wild-type and UHM150 (Δ*hetN*). All phenotypes being compared were observed 48h after the removal of combined nitrogen (Table 13). Values written in green indicate a significant difference in the comparison being tested. Values written in red indicate no significant difference in the comparison being tested.

Assessment of protein levels with YFP fusions. When amino acids within a protein are mutated it is possible that any resulting impairments in protein activity could be caused by destabilization of the protein structure leading to degradation [13, 20]. It is therefore possible that the results presented above, which indicated that alleles harboring the *hetN*(M119L) mutation were non-functional, could be due to unforeseen changes in the protein structure rather than mutation of a translational start site. To determine if mutation of M119 significantly decreased levels of full-length HetN protein, the mutant

allele was translationally fused to yellow fluorescent protein (YFP) and assessed for fluorescence localization in a pattern analogous to HetN-YFP.

After 24 h N-, the wild-type containing the positive control vector, P_{petE}-*hetN*-YFP, had detectable YFP fluorescence localized to cell membranes and failed to produce heterocysts. Wild-type containing the negative control, empty vector, lacked detectable YFP fluorescence and differentiated 7.6 % ± 0.4 heterocysts (Figure 22, Table 15).

When *hetN*(M119L)-YFP was expressed in wild-type, YFP fluorescence was present, localized to cell membranes and the strain failed to differentiate heterocysts after 24 hours in N- medium (Figure 22, Table 15). The *hetN*(M119L)-YFP allele expressed in UHM163 produced detectable YFP fluorescence localized to cell membranes in vegetative cells and heterocysts when expressed from the *petE* promoter or in heterocysts alone when expressed from the *hetN* promoter (Figure 22, Figure 23, Table 15). The results indicate that a stable protein is produced when methionine 119 is changed to a leucine. Surprisingly, overexpression of *hetN*(M119L)-YFP also prevented the production of heterocysts in the wild-type background. This was unexpected given the mutant phenotypes above.

When *hetN*(M1L)-YFP was expressed in wild-type YFP fluorescence was absent and the strain failed to differentiate heterocysts after 24 hours in N- medium. (Figure 22, Table 15). YFP fluorescence was also absent when *hetN*(M1L)-YFP was expressed in UHM163 from both the *petE* and *hetN* promoters (Figure 22, Figure 23, Table 15). The results indicate that a stable protein with inhibitory activity is produced when *hetN*(M1L)-YFP is overexpressed. The results suggest the annotated start site of

HetN is necessary for detectable levels of protein fluorescence in the cell harboring a HetN-YFP fusion.

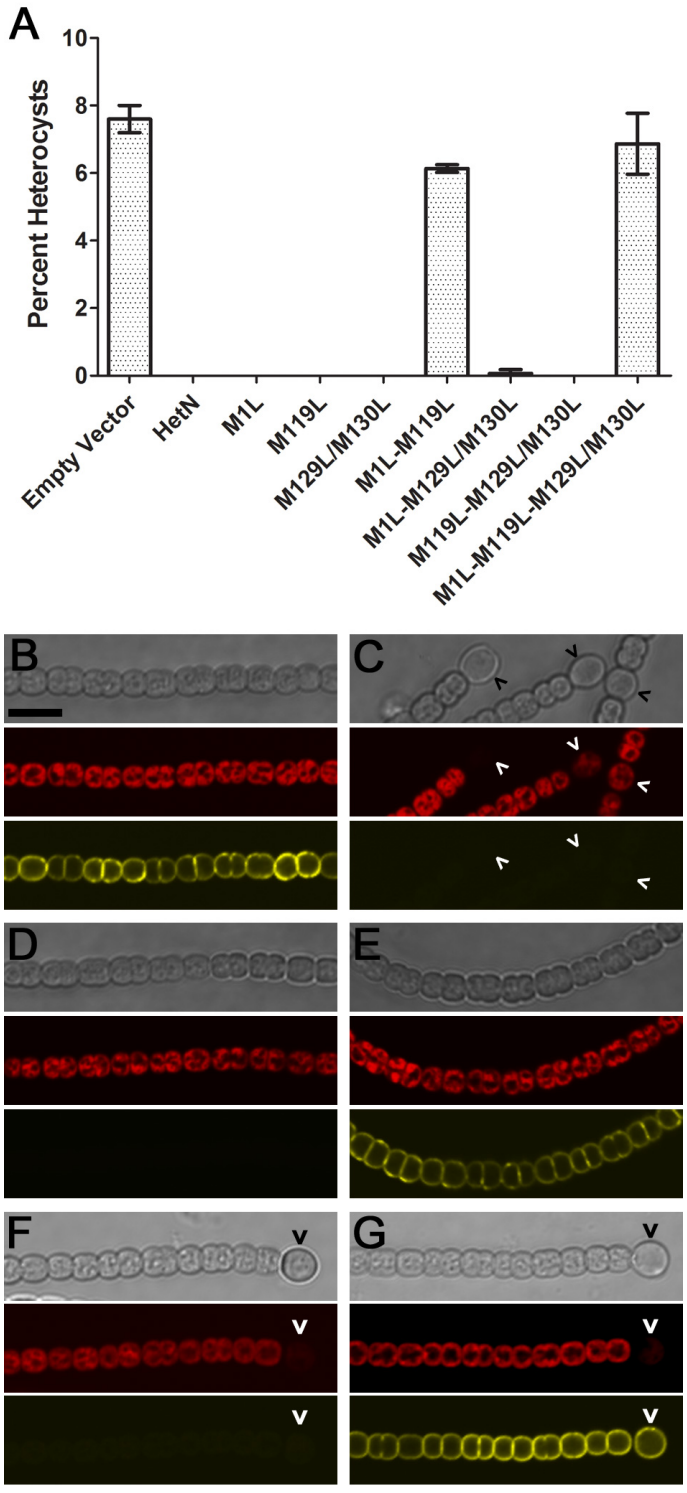

Figure 22. The M1 and M119 residues of *hetN* are required for the translation of inhibitory protein. Heterocyst percentages for the wild-type strain carrying either pPJAV153 as an empty vector control or plasmids harboring the indicated *hetN* alleles expressed by the *petE* promoter 24 h after the removal of combined nitrogen (A). The wild-type (B, C, D, E) or strain UHM163, which contains *hetR*(*R250K*) at the native locus and forms heterocysts even when *hetN* is overexpressed (F, G), 24 h after the removal of combined nitrogen with the following plasmids: pAD135 containing P_{petE}-*hetN*-YFP (B); pAD131 containing P_{petE}-*hetN*(*M1L*, *M119L*)-YFP (C); pAD128 containing P_{petE}-*hetN*(*M1L*)-YFP (D); pAD129 containing P_{petE}-*hetN*(*M119L*)-YFP (E); pAD128 containing P_{petE}-*hetN*(*M1L*)-YFP (F); or pAD129 containing P_{petE}-*hetN*(*M119L*)-YFP (G). From top to bottom: bright-field, red autofluorescence, yellow fluorescence from HetN-YFP alleles. Carets indicate heterocysts. Scale bar, 10 μm.

Table 15. Heterocyst percentages, statistical analysis, and presence or absence of YFP fluorescence when the indicated methionine alleles of *hetN* were expressed in wild-type and UHM163 translationally fused to YFP.

Plasmid Construct:	Percent Heterocysts after 24h N_2	ANOVA with post-hoc Tukey HDS test comparing each allele to the empty vector control: p-value	YFP detected in Wt from P*petE*	YFP detected in *hetR(R250K)* from P*petE*	YFP detected in *hetR(R250K)* from P*hetN*
ANOVA p-value	--	$7.77 * 10^{-16}$	--	--	--
Empty Vector	7.6 ± 0.4	--	No	No	No
hetN	0	0.001	Yes	Yes	Yes
hetN(M1L)	0	0.001	No	No	No
hetN(M119L)	0	0.001	Yes	Yes	Yes
hetN(M129L/M130L)	0	0.001	Yes	Yes	Yes
hetN(M1L, M119L)	6.13 ± 0.11	0.002	No	No	No
hetN(M1L, M129L/M130L)	0.06 ± 0.11	0.001	No	No	No
hetN(M119L, M129L/M130L)	0	0.001	Yes	Yes	Yes
hetN(M1L, M119L, M129L/M130L)	6.86 ± 0.9	0.26	No	No	No

The percent heterocysts 24 h N- with the indicated *hetN* allele, or the empty vector, expressed in wild-type. One-way ANOVA with post-hoc Tukey HDS test comparing the percent heterocysts produced by the empty vector control to the indicated *hetN* allele 24 h N-. Values written in green indicate a significant difference in the comparison being tested. Values written in red indicate no significant difference in the comparison being tested. The presence, Yes, or absence, No, of YFP fluorescence detected from the

indicated *hetN*-YFP allele expressed from the indicated promoter in wild-type or UHM163, Δ*hetR*.

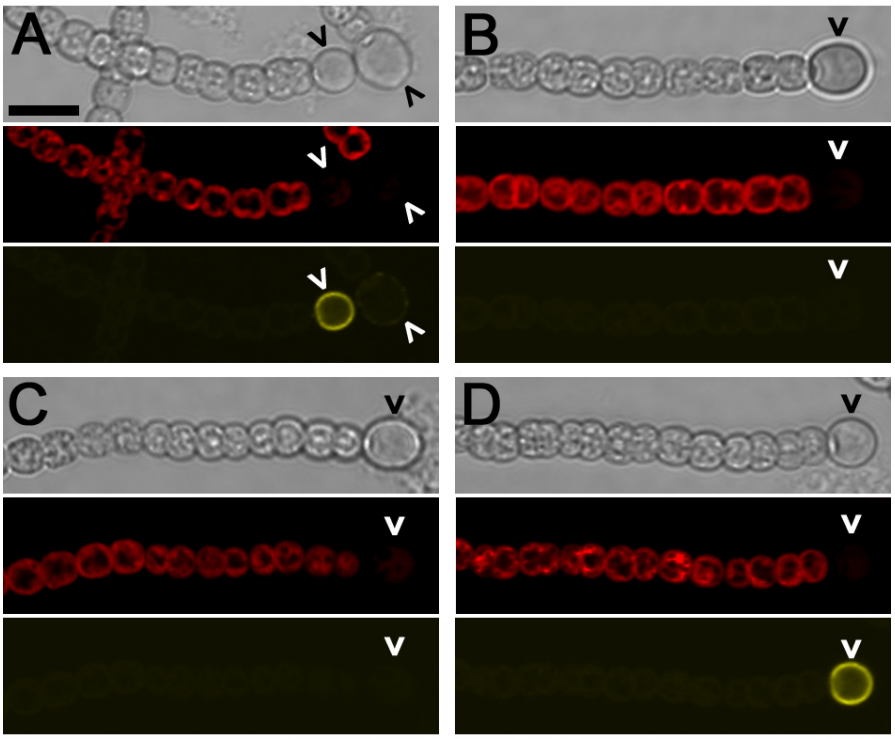

Figure 23. The M1 residue of *hetN* is required for heterocyst-specific translation of a *hetN*-YFP chimera. Strain UHM163, which contains *hetR*(*R250K*) at the native locus and forms heterocysts even when *hetN* is overexpressed, 24 h after the removal of combined nitrogen with the following plasmids: pAD127 containing P_{hetN}-*hetN*-YFP (A); pAD126 containing P_{hetN}-*hetN*(*M1L*, *M119L, M129L, M130L*)-YFP (B); pAD124 containing P_{hetN}-*hetN*(*M1L, M129L, M130L*)-YFP (C); or pAD125 containing P_{hetN}-*hetN*(*M119L, M129L, M130L*)-YFP (D). From top to bottom: bright-field, red autofluorescence, yellow fluorescence from HetN-YFP alleles. Carets indicate heterocysts. Scale bar, 10 μm.

Discussion

In order to test for the presence of a translational start site internal to the annotated start codon eight mutant strains were created. The phenotypes produced by the eight mutant strains indicate that M119 is the primary translational start site utilized by *Anabaena* for patterning of heterocysts. Strains in which M119 was mutated displayed

elevated heterocysts percentages and Mch phenotypes. In contrast, strains in which M119 was intact differentiated a wild-type percentage of heterocysts and did not display Mch phenotypes.

The mutant phenotypes could be the result of unstable protein production leading to immediate protein degradation or could be due to the loss of a translational start site. To distinguish between these two possibilities *hetN*-YFP translational fusions were expressed in wild-type and UHM163, *hetR*(R250K). Overexpression of the *hetN*(M119L)-YFP allele produced what appeared to be a stable protein that localized in a manner similar to the wild-type protein, suggesting that the loss of activity from this allele in the mutant strain was not the result of protein destabilization followed by rapid turnover.

It was surprising that overexpression of the *hetN*(M119L)-YFP allele also resulted in suppression of heterocyst formation given the mutational analysis that suggested M119 was necessary for patterning. However, the presence of inhibitory activity is likely an artifact of overexpression of the allele from a replicating plasmid with a copy number about 10-fold that of the chromosome [24]. Overexpression in a similar manner of two other proteins that also contain the RGSGR sequence prevented hetercyst formation even though neither is involved in development [25].

The combined results indicate that the loss of HetN-dependent inhibitory function when M119 is mutated in the chromosome is consistent with loss of a developmentally regulated translational start site. The ability to produce protein from both M1 and M119 of HetN suggests that use of the second translational start site may have been coopted over evolutionary time. Ancestral HetN may have functioned solely as a ketoacyl

reductase involved in heterocyst morphogenesis. The heterocyst specific transcription could have led to a more recent evolution in which HetN assumed a second function as an inhibitor. Cyanobacteria phylogeny supports this hypothesis with the presence of non-RGSGR containing homologues of *hetN* in some non-heterocyst forming cyanobacteria and RGSGR containing homologues of *hetN* in some heterocyst forming cyanobacteria [6].

References

1. Arteaga, M.F., et al., *Multiple translational isoforms give functional specificity to serum- and glucocorticoid-induced kinase 1.* Mol Biol Cell, 2007. **18**(6): p. 2072-80.
2. Borthakur, P.B., et al., *Inactivation of patS and hetN causes lethal levels of heterocyst differentiation in the filamentous cyanobacterium Anabaena sp. PCC 7120.* Mol. Microbiol., 2005. **57**: p. 111-123.
3. Buikema, W.J. and R. Haselkorn, *Expression of the Anabaena hetR gene from a copper-regulated promoter leads to heterocyst differentiation under repressing conditions.* Proc. Natl. Acad. Sci., U.S.A., 2001. **98**: p. 2729-2734.
4. Cai, Y. and C.P. Wolk, *Use of a conditionally lethal gene in Anabaena sp. strain PCC 7120 to select for double recombinants and to entrap insertion sequences.* J. Bacteriol., 1990. **172**: p. 3138-3145.
5. Callahan, S.M. and W.J. Buikema, *The role of HetN in maintenance of the heterocyst pattern in Anabaena sp. PCC 7120.* Mol. Microbiol., 2001. **40**: p. 941-950.
6. Corrales-Guerrero, L., et al., *Subcellular Localization and Clues for the Function of the HetN Factor Influencing Heterocyst Distribution in Anabaena sp. Strain PCC 7120.* Journal of Bacteriology, 2014. **196**(19): p. 3452-3460.
7. Elhai, J. and C.P. Wolk, *Conjugal transfer of DNA to cyanobacteria.* Methods Enzymol., 1988. **167**: p. 747-754.
8. Feldmann, E.A., et al., *Evidence for direct binding between HetR from Anabaena sp. PCC 7120 and PatS-5.* Biochemistry, 2011. **50**: p. 9212-9224.
9. Higa, K.C. and S.M. Callahan, *Ectopic expression of hetP can partially bypass the need for hetR in heterocyst differentiation by Anabaena sp strain PCC 7120.* Mol. Microbiol., 2010. **77**: p. 562-574.
10. Higa, K.C., et al., *The RGSGR amino acid motif of the intercellular signaling protein, HetN, is required for patterning of heterocysts in Anabaena sp. strain PCC 7120.* Mol. Microbiol., 2012. **83**: p. 682-693.
11. Higuchi, R., B. Krummel, and R.K. Saiki, *A general method of in vitro preparation and specific mutagenesis of DNA fragments: study of protein and DNA interactions.* Nucleic Acids Res., 1988. **16**: p. 7351-7367.
12. Kim, Y., et al., *Structures of complexes comprised of Fischerella transcription factor HetR with Anabaena DNA targets.* Proc. Natl. Acad. Sci. USA, 2013. **110**(19): p. E1716-1723.
13. Matthews, B.W., *Studies on Protein Stability With T4 Lysozyme*, in *Advances in Protein Chemistry*, F.M.R.J.T.E. C.B. Anfinsen and S.E. David, Editors. 1995, Academic Press. p. 249-278.
14. Mitschke, J., et al., *Dynamics of transcriptional start site selection during nitrogen stress-induced cell differentiation in Anabaena sp. PCC7120.* Proc. Natl. Acad. Sci., 2011. **108**: p. 20130-20135.
15. Omairi-Nasser, A., A.G. de Gracia, and G. Ajlani, *A larger transcript is required for the synthesis of the smaller isoform of ferredoxin: NADP oxidoreductase.* Molecular Microbiology, 2011. **81**(5): p. 1178-1189.

16. Orozco, C.C., D.D. Risser, and S.M. Callahan, *Epistasis analysis of four genes from Anabaena sp. strain PCC 7120 suggests a connection between PatA and PatS in heterocyst pattern formation.* J. Bacteriol., 2006. **188**(5): p. 1808-1816.
17. Ringquist, S., et al., *Translation initiation in Escherichia coli: sequences within the ribosome-binding site.* Molecular Microbiology, 1992. **6**(9): p. 1219-1229.
18. Risser, D.D. and S.M. Callahan, *Genetic and cytological evidence that heterocyst patterning is regulated by inhibitor gradients that promote activator decay.* Proc. Natl. Acad. Sci. USA, 2009. **106**(47): p. 19884-19888.
19. Rivers, O.S., P. Videau, and S.M. Callahan, *Mutation of sepJ reduces the intercellular signal range of a hetN-dependent paracrine signal, but not of a patS-dependent signal, in the filamentous cyanobacterium Anabaena sp. strain PCC 7120.* Mol. Microbiol., 2014. **94**(6): p. 1260-1271.
20. Shoichet, B.K., et al., *A relationship between protein stability and protein function.* Proceedings of the National Academy of Sciences of the United States of America, 1995. **92**(2): p. 452-456.
21. Vagner, S., et al., *Alternative translation of human fibroblast growth factor 2 mRNA occurs by internal entry of ribosomes.* Mol Cell Biol, 1995. **15**(1): p. 35-44.
22. Videau, P., et al., *Transcriptional dynamics of developmental genes assessed with an FMN-dependent fluorophore in mature heterocysts of Anabaena sp. strain PCC 7120.* Microbiol., 2014. **160**(9): p. 1874-1881.
23. Videau, P., et al., *ABC transporter required for intercellular transfer of developmental signals in a heterocystous cyanobacterium.* J. Bacteriol., 2015. **197**(16): p. 2685-2693.
24. Wei, T.-F., R. Ramasubramanian, and J.W. Golden, *Anabaena sp. strain PCC 7120 ntcA gene required for growth on nitrate and heterocyst development.* J. Bacteriol., 1994. **176**: p. 4473-4482.
25. Wu, X., et al., *patS minigenes inhibit heterocyst development of Anabaena sp. strain PCC 7120.* J. Bacteriol., 2004. **186**: p. 6422-6429.

Appendix 1. HetN and PatS are Not Functionally Redundant

Introduction

Though HetN and PatS regulate the progression of development differently, they share a conserved RGSGR motif that is absolutely required for function. Mutations in the RGSGR motif result in greatly decreased or non-functional *patS* and *hetN* alleles. Exogenous addition of the RGSGR pentapeptide to cultures inhibits heterocyst formation and *in vitro* studies have shown that this pentapeptide interacts directly with HetR [8]. However, the addition of one conserved amino acid (ERGSGR) results in binding with a much higher affinity [9]. Mutational analysis of the entire *patS* gene identified amino acids required for activity and showed that mutation of the conserved glutamate in the ERGSGR motif resulted in a *patS* allele with decreased function [4]. Mutation of the four regions of *hetN* that show differences in hydrophobicity demonstrated that the E/RGSGR motif and the region upstream of it are required for protein function [7]. Despite these studies, the exact nature of the mature PatS and HetN inhibitors remain unknown.

The implied similarities between the amino acids required for the inhibitory function of HetN and PatS does not define a conserved inhibitory protein within the two. HetN is 287 aa and PatS is 17 aa, the proteins are produced at different times during differentiation, *patS* during pattern formation and *hetN* during pattern maintenance, and the level of expression upon induction is not comparable between the two proteins with *patS* induction being higher than that of *hetN*. Regardless of these stark differences, the similarity in the regions required for inhibition suggests that the two protein produce an identical inhibitory signal. In this case the proteins may be functionally redundant.

To determine if HetN and PatS are functionally redundant, the coding region of one was replaced by the coding region of the other in the chromosome and vice versa. The two mutants produced, UHM357 and UHM358, had either two copies of *hetN,* one expressed from the native promoter and the other expressed from the *patS* promoter, or two copies of PatS, one expressed from the native promoter and the other expressed from the *hetN* promoter. The phenotypes of the two mutants were compared to wild-type and UHM114 (Δ*patS*) or UHM150 (Δ*hetN*), depending on the mutant. The phenotypes of the five strains were used to determine if HetN and PatS are functionally redundant. Functional redundancy would be indicated by the phenotypes of UHM357 and UHM358 resembling that of the wild-type.

Materials and Methods

Culture conditions. The growth of *Escherichia coli, Anabaena* sp. strain PCC 7120 and its derivatives, concentrations of antibiotics, and the induction of heterocysts in media lacking a source of combined nitrogen were as previously described [1, 6]. Growth medium containing 6 mM ammonia as a nitrogen source was prepared as previously described and used to grow strains prior to the induction of heterocyst differentiation [10]. Heterocyst percentages, frequency of single, double, and higher numbers of contiguous heterocysts, and the mean vegetative cell interval between heterocysts were determined as previously described [12]. Plasmids were introduced into *Anabaena* strains by conjugation from *E. coli* as previously described [5].

Plasmid construction. Plasmid pPJAV348 is a suicide vector based on pRL277 to replace the coding region of *hetN* with *patS* at the native *hetN* locus. Regions directly up- and downstream of the *hetN* coding region were amplified by PCR from *Anabaena*

chromosomal DNA with the primer pairs hetMF-BamHI and dhetNup-S-OEX-R and dhetNup-S-OEX-F and hetIR-SacI, respectively. The products were fused together by overlap extension PCR, such that the region of overlap on the primers introduced the *patS* coding region, and cloned into the *Nru*I site of pRL277 to create pPJAV348.

Plasmid pPJAV349 is a suicide vector based on pRL277 to replace the coding region of *patS* with *hetN* at the native *patS* locus. Regions directly up- and downstream of the *patS* coding region were amplified from *Anabaena* chromosomal DNA with the primer pairs 5'patSSacF and dpatSup-N-OEX-R and dpatSdn-N-OEX-F and 3'patSBglIIR, respectively, and the coding region of *hetN* was amplified with the primers dpatS-N-OEX-F and dpatS-N-OEX-R. The *hetN* coding region and regions up- and downstream of *patS* were fused together by overlap extension PCR and the product was cloned into the *Nru*I site in pRL277 to create pPJAV349.

Strain construction. The coding region of *hetN* was replaced with the coding region of *patS* at the *hetN* locus with the plasmid pPJAV348 to create UHM357. The coding region of *patS* was replaced with the coding region of *hetN* at the *patS* locus with the plasmid pPJAV349 to create UHM358. Strains with mutations in the *hetN* and *patS* genes were verified by PCR with the primer sets patSfor and patSrev and up-hetN-F and down-hetN-R, respectively, which anneal outside of the regions used to make the mutations.

Microscopy. Cells were routinely viewed and imaged as previously described [1]. All images were processed in Adobe Photoshop CS2.

Table 16. Strains and Plasmids used in Appendix 1.

Strain or Plasmid	**Relevant Characteristic(s)***	**Source or Reference**
***Anabaena* sp. strains**		
PCC 7120	Wild-type	Pasteur Culture Collection
UHM114	Δ*patS*	[1]
UHM150	Δ*hetN*	[7]
UHM357	*patS* replacing *hetN* in the *hetN* locus	This study
UHM358	*hetN* replacing *patS* in the *patS* locus	This study
Plasmids		
pRL277	Suicide vector; Sp^r Sm^r	[2]
pPJAV348	pRL277 to make UHM357	This study
pPJAV349	pRL277 to make UHM358	This study

*Km, kanamycin; Nm, neomycin; Sm, streptomycin; Sp, spectinomycin

Table 17. Oligonucleotide primers used Appendix 1.

Oligonucleotide*	Sequence
hetMF-BamHI	GGATCCTAGAACGCTGGTCTGATGAACAA
dhetNup-S-OEX-R	CTCATCACAGAAATTCACTAACATAATTGCCTTCATT GTAACCTGCTAGTCTCCAAATTC
dhetNup-S-OEX-F	GTGAATTTCTGTGATGAGCGCGGTAGTGGTAGATAG CTCCGCAGTTGCTTAGGGAATGAG
hetIR-SacI	GAGCTCTGGAACCAGGGCAAGTTAAATTT
dpatS-N-OEX-F	TTTAAGATTATGACAACTCTTACAGGTAAGACAGTAC
dpatS-N-OEX-R	ACACTCGTTTCATGAGCGATGAGACTCAACAGCTACA TAG
dpatSdn-N-OEX-F	CGCTCATGAAACGAGTGTAAAATTCTGCCTCGACTAT CG
3'patSBglIIR	AGATCTGGGAGTAAATTGTAAATCATAGAAC
5'patSSacF	GAGCTCCGCATCTTTTATTCAAGCTAACTAGC
dpatSup-N-OEX-R	AGTTGTCATAATCTTAAAATCGGTGAATTACTTTTCA ACAG
patSfor	GATATCTAATCGATGCCACATCTAAG
patSrev	CACATTAATCTCACTAACTTCTACATC
up-hetN-F	GAGCTCGGCAAGCAGAGTTAATC
down-hetN-R	GGATCCGCCCATTAATATAAGTCTC

*Oligonucleotides are shown in the 5’ to 3’ direction

Results

Strains UHM358 (*ΔpatS::hetN*) and UHM357 (*ΔhetN::patS*) were created and their ability to differentiate heterocysts was determined 24 and 48 h N-. After 24 h, the wild-type and UHM114 (*ΔpatS*) produced 9.1 % ± 0.31 and 21.3 % ± 3.1 heterocysts, respectively, while UHM358 produced 0.3 % ± 0.23 heterocysts (Figure 24, Table 18). After 48 h N-, the wild-type and UHM150 (*ΔhetN*) produced 9.5 % ± 0.31 and 16.2 % ± 0.2 heterocysts, respectively, while UHM357 produced 11.4 % ± 0.4 heterocysts (Figure 24, Table 18). When *hetN* replaced *patS* in UHM358, heterocyst differentiation did not exceed ~3% indicating that expression of *hetN* at levels comparable to *patS* is sufficient to inhibit differentiation. In contrast, when *patS* replaced *hetN* and was controlled by the *hetN* promoter, an increased but intermediate number of heterocysts between wild-type and UHM150 was formed. These results indicate that *hetN* and *patS* are not functionally redundant due to the strongly inhibitory influence of *hetN* in the *patS* locus and the decrease in inhibition by *patS* in the *hetN* locus.

Table 18. Patterns of heterocysts produced by strains of *Anabaena*.

Strain (Genotype)	Hours N-	Heterocyst Percentage	Mean Vegetative Cell Interval	Heterocyst Occurrence
Wild-type	24	9.07 ± 0.31	10.3 ± 0.46	96 ± 1.73; 4 ± 1.73
	48	9.47 ± 0.31	11.5 ± 0.31	96.67 ± 1.53; 3.33 ± 1.53
	72	8.93 ± 0.23	12.7 ± 0.38	95.33 ± 0.58; 6.67 ± 0.58
UHM150 (Δ*hetN*)	24	9.47 ± 0.5	10.4 ± 0.32	88.33 ± 3.79; 10.67 ± 2.08 1 ± 1.73
	48	16.2 ± 0.2	5.9 ± 0.17	41.67 ± 2.08; 33.33 ± 4.04; 25 ± 4.36
	72	16.07 ± 0.12	6.1 ± 0.45	29 ± 1; 29.11 ± 2.08; 42 ± 2.52
UHM114 (Δ*patS*)	24	21.3 ± 3.1	3.8 ± 0.52	51.56 ± 2.52; 40.78 ± 2.31; 7.67 ± 3.61
	48	18.07 ± 2.37	4.5 ± 0.34	56.11 ± 7.57; 39.56 ± 8.19; 6.33 ± 3.61
	72	15.85 ± 1.82	5.9 ± 1.08	61.67 ± 0.67; 33.12 ± 1.84; 5.21 ± 2.08
UHM357 (Δ*hetN::patS*)	24	9.27 ± 0.76	10.6 ± 0.07	88.17 ± 3.51; 11.83 ± 3.51
	48	11.4 ± 0.4	8.4 ± 0.29	56.33 ± 4.04; 17.34 ± 6.65; 7.33 ± 3.51
	72	11.13 ± 0.61	7.5 ± 0.89	52.33 ± 4.04; 18.33 ± 6.65; 10.34 ± 3.51
UHM358 (Δ*patS::hetN*)	24	0.33 ± 0.23	-	-
	48	2.67 ± 0.12	-	-
	72	3.2 ± 0.35	-	-

At the indicated times following nitrogen stepdown, 500 cells were counted in triplicate and total heterocysts are presented as the mean ± the standard deviation. The presence of single (top line), double (second line), or multiple contiguous heterocysts (third line) was determined for 300 heterocyst occurrences in triplicate and are presented as the average percent ± the standard deviation. The number of vegetative cell between heterocysts was counted for 300 intervals and is presented as the mean ± the standard deviation of the mean.

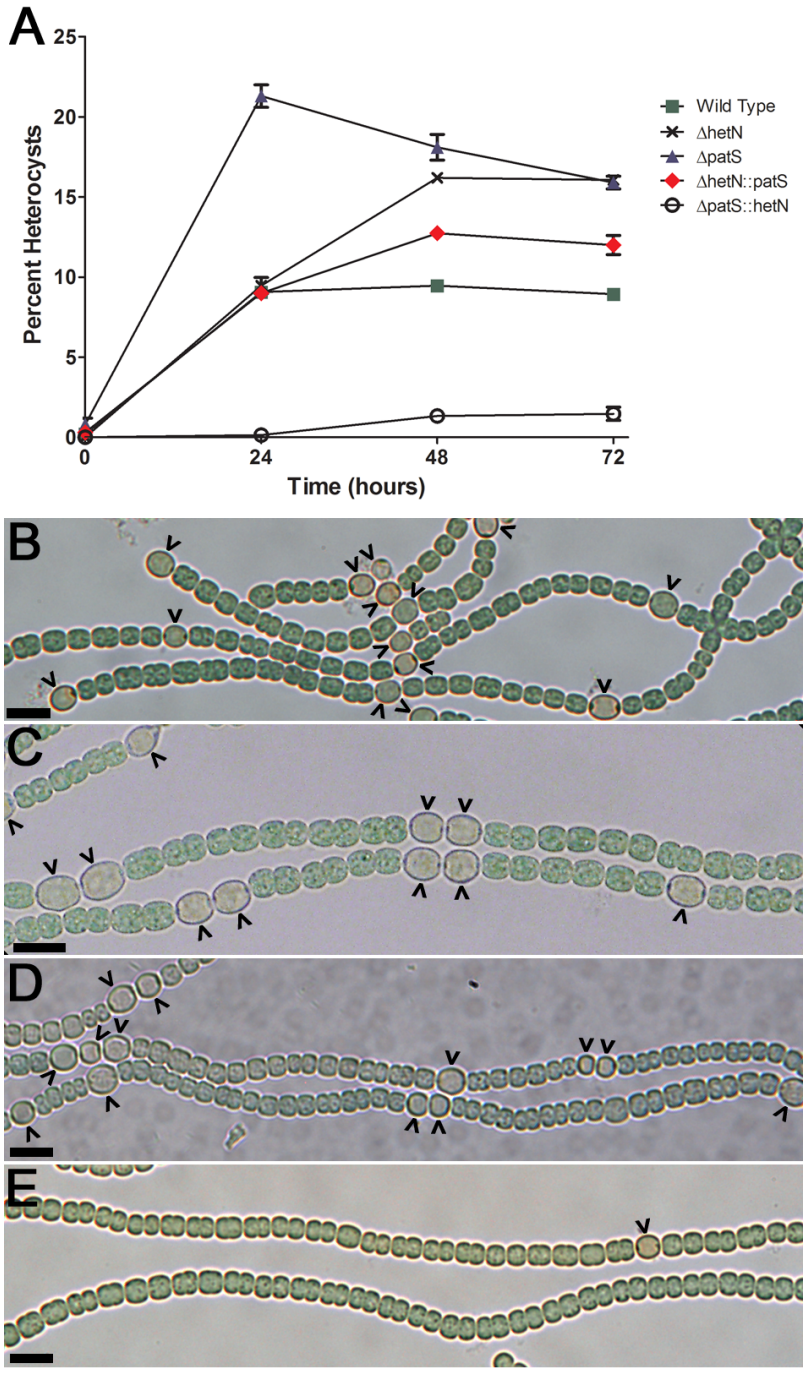

Figure 24. The proper positioning of *patS* and *hetN* in the genome is involved in their function as inhibitors. Heterocyst percentages from 500 cells were determined in triplicate various times after nitrogen stepdown for the wild-type, Δ*hetN*, Δ*patS*, Δ*hetN*::*patS* strains, and Δ*patS*::*hetN* strains and presented as the average ± standard deviation (A). Brightfield micrographs of wild-type (B), Δ*patS* (UHM114; C), Δ*hetN*::*patS* (UHM357, D), and Δ*patS*::*hetN* (UHM358, E). Micrographs were taken either 24 h (B, C, E) or 48 h (D) after the removal of combined nitrogen. Carets indicate heterocysts. Scale bars, 10 μm.

Discussion

The plasticity of bacterial genomes leads to different levels of interrelatedness between different genes within the genomes of closely and distantly related bacteria. Homologous genes are those that have a common ancestral gene, with genetic differences arising from either speciation, producing orthologs that retain the function of the ancestral gene, or duplication within a genome, producing paralogs with dissimilar functions. The genetic differences between the *hetN* and *patS* loci, as well as the similarity of HetN to proteins involved with fatty acid synthesis suggest that the similarity in function shared by *hetN* and *patS* is not due to a shared ancestral gene. Rather it may be the result of convergent speciation of gene function within a single organism.

In order to determine the functional relatedness of HetN and PatS, two mutants were created in which the coding region of one gene was replaced by the coding region of the other and vice versa. The phenotypes of the two mutants were dissimilar to wild-type, UHM114 (Δ*patS*), and UHM150 (Δ*hetN*). HetN produced from the *patS* promoter, UHM358, was sufficient to inhibit sustainable levels of differentiation in N- medium. PatS produced from the *hetN* promoter, UHM357, resulted in an intermediate percentage of heterocysts between that of wild-type and UHM150, indicating incomplete complementation. The results indicate that HetN and PatS do not functionally complement one another.

The inability to complement one another is not an unexpected result. Known differences in the levels of transcription could account for the mutant phenotypes alone, while many other differences between the two proteins could also be implicated. The

topology of HetN requires some amount of protein processing to produce a peptide of a similar length to PatS, which itself is thought to be processed to a smaller mature peptide [4]. This processing could be increase in vegetative cells and result in excessive export of the inhibitory signal from developing heterocysts. Further, the protein channels connecting adjacent cells within filaments may be different between two vegetative cells and a vegetative cell and heterocyst, leading to a decrease in the transport of PatS away from source heterocysts when it is expressed from the *hetN* promoter. The inherent number of possibilities explaining the mutant phenotypes of UHM357 and UHM358 make it difficult to use the results in identification of the inhibitory signal within the *Anabaena* developmental system. The exact identity of the inhibitory signal(s) within *Anabaena* remains unknown, while identification and description to the current degree of proteins like HetN and PatS remains an important part of developmental biology.

References

1. Borthakur, P.B., et al., *Inactivation of patS and hetN causes lethal levels of heterocyst differentiation in the filamentous cyanobacterium Anabaena sp. PCC 7120.* Mol. Microbiol., 2005. **57**: p. 111-123.
2. Cai, Y. and C.P. Wolk, *Use of a conditionally lethal gene in Anabaena sp. strain PCC 7120 to select for double recombinants and to entrap insertion sequences.* J. Bacteriol., 1990. **172**: p. 3138-3145.
3. Callahan, S.M. and W.J. Buikema, *The role of HetN in maintenance of the heterocyst pattern in Anabaena sp. PCC 7120.* Mol. Microbiol., 2001. **40**: p. 941-950.
4. Corrales-Guerrero, L., et al., *Functional dissection and evidence for intercellular transfer of the heterocyst-differentiation PatS morphogen.* Mol. Microbiol., 2013. **88**(6): p. 1093-1105.
5. Elhai, J. and C.P. Wolk, *Conjugal transfer of DNA to cyanobacteria.* Methods Enzymol., 1988. **167**: p. 747-754.
6. Higa, K.C. and S.M. Callahan, *Ectopic expression of hetP can partially bypass the need for hetR in heterocyst differentiation by Anabaena sp strain PCC 7120.* Mol. Microbiol., 2010. **77**: p. 562-574.
7. Higa, K.C., et al., *The RGSGR amino acid motif of the intercellular signaling protein, HetN, is required for patterning of heterocysts in Anabaena sp. strain PCC 7120.* Mol. Microbiol., 2012. **83**: p. 682-693.
8. Kim, Y., et al., *Structure of the transcription factor HetR required for heterocyst differentiation in cyanobacteria.* Proc. Natl. Acad. Sci., 2011. **108**: p. 10109-10114.
9. Kim, Y., et al., *Structures of complexes comprised of Fischerella transcription factor HetR with Anabaena DNA targets.* Proc. Natl. Acad. Sci. USA, 2013. **110**(19): p. E1716-1723.
10. Mitschke, J., et al., *Dynamics of transcriptional start site selection during nitrogen stress-induced cell differentiation in Anabaena sp. PCC7120.* Proc. Natl. Acad. Sci., 2011. **108**: p. 20130-20135.
11. Rivers, O.S., P. Videau, and S.M. Callahan, *Mutation of sepJ reduces the intercellular signal range of a hetN-dependent paracrine signal, but not of a patS-dependent signal, in the filamentous cyanobacterium Anabaena sp. strain PCC 7120.* Mol. Microbiol., 2014. **94**(6): p. 1260-1271.
12. Videau, P., et al., *ABC transporter required for intercellular transfer of developmental signals in a heterocystous cyanobacterium.* J. Bacteriol., 2015. **197**(16): p. 2685-2693.